# The VEGFC/VEGFR3 pathway in the malignancy of ovarian carcinoma

## Thesis

# THE VEGFC/VEGFR3 PATHWAY IN THE MALIGNANCY OF OVARIAN CARCINOMA

Thesis submitted by

Alessandra Agnese Decio

IRCCS - Istituto di Ricerche Farmacologiche Mario Negri, Bergamo, Italy

for the degree of

Doctor of Philosophy

Open University Research School, UK

Discipline of Life Sciences

September 2013

# THE VEGFC/VEGFR3 PATHWAY IN THE MALIGNANCY OF OVARIAN CARCINOMA

**Alessandra Agnese Decio**
IRCCS - Istituto di Ricerche Farmacologiche Mario Negri, Bergamo, Italy
Open University Research School, UK
**Doctor of Philosophy**
September 2013

---

# ABSTRACT

Vascular endothelial growth factor C (VEGFC) promotes tumor progression in several tumor types, mainly through the stimulation of lymphangiogenesis and lymphatic metastasis.
The expression and biological significance of the VEGFC/VEGFR3 pathway in ovarian cancer growth and dissemination has been investigated in this thesis using ovarian carcinoma cell lines and tumor animal models.

In patient-derived ovarian carcinoma xenografts (HOC), high levels of soluble VEGFC in ascites and serum were detected, in association with disease progression and tumor burden. Peak VEGFC expression preceded para-aortic lymph node infiltration by HOC8 neoplastic cells. Histological detection of tumor cells in blood and lymphatic vessels indicated both hematogenous and lymphatic dissemination.

VEGFC was over-expressed in the VEGFR3-positive and luciferase-expressing 1A9 and IGROV1 ovarian cancer cells. *In vitro*, VEGFC released by the expressing tumor cells stimulated tumor cell migration in an autocrine manner. *In vivo*, over-expression of VEGFC

promoted IGROV1 dissemination after orthotopic intraovarian transplantation in nude mice. VEGFC released in serum of mice correlated with tumor burden and metastasis.

Cediranib, a small molecule receptor tyrosine kinase inhibitor of VEGFR1-3 and c-Kit, inhibited *in vivo* metastasis of VEGFC-overexpressing IGROV1 and *in vitro* autocrine effects on tumor cell migration; cediranib improved the survival of mice bearing the four HOC xenografts analyzed. The therapeutic benefit was proportional to soluble VEGFC levels in serum and ascites and to VEGFR3 expression by tumor cells.

Different schedules of cediranib were tested on HOC8 xenograft. The survival benefit of cediranib in maintenance regimen (14 weeks) was superior to 3-weeks treatment. A significant prolongation of mice survival was observed in mice treated with advanced tumor. Treatment benefits were improved combining cediranib with chemotherapy (paclitaxel plus cisplatin).

These findings suggest that the VEGFC/VEGFR3 pathway acts as an enhancer of ovarian cancer progression through autocrine and paracrine mechanisms, hence offering a potential target for therapy.

# Preface

The work described herein was performed at the IRCCS – Istituto di Ricerche Farmacologiche Mario Negri, Bergamo, Italy from 2009 to 2013. The work was performed under the supervision of Dr. Dorina Belotti (director of studies) and Prof. Dylan R Edwards (external supervisor).

# Declaration

This thesis has not been submitted in whole or in part for a degree or diploma or other qualification to any other university.

The experimental work described herein was performed by myself, Alessandra Agnese Decio and includes work carried out in collaboration with:

*Research collaborators:*

- Dr. Enrico Pesenti (Nerviano Medical Sciences Oncology, Nerviano, Italy) together with members of his lab, taught and helped me to generate the lentivirus infected cell lines (Chapter 4).
- Dr. Veronica Patton and Dr. Rachele Alzani (Nerviano Medical Sciences Oncology, Nerviano, Italy) are expert pathologists who performed all the histological and immunohistochemical analysis (Chapters 3, 4 and 5).
- Dr. Sergio Bernasconi (IRCCS – Istituto di Ricerche Farmacologiche Mario Negri, Milan, Italy) is the expert technician who performed the FACS analysis of Katushka-infected cells (Chapter 4).

# Acknowledgements

First and foremost, I would like to thank my supervisor Dr. Dorina Belotti for her guidance and support throughout these years. Thank you also for your time and dedication.

Special thanks go to Dr. Raffaella Giavazzi, head of the lab, for constantly challenging and encouraging me. Another important thank you goes to Dr. Giulia Taraboletti, head of the Tumor Angiogenesis Unit, for welcoming me in her lab and for her always appropriate suggestions.

I would like to thank Prof. Dylan R. Edwards, my external supervisor, for his precious guidance and advice throughout these years.

Thank you also to the many members of the Giavazzi lab, both in Bergamo and Milan, whom I have met over the years. It has been a pleasure to work with each of you, and I was so lucky to find also some very good friends.

My gratitude goes to Prof. Silvio Garattini, director of the IRCCS Istituto di Ricerche Farmacologiche Mario Negri, for offering the PhD program in the institute. I deeply esteem him for always defending science and research in the first person. I wish I'll become an honest scientist like him.

Finally my most important thanks go to my parents, my brother, and Matteo, for their constant patience, support, and encouragement.

# List of Abbreviations

| | |
|---|---|
| ΔCt | delta Ct |
| µg | Micrograms |
| µm | Micrometers |
| Abs | Absorbance |
| ADP | Adenosine diphosphate |
| Ang1 | Angiopoietin 1 |
| Ang2 | Angiopoietin 2 |
| ANOVA | Analysis of variance |
| AM | Adrenomedullin |
| AP-2 | Activating Protein 2 |
| ARID1A | AT rich interactive domain 1A (SWI-like) |
| Arg | Arginine |
| ATCC | American Type Culture Collection |
| ATP | Adenosine triphosphate |
| BEC | Blood endothelial cells |
| bFGF /FGF-2 | Basic fibroblast growth factor |
| BL-2 | Biosafety level 2 |
| BL | Bioluminescence |
| BLI | Bioluminescence imaging |
| bp | Base pairs |
| BRAF | v-raf murine sarcoma viral oncogene homolog B |
| BRCA1 | Breast Cancer Type 1 susceptibility protein |
| BRCA2 | Breast Cancer Type 2 susceptibility protein |

| | |
|---|---|
| BSA | Bovine serum albumin |
| °C | degree Celsius |
| cDNA | Complementary deoxyribonucleic acid |
| CD31 /PECAM-1 | Platelet endothelial cell adhesion molecule-1 |
| CMV | Cytomegalovirus |
| CREB | cAMP response-element binding protein |
| Ced | Cediranib |
| Ct | Threshold cycle |
| CTNNB1 | Catenin (cadherin-associated protein), beta 1 |
| C-terminal | Carboxyl-terminal |
| Cys | Cysteine |
| DDP | Cis-diamminedichloroplatinum |
| DMEM | Dulbecco's modified Eagle medium |
| DMSO | Dimethylsulphoxide |
| DNA | Deoxyribonucleic acid |
| EC | Endothelial cells |
| ECD | Extracellular domain |
| ECGS | Endothelial cell growth supplement |
| EDTA | Ethylenediaminetetraacetic acid |
| ELISA | Enzyme-linked immunosorbent assay |
| EOC | Epithelial ovarian cancer |
| ERK1/2 | Extracellular signal-regulated kinase 1/2 |
| F4/80 | Mature macrophage antigen |
| FBS | Fetal bovine serum |
| FGF/-1/-2 | Fibroblast growth factor/-1/-2 |

| | |
|---|---|
| FGFR/-1 | Fibroblast growth factor receptor/-1 |
| FIGO | Federation of Gynecologists and Obstetricians |
| FLI | Fluorescence imaging |
| Flt4 | fms-related tyrosine kinase 4 |
| GCIG | Gynaecologic Cancer InterGroup |
| GEM | Genetically engineered models |
| H&E | Hematoxylin and eosin |
| HBSS | Hank's Balanced Salt Solution |
| HGF | Hepatocyte growth factor, also referred to as scatter factor (SF) |
| HIV | Human immunodeficiency virus |
| HOC | Human ovarian carcinoma |
| HPRT1 | Hypoxanthine phosphoribosyltransferase 1 |
| kDa | Kilodalton |
| kg | Kilograms |
| KRAS | Kirsten rat sarcoma viral oncogene homolog |
| Ig | Immunoglobulin |
| IGF-1/-2 | Insulin-like growth factor 1/2 |
| ILS | Increment of life span |
| i.o. | Intraovarian |
| i.p. | Intraperitoneal |
| i.v. | Intravenous |
| LEC | Lymphatic endothelial cells |
| LYVE-1 | Lymphatic vessel endothelial hyaluronic acid receptor 1 |
| MELC | Mouse endothelial lymphatic cells |
| MEM | Minimum essential medium Eagle |

| | |
|---|---|
| MiSEP | Multiplex in situ epitope profiling |
| ml | Milliliter |
| MMP2 | Matrix metalloprotease-2 |
| mRNA | Messenger RNA |
| MST | Median survival time |
| NCIC | National Cancer Institute of Canada |
| NEAA | Non-essential amino acids |
| NF-kB | Nuclear factor kappa light polypeptide gene enhancer in B cells |
| nm | Nanometers |
| Nrp/-1/-2 | Neuropilin/-1/-2 |
| NSCLC | Non-small cell lung cancer |
| N-terminal | Amino-terminal |
| ORF | Open reading frames |
| ORR | Objective response rate |
| OS | Overall survival |
| PARP | Poly(adenosine diphosphate [ADP]-ribose |
| PBS | Phosphate buffered saline |
| PCR | Polymerase chain reaction |
| PDGF | Platelet derived growth factor |
| PDGFR/-α/-β | Platelet derived growth factor receptor/-α/-β |
| PDTX | Patient-derived tumor xenografts |
| PFS | Progression-free survival |
| PIK3CA | Phosphatidylinositol-4,5-bisphosphate 3-kinase, catalytic subunit alpha |
| PKB /Akt | Protein kinase B |
| PLD | Pegylated liposomaldoxorubicin |

| | |
|---|---|
| PlGF | Placenta growth factor |
| pg | Picograms |
| p.o. | Per os |
| PPP2R1A | Protein phosphatase 2, regulatory subunit A, alpha |
| PTEN | Phosphatase and tensin homolog |
| PTX | Paclitaxel |
| RNA | Ribonucleic acid |
| ROI | Region of interest |
| rpm | Revolutions per minute |
| RPMI | Roswell Park Memorial Institute cell culture medium |
| RRE | Rev response element |
| RT | Reverse transcription |
| SD | Standard deviation |
| SEM | Standard error of mean |
| Ser | Serine |
| Sp-1 | Specificity Protein 1 |
| SV40 | Simian virus 40 |
| TAM | Tumor-associated macrophages |
| TATA | Thymine Adenine Thymine Adenine |
| Tie1 | Tyrosine kinase with immunoglobulin-like and EGF-like domains 1 |
| Tie2 | TEK tyrosine kinase, endothelial |
| TK(R)I | Tyrosine kinase (receptor) inhibitor |
| TP53 | Tumor protein p53 |
| Tween-80 | Polysorbate 80 |
| VEGF | Vascular endothelial growth factor |

| | |
|---|---|
| VEGFA | Vascular endothelial growth factor A, also referred to as VEGF |
| VEGFC | Vascular endothelial growth factor C |
| VEGFCfl | Full length vascular endothelial growth factor C |
| VEGFCmf | Mature form vascular endothelial growth factor C |
| VEGFD | Vascular endothelial growth factor D |
| VEGFE | Vascular endothelial growth factor E |
| VEGFR1 | Vascular endothelial growth factor receptor-1 |
| VEGFR2 | Vascular endothelial growth factor receptor-2 |
| VEGFR3 | Vascular endothelial growth factor receptor-3 |
| VHD | VEGF homology domain |

# Table of Contents

Chapter 1

# Introduction

## 1.1 Epithelial ovarian cancer

### *1.1.1 Epidemiology*

Epithelial ovarian cancer (EOC) is the fifth highest cancer-related cause of death in women in Western countries (Siegel, Naishadham *et al.* 2013). In 2008, it was estimated that 225500 women were diagnosed with ovarian cancer and the estimated deaths worldwide were 140200. These values make ovarian cancer the eighth most common type of cancer worldwide, and the seventh most common cause of death related to cancer among women (Jemal, Bray *et al.* 2011). Ovarian cancer has the highest mortality rate of any gynecological malignancy in developed regions of the world and is second to cervical cancer in developing regions (Jemal, Bray *et al.* 2011).

The high mortality of ovarian cancer is primary due to difficulties in diagnosing early stage disease indeed most patients (about 75%) present with advanced stage tumors (Karst and Drapkin 2010). Stage at diagnosis has a profound influence on the overall prognosis and survival of the patient, with only a 27% of the women diagnosed with distant disease surviving at least 5 years post-diagnoses (Lowe, Chia *et al.* 2013).

Unfortunately, the current screening modalities are not effective for detecting ovarian cancer in asymptomatic patients. Typical symptoms are vague and are often confused with gastrointestinal diseases, and in many cases symptoms may not even present until the tumor has reached an advanced stage (Karst and Drapkin 2010).

### *1.1.2 Risk factors*

The most important risk factor is strong family history of ovarian or breast cancer, although an identifiable genetic predisposition, such as Breast Cancer Type 1 and 2 Susceptibility Proteins (BRCA1/BRCA2) tumor suppressor gene mutations, is present only in 10-15% of patients (Bast, Hennessy *et al.* 2009). Early menarche, late menopause, nulliparity, and

increasing age are also associated with increased risk, whereas oral contraceptive use, pregnancy, breast-feeding, and tubal ligation are associated with reduced risk (Edmondson and Monaghan 2001). These epidemiological data could be explained by the incessant ovulation hypothesis that postulates that repetitive wounding of the ovarian surface epithelium and cell proliferation in postovulatory repair result in a stepwise accumulation of genomic abnormalities. Ovarian epithelial inclusion cysts occur as a result and might increase the risk of carcinogenesis by entrapping cells in a growth factor rich environment (Fathalla 1971). Furthermore, surges of pituitary gonadotropins at ovulation and persistent high concentrations after menopause stimulate surface epithelium cells, resulting in accumulation of genetic changes and carcinogenesis (Cramer and Welch 1983). Inflammation and changes in redox potential might have a role in the setting of ovulation and surface-epithelium repair and might account for the increased risk of epithelial ovarian cancer associated with talc or asbestos exposure, endometriosis, pelvic inflammatory disease and mumps (Cramer, Hutchison *et al.* 1983).

### *1.1.3 Pathology*

The term "ovarian cancer" refers not to a single disease, but to a heterogeneous group of malignancies affecting the ovary. In general, ovarian tumors may develop from one of three cell types: epithelial cells, sex cord-stromal cells (including granulosa, theca, and hilus cells), or germ cells (oocytes). Although about 40% of all ovarian tumors are non-epithelial in origin, such lesions rarely progress to a malignant state and account for 10% of ovarian cancers (Chen, Ruiz *et al.* 2003).

Epithelial ovarian carcinomas are themselves a heterogeneous group of neoplasms that exhibit a wide range of tumor morphologies, clinical manifestations, underlying genetic alterations. According to the International Federation of Gynecology and Obstetrics (FIGO)

classification, epithelial ovarian cancers are classified by diagnosis of malignancy in 4 stages on the basis of the extension of the tumor beyond the ovary (Benedet, Bender *et al.* 2000):

- stage I indicates confinement to the ovary;
- stage II tumors extend beyond the ovary to adjacent pelvic structures such as the fallopian tube or uterus;
- stage III indicates metastasis to the peritoneum and/or regional lymph nodes;
- stage IV tumors have metastasized beyond the peritoneum to distant sites.

Additionally, tumors are classified by histopathological grade (I-III) and appearance into serous, endometrioid, mucinous and less commonly, clear cell, transitional cell, squamous cell, mixed epithelial, and undifferentiated subtypes (Tavassoli and Devilee 2003). Within each subtype, tumors are further described as either benign, malignant, or borderline and, depending upon tumor subtype, classified as low- or high-grade. Borderline tumors are considered to have low malignant potential and/or indolent behavior. There are major differences in incidence, tumor behavior (low versus high malignant potential), and clinical outcome between each histologic subtype.

The traditional view of ovarian cancer asserts that all tumor subtypes share a common origin in ovarian surface epithelium, that is a flat-to-cuboidal layer of uncommitted mesothelial cells covering the exterior surface of the ovary. Subsequent metaplastic changes lead to the development of the different cell types. Recent studies have provided evidences that what have been traditionally thought to be primary ovarian tumors actually originate in other pelvic organs and involve the ovary secondarily. Thus, it has been suggested that serous carcinoma arise from the implantation of epithelium from the fallopian tube, while endometriosis is considered the precursor of endometrioid and clear cell tumors (Kurman and Shih Ie 2010).

Consequently, over the last several years, a dualistic model for the pathogenesis of ovarian carcinoma has emerged. In this model, epithelial tumors are divided into two groups, types I

and II (Kurman and Shih Ie 2010), based on their distinctive clinicopathologic and molecular genetic features. It also links specific histologic types with their putative precursor lesions.

Type I tumors comprise low-grade serous carcinomas, low-grade endometrioid, clear cell, and mucinous carcinomas, which develop in a stepwise fashion from well-established precursor lesions, such as borderline tumors and endometriosis.

They typically present as large masses that are confined to one ovary (stage Ia), are indolent, and have a good prognosis. The type I tumors are relatively genetically stable and typically display a variety of somatic sequence mutations that include Kirsten rat sarcoma viral oncogene homolog (KRAS), v-raf murine sarcoma viral oncogene homolog B (BRAF), Phosphatase and tensin homolog (PTEN), Phosphatidylinositol-4,5-bisphosphate 3-kinase, catalytic subunit alpha (PIK3CA), Catenin (cadherin-associated protein), beta 1 (CTNNB1), AT rich interactive domain 1A (SWI-like) (ARID1A), and Protein phosphatase 2, regulatory subunit A, alpha (PPP2R1A) but very rarely Tumor protein p53 (TP53) (Shih Ie and Kurman 2004; Jones, Wang *et al.* 2010).

In contrast, type II tumors comprise high-grade serous carcinoma, high-grade endometrioid carcinoma, malignant mixed mesodermal tumors (carcinosarcomas), and undifferentiated carcinomas, which present in advanced stage (stages II-IV) in more than 75% of cases; they grow rapidly and are highly aggressive. Type II tumors, of which high-grade serous carcinoma is the prototypic type, are chromosomally highly unstable and harbor TP53 mutations in more than 95% of cases (Ahmed, Etemadmoghadam *et al.* 2010) and they rarely display the mutations found in the type I tumors. BRCA inactivation, either by mutation or inactivation of expression of BRCA and its downstream genes via promoter methylation, occurs in up to 40% to 50% of high-grade serous carcinoma (Senturk, Cohen *et al.* 2010). BRCA inactivation has not been reported in the type I tumors.

### 1.2 Lymph node metastasis and lymphatic dissemination

Ovarian cancer metastasizes either by direct extension from the ovarian/fallopian tumor to neighboring organs (bladder/colon) or by detachment of cancer cells from the primary tumor. Exfoliated tumor cells are transported throughout the peritoneum by ascites and disseminate within the abdominal cavity (Lengyel 2010). Cancer cells do not immediately adhere to a peritoneal surface, but move with ascites vehicle to distant sites by physical forces such as fluid hydrodynamics and gravity. In contrast, in the absence of ascites, cancer cells are restricted in motion and implant near the primary site (Carmignani, Sugarbaker *et al.* 2003).

Malignant cells implant anywhere in the peritoneal cavity but likely along the preferential flow and site of peritoneal fluid stasis, such as in the pelvis, near the ileocecal valve region and along the right paracolic gutter. Frequent invasion of the diaphragm and greater omentum may be explained by the presence of lymphatic lacunae on the peritoneal surface of the diaphragm and lymphoid tissue present on the greater omentum. These tissues absorb peritoneal fluid and thereby draw cancer cells to their surface (Feki, Berardi *et al.* 2009).

Besides the dissemination through peritoneal fluid, lymphatic invasion and hematogenous dissemination are common in ovarian cancer (Feki, Berardi *et al.* 2009).

In particular, lymphangiogenesis, the formation of new lymphatic vessels may play a role in lymphatic dissemination (Skobe, Hawighorst *et al.* 2001; Stacker, Caesar *et al.* 2001; Beasley, Prevo *et al.* 2002).

Physiological lymphangiogenesis is primarily a developmental process and is uncommon in adult tissues. However, new lymphatic vessels form in adult tissues during follicle maturation and wound healing (Paavonen, Puolakkainen *et al.* 2000; Saaristo, Tammela *et al.* 2006).

Lymphatic vessel growth is also associated with pathological conditions such as tumor metastasis and inflammation in different types of tumors (Karpanen and Alitalo 2008). Animal models suggest that lymphangiogenesis occurs in malignancy and that inhibiting this

process can halt the spread to lymphatics (Makinen, Jussila *et al.* 2001; Mandriota, Jussila *et al.* 2001; Shimizu, Kubo *et al.* 2004). However, tumour cell invasion of pre-existing lymphatics at the tumour margin can also occur (Jackson, Prevo *et al.* 2001; Pepper 2001). Thus, regional lymph nodes are the first site to develop metastases, either draining via pre-existing afferent lymphatic vessels or via newly formed lymphatic capillaries (Skobe, Hawighorst *et al.* 2001; Stacker, Achen *et al.* 2002).

In particular, the incidence of positive lymph nodes in patients with early stage ovarian cancer is 5.1–15% (Cass, Li *et al.* 2001), but lymphatic dissemination to the pelvic and para-aortic lymph nodes is common in an advanced-stage disease (50% of patients have positive lymph nodes) (Plentl and Friedman 1971; Chen and Lee 1983; Burghardt, Pickel *et al.* 1986). For this reason, the lymph nodes status is currently the most valuable prognostic factor for patients with early-stage ovarian tumors confined to the ovary (Maggioni, Benedetti Panici *et al.* 2006; Yavuzcan, Baloglu *et al.* 2009), as tumor metastasis to regional (sentinel) lymph nodes often represents the first step of tumor dissemination and serves as a major prognostic indicator for the progression of human cancers (Tobler and Detmar 2006).

Over the past 2 decades, members of the Vascular Endothelial Growth Factor (VEGF) family have been shown to be essential regulators of lymphangiogenesis (Figure 1.1) (Lohela, Bry *et al.* 2009). In particular, the main lymphangiogenic factor in both physiological and pathological settings is VEGFC (Joukov, Pajusola *et al.* 1996; Karkkainen, Haiko *et al.* 2004). VEGFD has similar properties, but its role as an endogenous regulator of lymphangiogenesis is less clear (Achen, McColl *et al.* 2005).

Although VEGFC and VEGFD, acting through VEGFR3 (Flt4), the first lymphatic-specific growth factor receptor identified (Kaipainen, Korhonen *et al.* 1995), and, to some extent, VEGFR2, are the key growth factors that can directly stimulate the lymphatic endothelium, other growth factors have been implicated in lymphangiogenesis. Both VEGFA and VEGFE

have been shown to promote the growth of lymphatic vessels, which express low levels of VEGFR2 (Nagy, Vasile *et al.* 2002; Saaristo, Veikkola *et al.* 2002; Wirzenius, Tammela *et al.* 2007). In addition, fibroblast growth factor-2, insulin-like growth factor-1 and -2, hepatocyte growth factor, lymphotoxin, and platelet-derived growth factor-B have been shown to induce lymphangiogenesis in experimental models (Cueni and Detmar 2006; Mounzer, Svendsen *et al.* 2010).

The Angiopoietin 1 (Ang1) receptor Tyrosine kinase with immunoglobulin-like and EGF-like domain 2 (Tie2) is expressed in cultured lymphatic endothelial cells (LECs) and in lymphatic vessels *in vivo* (Kriehuber, Breiteneder-Geleff *et al.* 2001; Makinen, Veikkola *et al.* 2001; Morisada, Oike *et al.* 2005; Tammela, Saaristo *et al.* 2005; Kim, Cho *et al.* 2007).

Analysis of gene-targeted mice has shown that Angiopoietin 2 (Ang2) is essential for the proper patterning of lymphatic vessels, whereas Ang1 is able to rescue the lymphatic phenotype, suggesting that both ligands act as receptor agonists in LECs (Morisada, Oike *et al.* 2005; Tammela, Saaristo *et al.* 2005; Kim, Cho *et al.* 2007).

### 1.3 Vascular Endothelial Growth Factor C (VEGFC)

The expression of several growth factors and their cognate receptors determines the aggressive phenotype of cancer cells and regulates tumor invasion and metastasis (Avraham, Park *et al.* 2000). In particular, the expression of vascular endothelial growth factor C (VEGFC), the main promoter of lymphatic vessel formation, is considered essential for the spread of tumor cells to lymph nodes (Skobe, Hawighorst *et al.* 2001; Stacker, Achen *et al.* 2002).

VEGFC is a member of the VEGF family of vascular growth factors, which comprises VEGFA, B, C, and D and Orf virus VEGFs (or VEGFE) (Figure 1.2) (Eriksson and Alitalo 1999; Ferrara 1999).

The secreted glycoprotein VEGFC was first isolated as the cognate ligand of VEGFR3 by Alitalo and co-workers (Joukov, Pajusola *et al.* 1996) and was associated with the broader VEGF family of receptors and growth factors (Achen, Clauss *et al.* 1995; Achen, Gad *et al.* 1997; Achen and Stacker 1998; Ferrara and Alitalo 1999), that play a major role in the growth and development of blood vessels. VEGFC subsequently became the first defined lymphangiogenic growth factor (Jeltsch, Kaipainen *et al.* 1997).

*1.3.1 VEGFC - Gene structure*

VEGFC is comprised of over 40 kilobase pairs of genomic DNA and its gene structure consists of seven exons, which all contain coding sequences. The exon structure of VEGFC resembles that of the other VEGF family members, particularly in exons 3 and 4 encoding the core growth factor domain, which contains the eight cysteine residues (Figure 1.3) and the signature sequence PXCVXXXRCXGCC conserved in all Platelet Derived Growth Factor (PDGF)/VEGF family members. Analysis of the distribution of the various motifs encoded by human VEGFC gene shows that the signal sequence and the first residues of the N-terminal propeptide are encoded by exon 1 (Figure 1.3). The second exon encodes the carboxyl-terminal part of the N-terminal peptide and the amino terminus of the VEGF homology domain. The region encoding the 21-kDa form of VEGFC (Joukov, Sorsa *et al.* 1997) after proteolytic processing of both the N and C termini is marked black in Figure 1.3. Exon 4 encodes the sequence for the major proteolytic cleavage site of the VEGFC precursor between the VEGF homology domain and the C-terminal propeptide (Joukov, Sorsa *et al.* 1997). Notably, in contrast with the other VEGF genes, exon 4 contains a 24-amino acid C-terminal extension after the last cysteine residues conserved in the VEGF homology domain. The most variable parts of these genes are the regions encoded by the sixth and seventh exons, which are alternatively spliced in all other members except VEGFC. A short fifth exon is present in

all splicing variants of the other genes, but VEGFC appears to lack such an exon. Exons 5 and 7 encode cysteine-rich motifs of the type $C_6C_{10}CRC$, and exon 6 encodes additional $C_{10}CXCXC$ motifs typical of a silk protein (Tischer, Mitchell *et al.* 1991). A putative alternatively spliced rare RNA form lacking exon 4 was identified in human fibrosarcoma cells (Chilov, Kukk *et al.* 1997), and a major transcription start site was located in the human VEGFC gene 523 base pairs upstream of the translation initiation codon (Chilov, Kukk *et al.* 1997). The upstream promoter sequences contain conserved putative binding sites for Specificity Protein 1 (Sp-1) (Pugh and Tjian 1990), Activating Protein 2 (AP-2) (Imagawa, Chiu *et al.* 1987; Mitchell, Wang *et al.* 1987; Gille, Swerlick *et al.* 1997), and Nuclear factor kappa light polypeptide gene enhancer in B cells (NF-kB) (Lenardo and Baltimore 1989; Baeuerle and Baltimore 1996) transcription factors but no Thymine Adenine Thymine Adenine (TATA) box.

### *1.3.2 VEGFC - Protein*

VEGFC is synthesized as a proprotein (Figures 1.4 and 1.5) that is 30% identical in amino acid sequence to $VEGF_{165}$ (Joukov, Pajusola *et al.* 1996; Joukov, Sorsa *et al.* 1997). Nascent VEGFC consists of a signal sequence, an N-terminal extension, the VEGF homology domain (VHD), and a C-terminal extension that has cysteine-rich sequences resembling insect silk proteins (Li and Eriksson 2001). After the signal sequence has been removed, two VEGFC precursors are held together by intermolecular disulfide bonds to form an antiparallel homodimer. Subsequently, this dimer undergoes a series of proteolytic processes that increase the protein binding affinity to VEGFR3 and VEGFR2 (Figure 1.5) (Joukov, Sorsa *et al.* 1997). Firstly, VEGFC precursor is divided between Arg227 and Ser228 into nearly equal halves, a N-terminal (~31 kDa) and a cysteine-rich C-terminal (~29 kDa) polypeptides, by furin convertase (Siegfried, Basak *et al.* 2003) or plasmin (McColl, Baldwin *et al.* 2003).

Then, a proteolytic cleavage between the growth factor domain and the silk domain activates VEGFC binding to VEGFR3 and the N-terminal propeptide is removed extracellularly (Joukov, Sorsa *et al.* 1997). Finally, mature VEGFC is given rise and it is composed of two VEGF homology domains bound by non-covalent interactions (Figure 1.5) (Joukov, Sorsa *et al.* 1997).

*1.3.3 Lymphatic versus vascular endothelial response to VEGFC*

VEGFC binds to VEGFR3 and VEGFR2 cell-surface-receptor tyrosine kinases that are predominantly expressed on lymphatic and vascular endothelial cells, respectively (Kaipainen, Korhonen *et al.* 1995). Lymphatic endothelium also expresses VEGFR2, which might contribute to signalling for mitogenesis (Stacker, Achen *et al.* 2002). In particular, the secreted 31 kD VEGFC protein predominantly activates VEGFR3 whereas the mature, fully processed 21 kD form additionally activates VEGFR2 (Joukov, Sorsa *et al.* 1997).

Depending on the degree of proteolytic processing of VEGFC precursor, and on the expression of its receptors in the lymphatic versus blood endothelial cells of the target tissue, the lymphangiogenic versus angiogenic responses to VEGFC are induced. Signalling via VEGFR3 alone is sufficient for the lymphangiogenic signals, since VEGFC C156S, which only activates VEGFR3 but not VEGFR2, induced a similar phenotype (Veikkola, Jussila *et al.* 2001). VEGFC/VEGFR3 interaction (Kaipainen, Korhonen *et al.* 1995; Joukov, Sorsa *et al.* 1997) induces growth, migration, and survival of primary lymphatic endothelial cells (Makinen, Veikkola *et al.* 2001).

VEGFC also has synergistic effects with VEGFA during the induction of angiogenesis, and this effect is more prominent in cells that express both of its receptors (Pepper, Mandriota *et al.* 1998).

Like VEGFA, VEGFC stimulates the migration of endothelial cells and induces vascular permeability and endothelial-cell proliferation (Joukov, Pajusola *et al.* 1996; Joukov, Sorsa *et al.* 1997).

VEGFR3 deficient embryos succumb due to vascular defects (Dumont, Jussila *et al.* 1998). In addition, VEGFC affects early vascular development in the chorioallantoic membrane before the emergence of the lymphatics. Finally, angiogenesis is enhanced in the ischemic limb and in the cornea by VEGFC (Cao, Linden *et al.* 1998; Witzenbichler, Asahara *et al.* 1998; Marconcini, Marchio *et al.* 1999).

The VEGFRs have a similar organization; an extracellular domain composed of immunoglobulin (Ig)-like loops for ligand-binding, a transmembrane domain, a cytoplasmic juxtamembrane domain, a catalytic tyrosine kinase domain split by a kinase insertion domain and a C-terminal tail (Figure 1.4) (Koch, Tugues *et al.* 2011). Previous studies have indicated that VEGFC binding requires Ig-Loops 1 and 2 in VEGFR3 (Jeltsch, Karpanen *et al.* 2006), whereas binding to VEGFR2 involves Loops 2 and 3 (Leppanen, Prota *et al.* 2010). Since VEGFC can bind to more than one receptor, this allows for the potential formation of receptor hetero- and homodimers (Dixelius, Makinen *et al.* 2003; Nilsson, Bahram *et al.* 2010). Indeed, VEGFC can induce the formation and activation of VEGFR3 homodimers and VEGFR2/VEGFR3 heterodimers, but not VEGFR2 homodimers, that can be induced by VEGFA (Nilsson, Bahram *et al.* 2010).

### *1.3.4 Physiological and pathological role of VEGFC*

VEGFC is produced by different tissues during embryogenesis (e.g. lung, heart and skin) and adult life (e.g. macrophages) (Figure 1.6).

It has a role in the development of the lymphatic vessels in embryos, since deletion of the VEGFC gene results in embryonic lethality because of failure of lymphatic vessel

development. Furthermore, a paracrine expression pattern is seen between VEGFC and VEGFR3 at sites in which the first lymphatic sprouts occur (Kukk, Lymboussaki *et al.* 1996). In the adult, the lymphatic vasculature is rather quiescent, and survival of lymphatic endothelial cells is no longer dependent on VEGFR3 signalling (Karpanen, Wirzenius *et al.* 2006). Under normal physiological conditions the *de novo* formation of lymphatic vasculature is restricted to the endometrium during pregnancy.

However, in several pathological situations, including wound healing, tissue repair and organ transplant rejection new lymphatic vasculature is generated.

Lymphatic vessels have a major role in some diseases such as lymphedema and, in particular, cancer.

Lymphedema is the accumulation of fluid in the intersititum of the tissues and can be caused by a number of factors relating to lymphatic function (Baldwin, Stacker *et al.* 2002). In particular, in primary lymphedema patients, VEGFR3 has been shown to contain mutations which alter the function of the receptor, including autophosphorylation, and prevented signal transduction after ligand stimulation, thus stopping the activation of downstream effector genes (Ferrell, Levinson *et al.* 1998; Irrthum, Karkkainen *et al.* 2000; Karkkainen, Ferrell *et al.* 2000). Furthermore, both *Vegfc* alleles are required for normal lymphatic development. In *Vegfc*$^{+/-}$ mice it was observed that VEGFC haploinsufficiency resulted in lymphedema in adult mice (Karkkainen, Ferrell *et al.* 2000).

### *1.3.5 VEGFC in cancer*

Regarding the role of VEGFC in cancer, tumor cells disseminate into the lymphatics via invasion into pre-existing lymphatic vessels in the surrounding tissue or by invasion of intratumoral lymphatics (Stacker, Achen *et al.* 2002; Achen, McColl *et al.* 2005). Both peritumoral and intratumoral lymphangiogenesis increase the number of the lymphatic vessels

around the primary tumor and increases contact between the lymphatic endothelial cells and tumor cells (Ji 2007). The microenvironment of the tumor, the stroma, and inflammatory cells produce multiple lymphangiogenic growth factors that may stimulate tumor-induced lymphangiogenesis (Joukov, Pajusola et al. 1996). The expression of VEGFC correlates with lymphatic metastasis in multiple human cancers, including prostate, gastric, thyroid, colorectal, esophageal, and lung carcinoma (Stacker, Achen *et al.* 2002; Stacker, Baldwin *et al.* 2002; Achen and Stacker 2008).

VEGFC overexpression in tumors increases intratumoral lymphangiogenesis, which has been correlated with enhanced metastasis to regional lymph nodes and distant sites (Karpanen, Egeblad *et al.* 2001; Mandriota, Jussila *et al.* 2001; Skobe, Hawighorst *et al.* 2001). VEGFC has been reported to induce hyperplasia and dilation of tumor lymphatic vessels (Mandriota, Jussila *et al.* 2001; Skobe, Hawighorst *et al.* 2001), increase in lymphatic density (Dadras, Paul *et al.* 2003), increase in flow rates of lymph (Hoshida, Isaka *et al.* 2006; Harrell, Iritani *et al.* 2007), and even to induce metastasis to lymph nodes in previously non-metastatic tumor cells. Interestingly, lymph node lymphangiogenesis has been observed even before the onset of metastasis. Recent studies have demonstrated that lymphangiogenesis occurs not only at the primary site, but also within draining lymph nodes, prior to tumor cells arriving in the lymph node (Qian, Berghuis *et al.* 2006; Harrell, Iritani *et al.* 2007; Hirakawa, Brown *et al.* 2007; Van den Eynden, Vandenberghe *et al.* 2007).

Tumor-released VEGFC may travel via the lymphatics to draining lymph nodes where it induces lymphangiogenesis within the lymph node and expansion of the lymphatic network (Rinderknecht and Detmar 2008). Thus, lymphangiogenic growth factors derived from the primary tumor prepare the lymph nodes for future metastasis (Qian, Berghuis *et al.* 2006; Hirakawa, Brown *et al.* 2007; Rinderknecht and Detmar 2008); the arrival of tumor cells to the lymph nodes further enhances VEGFC-induced lymphangiogenesis.

The lymphatic system may also directly facilitate tumor cell recruitment into lymphatic vessels. Factors expressed in LECs may facilitate tumor cell invasion, similar to the directed migration of lymphocytes into the lymphatic vessels (Petrova, Makinen *et al.* 2002; Podgrabinska, Braun *et al.* 2002).

The expression of VEGFC has been observed in several tumors, such as breast cancer, cervical cancer, colorectal cancer, gastric cancer, non-small-cell lung cancer and pancreatic cancer (Stacker, Achen *et al.* 2002), while the expression of VEGFR2 and VEGFR3 by cancer cells is still controversial. Indeed, it has been shown that a wide variety of cancer cells such as oral squamoid cancer (Matsuura, Onimaru *et al.* 2009), gallbladder cancer (Chen, Jiang *et al.* 2010), breast cancer (Issa, Le *et al.* 2009) and gastric cancer (Kodama, Kitadai *et al.* 2008) expressed VEGFR3 and VEGFR2, suggesting that the role of VEGFC signaling pathways extends beyond lymphangiogenesis and angiogenesis (Su, Yang *et al.* 2006). On the other hand, it was reported that VEGFR2 and VEGFR3 are localized primarily to intratumoral blood and lymphatic vessels but not on malignant cells in human solid tumors (Smith, Baker *et al.* 2010).

### *1.3.6 VEGFC in ovarian cancer*

The involvement of VEGFC in ovarian cancer progression is still debated. It has been shown that tissue expression of VEGFC is associated with peritoneal and lymph node metastases and matrix metalloprotease-2 (MMP2) expression in ovarian carcinoma patients (Nishida, Yano *et al.* 2004; Ueda, Hung *et al.* 2005; Huang and Sui 2012).

Tissue over-expression of VEGFR3 reflects the aggressiveness of ovarian carcinoma spread and has predictive value for identifying high-risk patients with poor prognosis (Klasa-Mazurkiewicz, Jarzab *et al.* 2011). Recent studies evidenced dysfunctional lymphatic vessels in mesentery and diaphragm of mice transplanted with human ovarian carcinoma cells (Jeon,

Jang *et al.* 2008). However, no significant relation between lymphatic microvessel density and overall survival or disease-free survival in patients was evidenced (Schoppmann, Horvat *et al.* 2002; Sundar, Zhang *et al.* 2006).

Despite all these evidences, the biological significance of VEGFC in ovarian cancer progression remains uncertain.

## 1.4 Ovarian cancer therapy

### *1.4.1 Cytoreductive surgery*

Ovarian cancer is associated with the highest case-fatality ratio of all gynecologic cancers, reflecting a propensity for early peritoneal dissemination, and advanced disease at clinical diagnosis. Thus, surgery continues to have a major role in the management of patients with ovarian cancer, both for accurate staging and for removal of bulk disease (cytoreduction).

The surgical staging included peritoneal washings and aspiration of ascites for cytologic analysis, hysterectomy and bilateral salpingo-oophorectomy, pelvic and para-aortic lymph node sampling, diaphragmatic biopsies, omentectomy, biopsy of suspicious lesions and random biopsies through the peritoneum. Such a comprehensive laparotomy is essential since postoperative treatment is based on clinicopathologic features documented at surgery. In addition to accurate staging, the initial surgery is important to remove as much disease as possible (cytoreduction). Optimal cytoreduction is considered to have been accomplished when no tumor nodule greater than 1 cm remains after surgery (Ozols 2003).

Numerous studies have demonstrated that the bulk of residual disease after surgery correlates with prognosis (Ozols, Rubin *et al.* 2000). Moreover, the timing of cytoreduction is becoming a critical issue. Cytoreduction at the time of diagnosis is a standard practice, although only approximately 50% of patients can be effectively cytoreduced at the initial laparotomy. Patients in whom the initial cytoreduction was not successful, receive three cycles of

chemotherapy, and then if they have a response to treatment, undergo another attempt at cytoreduction (interval cytoreduction) followed by additional chemotherapy (van der Burg, van Lent *et al.* 1995). Those patients undergoing interval debulking surgery had a statistically significant improvement, both in time to progression and in median survival (6 months).

An alternative approach to initial cytoreduction consists of neoadjuvant chemotherapy in patients with advanced-stage disease.

Ovarian cancer is frequently considered to be a chronic disease, and while cure remains the ultimate goal of cancer therapy, prolongation of survival, together with palliation of symptoms, is a clinically meaningful accomplishment.

### *1.4.2 Chemotherapy*

The 2010 consensus meeting defined standard of care in ovarian cancer. The recommended treatment paradigm for advanced disease has been debulking surgery followed by platinum-based chemotherapy, initially cisplatin-based and more recently with carboplatin/paclitaxel (Stuart, Kitchener *et al.* 2011).

Platinum-derivatives were introduced as chemotherapeutic agents in 1960s. Cisplatin was the first platinum-based drug developed, before carboplatin, a drug with fewer and less severe side effects introduced in the 1980s, and oxaliplatin.

Cisplatin is a cytotoxic drug, classified as alkylating agent whose mechanism of action is the formation of a platinum complex interacting with DNA. The formation of DNA adducts, primarily intrastrand crosslink adducts, activates several signal transduction pathways and culminates in the activation of apoptosis.

Paclitaxel was isolated in 1967 from the bark of the Pacific yew tree, *Taxus brevifolia.* Together with docetaxel, it forms the drug category of the taxanes. Paclitaxel is a mitotic inhibitor that stabilizes microtubules (tubulin dimers) and as a result, interferes with the

normal breakdown of microtubules during cell division because chromosomes are thus unable to achieve a metaphase spindle configuration. This blocks progression of mitosis, and prolonged activation of the mitotic checkpoint triggers apoptosis or reversion to the G-phase of the cell cycle without cell division.

The consensus meeting 2010 acknowledged that acceptable variations to the recommended therapies existed, but their use must be supported by at least one trial demonstrating superiority or noninferiority. Initially, improvements to standard platinum/taxane chemotherapy were seen through the addition of a third chemotherapeutic agent with demonstrable activity in the relapsed setting. First-line trials investigated the addition of drugs, including pegylated liposomal doxorubicin (PLD), topotecan and gemcitabine (Bookman, Brady *et al.* 2009; Bolis, Scarfone *et al.* 2010; du Bois, Herrstedt *et al.* 2010; Hoskins, Vergote *et al.* 2010)), but unfortunately demonstrated only increased toxicity without survival benefits.

Pegylated liposomal doxorubicin is a new available formulation of doxorubicin, an anthracycline antibiotic intercalating DNA, that is encapsulated in a pegylated liposome. The size of the liposomes prevents them from entering tissues with tight capillary junctions, such as the heart and gastrointestinal tract and in contrast to other nanoparticles, the pegylation allows these molecules to be protected from destruction by reticuloendothelial system.

Topotecan is a derivative of camptothecin that inhibits topoisomerase I, thus blocking cell cycle S-phase.

Gemcitabine is a nucleoside analog of deoxycytidine that replaces cytidine, during DNA replication, thus blocking DNA synthesis and inducing apoptosis.

Recently, trabectedin demonstrated efficacy as second-line treatment in platinum-sensitive ovarian cancer. The mechanism of action is binding the DNA minor groove and interfering with cell division, gene transcription mechanisms and DNA repair (Colombo 2011).

A more successful strategy seems likely to be the addition of targeted therapies to chemotherapy.

*1.4.3 Targeted therapies*

During the least years the search for new cancer therapies has been addressed to the development of specific target drugs that block cancer growth and dissemination by interfering with multiple molecular targets such as growth factor receptors, signal transduction pathways, cell cycle regulators, and angiogenic mechanisms specifically expressed by tumor cells or tumor environment. For this reason, these therapies are very effective on cancer cells and less harmful to normal cells.

Two of the major molecular targeted agents applied to ovarian cancer treatments are inhibitors of angiogenesis (chapter 1.5) and the PARP inhibitor Olaparib, a potent oral inhibitor of poly(adenosine diphosphate [ADP]–ribose) polymerase that induces synthetic lethality in BRCA1/2-deficient tumor cells (Evers, Drost *et al.* 2008; Rottenberg, Jaspers *et al.* 2008).

**1.5 Inhibitors of angiogenesis**

Angiogenesis is a complex process similar to the above described lymphangiogenesis. Angiogenesis is the formation of new blood vessels from existing ones: as described for lymphatic endothelial cells, vascular endothelial cells proliferate, migrate and penetrate host stroma, generating capillary sprouts.

In the adult, physiological angiogenesis is involved in normal processes. Examples of physiological angiogenesis are in the formation of the uterus lining prior to menstruation in females and of the placenta after fertilization, and wound healing (Carmeliet and Jain 2000).

Angiogenesis is a critical component for the growth and metastasis of cancer (Ellis and Hicklin 2008) and it is one of the hallmarks of cancers that have been extensively studied (Hanahan and Weinberg 2011).

Angiogenic factors control a discrete step called the "angiogenic switch", required for the induction of tumor vasculature (Hanahan and Folkman 1996). It has been widely recognized and shown that the angiogenic switch occurs when a tumor reaches approximately 1-2 $mm^2$, a critical size for the progression of its growth (Folkman 1995). Angiogenesis is tightly controlled by an angiogenic balance between molecules that promote angiogenesis (e.g., VEGFA, fibroblast growth factor) and those that inhibit angiogenesis (e.g., thrombospondin-1) (Figure 1.7) (Hanahan and Folkman 1996).

During pathological angiogenesis the tight balance and control of factors which regulated the process are lost and tumor vessels fail to remain quiescent (Bergers and Benjamin 2003).

Adequate tumor blood supply plays an important role in controlling the invasion of the metastatic cells in secondary sites. Indeed, experimental evidence showed that tumor vascularization correlates with high malignancy and bad prognosis, and that elevated levels of angiogenic factors, for example vascular endothelial growth factor (VEGF) and basic-fibroblast growth factor (bFGF/FGF-2), are associated with tumor growth (Giavazzi, Sennino *et al.* 2003; Dowlati, Gray *et al.* 2008; Ghosh, Sullivan *et al.* 2008).

Angiogenesis is important also for supporting tumor growth, as blood supply provides the tumor's main access to nutrients and oxygen at both primary and secondary sites.

VEGFA expression is higher in ovarian cancer tumors than in normal ovarian tissue or benign ovarian pathologies (Manenti, Riccardi *et al.* 2005).

Angiogenesis is more studied than lymphangiogenesis, thus a greater number of inhibitors is now available. Nevertheless, some inhibitors are able to target both pathways, for example, agents targeting members of the VEGF family.

In order to inhibit the VEGF pathway, there are two primary strategies: (1) inhibition of the VEGF ligand with antibodies or soluble receptors and (2) inhibition of the VEGF receptors (VEGFR) with tyrosine kinase inhibitors (TKIs), or receptor antibodies (Figure 1.8).

The most investigated VEGF inhibitor is a humanized monoclonal antibody that binds the VEGF ligand, known as bevacizumab (Avastin). It has recently been approved in Europe as a first-line treatment of advanced ovarian cancer in combination with chemotherapy, as several phase III studies showed that bevacizumab is active in ovarian cancer (Aghajanian, Finkler *et al.* 2011; Burger, Brady *et al.* 2011; Perren, Swart *et al.* 2011; Pujade-Lauraine, Hilpert *et al.* 2012).

*1.5.1 Inhibitors of lymphangiogenesis*

Several preclinical studies have investigated whether specific inhibition of the VEGFC/VEGFR3 pathway might inhibit cancer metastasis to lymph nodes and beyond. Inhibition of VEGFR3 activity by anti-VEGFR3 antibodies reduced the incidence of lymph node and organ metastasis in a mouse breast carcinoma model (Roberts, Kloos *et al.* 2006). As VEGFR3 may also have a role in tumor angiogenesis, the use of a VEGFR3-specific antibody has been shown to reduce primary tumor growth (Laakkonen, Waltari *et al.* 2007). Furthermore, inhibition of tumor cell VEGFC expression by stably transfected small interfering RNA reduced lymphangiogenesis, lymph node, and lung metastasis of murine mammary cancers (Chen, Varney *et al.* 2005). As an alternative approach, soluble VEGFR3 fusion protein (VEGFC/D-trap) has been shown to inhibit VEGFC-induced tumor lymphangiogenesis and metastatic spread in a breast cancer xenotransplant model (Karpanen, Egeblad *et al.* 2001). Overexpression of soluble VEGFR3 by lung cancer cells also reduced the number of intratumoral lymphatic vessels and the incidence of metastasis to the draining lymph nodes (He, Kozaki *et al.* 2002). Ectopic overexpression of soluble VEGFR3 in an immunocompetent rat mammary tumor model suppressed metastasis formation in lymph nodes and lungs (Krishnan, Kirkin *et al.* 2003). More recently, a gene therapy approach using recombinant adeno-associated virus expressing soluble VEGFR3 resulted in blockade of

lymph node metastasis in a melanoma model in mice (Lin, Lalani *et al.* 2005). Furthermore, a small molecule with high selectivity for VEGFR3, SAR131675, has been described to reduce lymphangiogenesis, angiogenesis, and tumor-associated macrophages (TAM) infiltration and consequently reduce tumor growth and metastasis in preclinical models (Alam, Blanc *et al.* 2012).

The double inhibition of VEGFR2 and VEGFR3 by combining the anti-VEGFR2 and anti-VEGFR3 antibodies more potently decreased lymph node and lung metastases than each antibody alone in a mouse breast carcinoma model (Roberts, Kloos *et al.* 2006), suggesting that a combination therapy with antiangiogenic agents may be a particularly promising approach for controlling metastases (Roberts, Kloos *et al.* 2006).

In particular, preclinical data in ovarian cancer suggested that inhibition of VEGFR1, VEGFR2 and VEGFR3 by gene therapy significantly reduced tumor size (Sallinen, Anttila *et al.* 2009; Sallinen, Anttila *et al.* 2011; Sopo, Anttila *et al.* 2012).

A number of small molecule kinase inhibitors of VEGFR2 have been found to also inhibit VEGFR3 signal transduction, including sunitinib, cediranib, sorafenib, PTK/ZK, MAZ51 and CEP-7055. These small molecular compounds also affect, however, a number of other tyrosine kinases, and their distinct effects on tumor lymphangiogenesis *in vivo* remain to be investigated.

There are several anti-angiogenic/anti-lymphangiogenic drugs under investigation in ovarian cancer. For example, tyrosine kinase inhibitors targeting VEGFRs and PDGFR (BIBF1120, cediranib, dorafenib, vandetanib and j1-101), an anti-angiopoetin antibody (AMG386) and VEGF-trap (Collinson, Seligmann *et al.* 2012).

### *1.5.2 Cediranib*

Among VEGF receptors tyrosine kinase inhibitors, cediranib is one of the most promising compound.

Cediranib (AZD2171) is an oral, small molecule tyrosine kinase inhibitor that inhibits all the three VEGF receptors (VEGFR1, VEGFR2 and VEGFR3), PDGFR-α/PDGFR-β, FGFR-1 and c-kit.

Cediranib was described effective in reducing lymphatic metastasis, independently of the effect on blood vessels (Padera, Kuo *et al.* 2008), but also blocking VEGFC-induced VEGFR3 activity and lymphangiogenesis in lung cancer (Heckman, Hyngstrom *et al.* 2008).

Cediranib competes for the ATP-binding site within the receptor kinase domain (Heckman, Holopainen *et al.* 2008), inhibiting VEGFC–induced phosphorylation of VEGFR3 and VEGFR2 in primary human endothelial cells. Consequently, a reduced activation of downstream signaling molecules ERK1/2, Akt, and CREB is observed. Additionally, cellular functions associated with VEGFR activation, including proliferation, survival, and migration, are all compromised by cediranib. Interestingly, cellular migration seems to be particularly sensitive to cediranib treatment. Low concentrations of the compound inhibit lymphatic and blood endothelial cell migration, but only slight inhibition of ligand-induced receptor phosphorylation at the same concentration was observed. Furthermore, cediranib compromises the growth of both tumor associated lymphatic and blood vessels. Growth of human non–small cell lung adenocarcinoma tumors in cediranib-treated animals is impaired (Heckman, Holopainen *et al.* 2008).

Cediranib has shown activity on human tumor xenografts. Encouraging preclinical data supported clinical testing in patients with a broad range of advanced cancers.

In the randomized, double-blind NCIC clinical trial BR24 study on advanced non-small-cell lung cancer (NSCLC), the addition of cediranib to carboplatin/paclitaxel resulted in improved response and PFS (Goss, Arnold *et al.* 2010).

In the double-blind, randomized phase III study (HORIZON III) on advanced metastatic colorectal cancer, cediranib activity, in terms of progression-free survival (PFS) and overall survival (OS), was comparable to that of bevacizumab when added to mFOLFOX6. However, the predefined boundary for PFS noninferiority was not met (Schmoll, Cunningham *et al.* 2012).

Cediranib monotherapy was studied in a phase II study in patients with recurrent glioblastoma. Encouraging proportions of radiographic response, 6-month progression-free survival were observed after cediranib treatments (Batchelor, Mulholland *et al.* 2010).

Cediranib monotherapy demonstrated significant evidence of antitumour activity in a randomised phase II study in patients with advanced renal cell carcinoma (Mulders, Hawkins *et al.* 2012).

In a prospective trial of systemic therapy for metastatic alveolar soft part sarcoma, it was observed that cediranib has substantial single-agent activity, producing an objective response rate (ORR) of 35% and a disease control rate of 84% at 24 weeks (Kummar, Allen *et al.* 2013).

In an open-label, phase I study of cediranib in patients with acute myeloid leukemia, cediranib showed preliminary evidence of activity as a monotherapy (Fiedler, Mesters *et al.* 2010).

In particular, in ovarian cancer cediranib has demonstrated widespread activity as monotherapy in two phase II single- agents studies with either platinum-resistant or -sensitive recurrent EOC (Hirte, Vidal *et al.* 2008; Matulonis, Berlin *et al.* 2009). A multi-stage phase III Gynaecologic Cancer InterGroup (GCIG) trial, ICON6, has now completed the recruitment of women with platinum-sensitive relapsed ovarian cancer. ICON6 is evaluating the safety and efficacy of platinum-based chemotherapy alone versus chemotherapy with concurrent and maintenance cediranib for 18 months. The primary outcome measure for stage I was safety: it has demonstrated that is feasible to add cediranib to carboplatin/cisplatin

(DDP) and paclitaxel chemotherapy without major unexpected toxicities (Raja, Griffin *et al.* 2011). Trial completion is expexted in October 2013.

**Aim of the study**

Epithelial ovarian cancer is still a leading cause of cancer death because of difficulties in diagnosis and lack of effective therapies.

Thus there is an ongoing need to identify selective pathways and investigate targets for therapy.

The aim of the study is to investigate the role of VEGFC and VEGFR3 in ovarian cancer invasion and metastasis. It proposes to address such an idea by employing a panel of patient-derived human ovarian carcinoma xenografts spontaneously releasing VEGFC in biological fluids, that reproduces the features of ovarian cancer patients. Furthermore, the effects on tumor growth and metastasis induced by VEGFC are studied on human ovarian carcinoma cell lines infected to over-express VEGFC, directly comparing the wild-type and the VEGFC over-expressing tumors.

Altogether, the aims of this project are to:

- characterize models of human ovarian tumor xenografts growing in the peritoneal cavity and under the bursa of the ovary of immunodeficient mice focusing on their pattern of invasion and metastasis;
- investigate the role of the VEGFC and VEGFR3 axis in ovarian cancer cell growth and invasive phenotype;
- inhibit the VEGFC/VEGFR3 pathway.

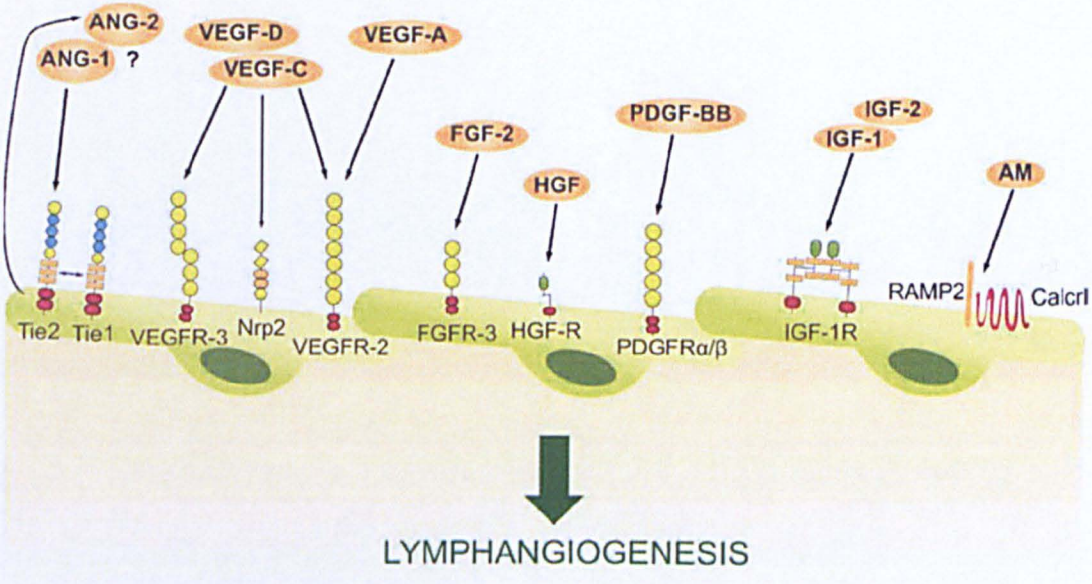


**Figure 1.1 Representation of lymphangiogenic growth factors and their receptors expressed by lymphatic endothelium.** Several vascular endothelial growth factors (VEGFA, VEGFC, VEGFD) promote lymphangiogenesis by activation of VEGF receptors-2 and -3 (VEGFR2, VEGFR3) and neuropilin-2 (Nrp2). Additional lymphatic growth factors include angiopoietin-1 (ANG-1), hepatocyte growth factor (HGF), fibroblast growth factor-2 (FGF-2), insulin-like growth factors (IGF-1, IGF-2), platelet-derived growth factor-BB (PDGF-BB), and adrenomedullin (AM). From Jurisic and Detmar 2009.

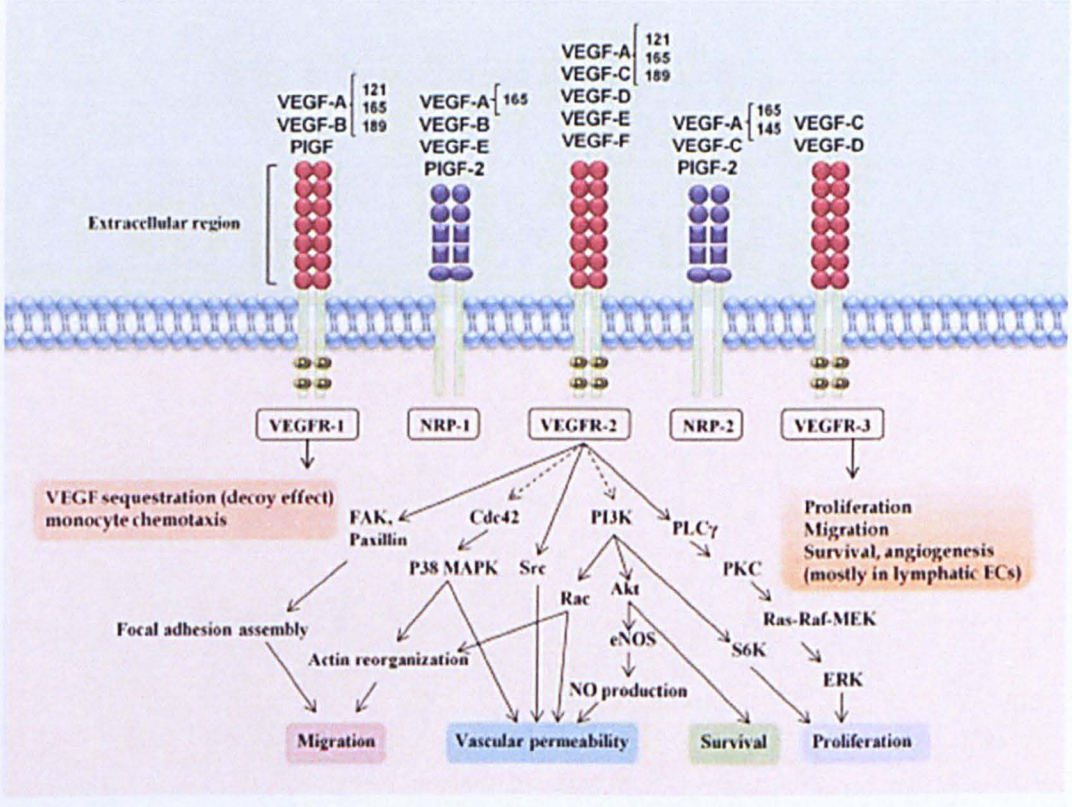


**Figure 1.2 Vascular endothelial growth factor (VEGF) family and their receptors.** VEGF family members bind to specific receptor tyrosine kinases VEGFR1, VEGFR2, and VEGFR3 and, through activating different cascades, exert their various biologic effects. From Masoumi Moghaddam, Amini et al. 2012.

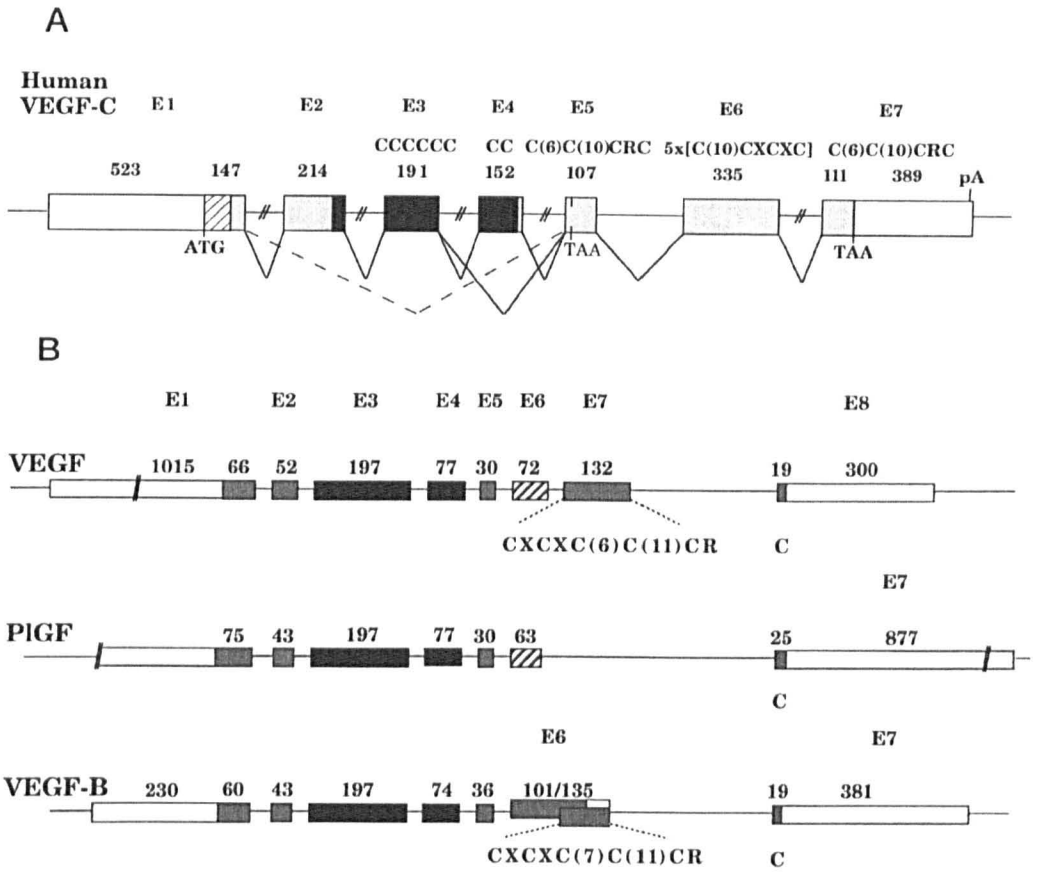


**Figure 1.3 Exon-intron organization of human VEGFC gene and other members of the VEGF family.** (A) The exons are shown as boxes and their lengths in bp are indicated. White boxes, noncoding portions; hatched boxes, signal sequences; grey boxes: sequences encoding C- and N-terminal propeptides that are removed during successive steps of proteolytic processing; black boxes, sequences encoding the fully processed VEGFC polypeptide. The cysteine motifs encoded by the different exons are indicated above the boxes. The translational start (ATG) and stop (TAA) codons are marked in boldface type, as is the polyadenylation signal (pA). The TAA stop codon in the 5th exon refers to the alternatively spliced mRNA form lacking exon 4, which is also marked. The putative mRNA form lacking exons 2–4 is indicated with the broken line. (B) The structures of the VEGF, VEGFB, and PlGF genes are shown for comparison. Black boxes indicate the cooling region, and the striped box indicates the exon encoding part of the heparin-binding region. The bars are drawn to scale. Modified from Chilov, Kukk et al. 1997.

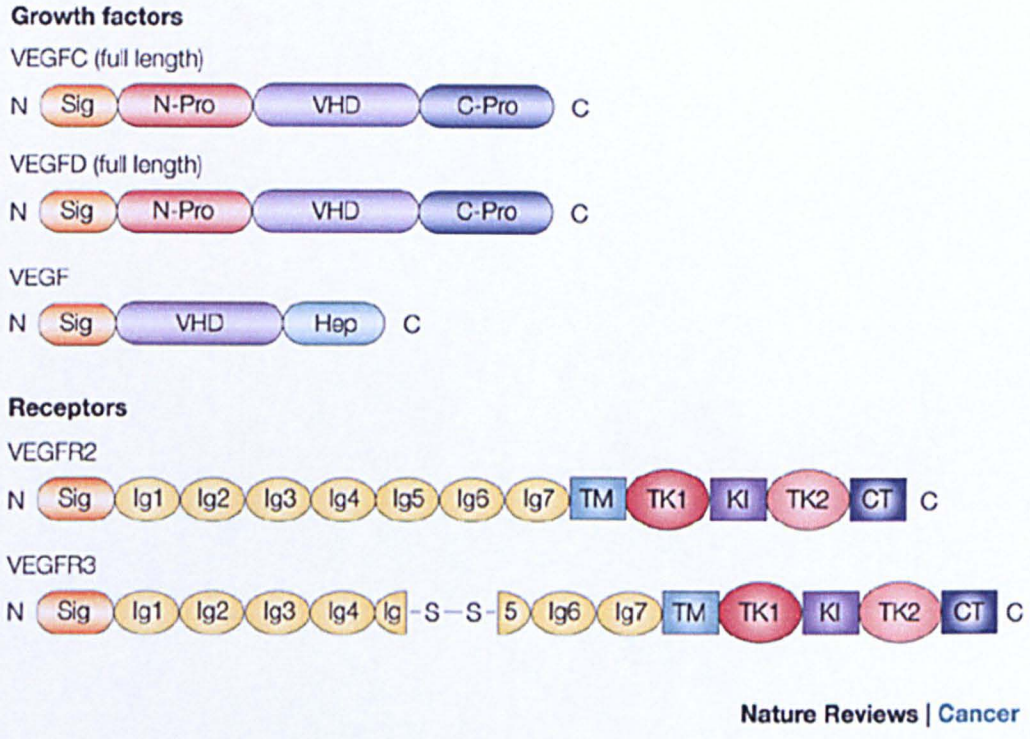


**Figure 1.4 The protein structure of growth factors and receptors associated with lymphangiogenesis.** Two members of the vascular endothelial growth factor (VEGF) family (VEGFC and VEGFD) are implicated in lymphangiogenesis — VEGF is shown for comparison. These are secreted homodimeric polypeptides that contain a hydrophobic amino-terminal signal sequence for protein secretion (Sig). All VEGF family members contain a central region that is termed the VEGF homology domain (VHD) and contains a cysteine-rich motif. A subfamily of these growth factors contains VEGFC and VEGFD, defined by their ability to bind VEGFR3 and the presence of amino- and carboxy-terminal propeptides (N-Pro and C-Pro). The receptors for VEGFC and VEGFD are VEGFR2 and VEGFR3, both of which can be expressed on lymphatic endothelial cells. These receptors are closely related in structure, consisting of an extracellular domain with seven immunoglobulin-like domains (Ig), a transmembrane domain (TM), a split tyrosine kinase domain (TK) with a kinase insert sequence (KI) and a cytoplasmic tail (CT) at the carboxyl terminus. The fifth Ig-like domain of VEGFR3 is proteolytically processed and the subunits are held together by a disulphide bond (-S-S-). From Stacker, Achen et al. 2002.

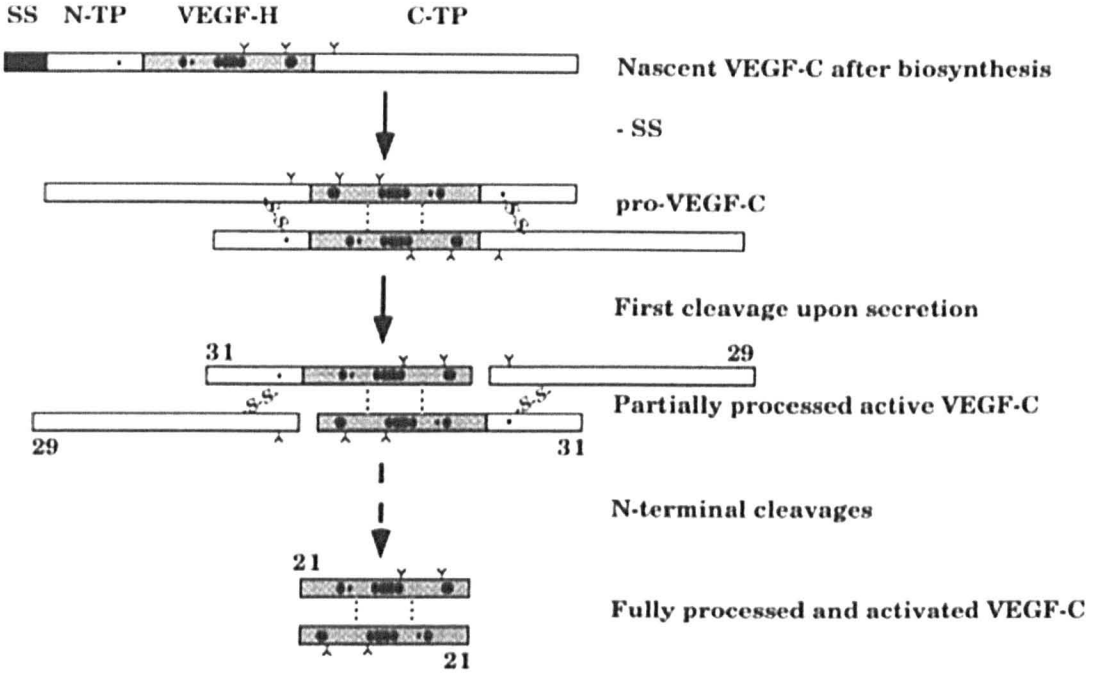


**Figure 1.5 Schematic model of the proteolytic processing of VEGFC.** Schematic model of the proteolytic processing of vascular endothelial growth factor C (VEGFC). The regions of the nascent VEGF-C precursor polypeptide are the signal sequence (SS, *black box*), N-terminal propeptide (N-TP), VEGF-homology domain (VEGF-H, *gray box*) and C-terminal propeptide (C-TP). Putative sites of N-linked glycosylation (Y) are shown; *black ovals* mark the Cys residues conserved among the platelet-derived growth factor (PDGF)/VEGF family of growth factors; the repeated cysteine residue motifs in the C-terminal propeptide are not marked for clarity. *Numbers* indicate molecular masses (kD) of the corresponding polypeptides in reducing conditions. Disulfide bonds joining the N- and C-terminal propeptides are marked as -S-S-; noncovalent bonds as *dotted lanes.* It is currently not known how the N-terminal cleavages are regulated and how much of the VEGF-C present in tissues is partially versus completely processed. Some intermediate forms are also omitted to simplify the scheme. From Enholm, Jussila et al. 1998.

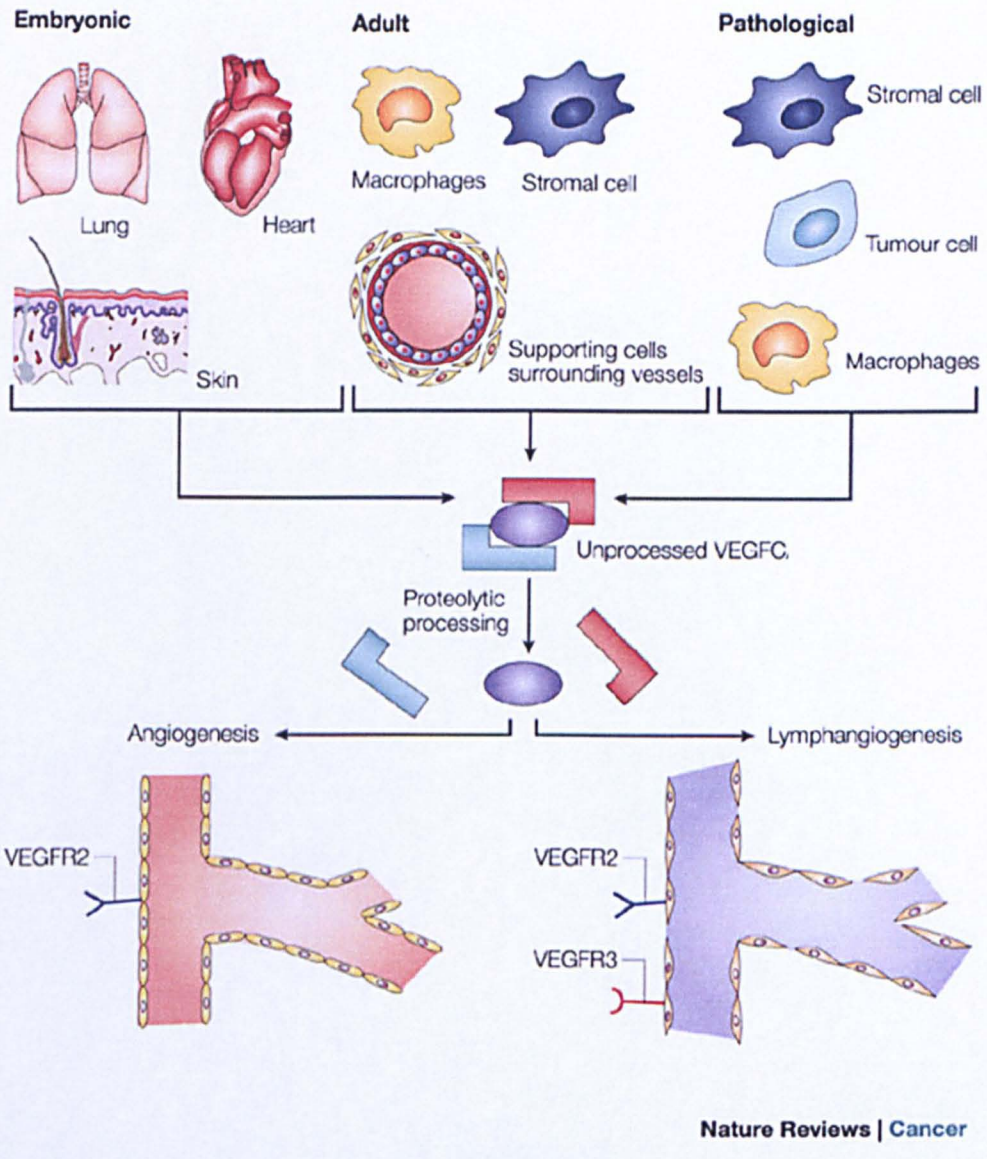


**Figure 1.6 Mode of action of lymphangiogenic growth factors.** The lymphangiogenic growth factor vascular endothelial growth factor C (VEGFC) is produced by a range of cells and tissues during embryogenesis, adult life and certain pathologies, including cancer. The full-length growth factor is processed by as yet uncharacterized proteases that cleave the amino- and carboxy-terminal propeptides (light blue and red L-shapes, respectively) from the VEGF homology domain (VHD) to generate a mature form that consists of dimers of the VHD (purple oval) that bind the receptors VEGFR2 and VEGFR3 with high affinity. Activation of VEGFR3 induces lymphangiogenesis, whereas activation of VEGFR2 is thought to drive angiogenesis. From Stacker, Achen et al. 2002.

## Angiogenesis regulation

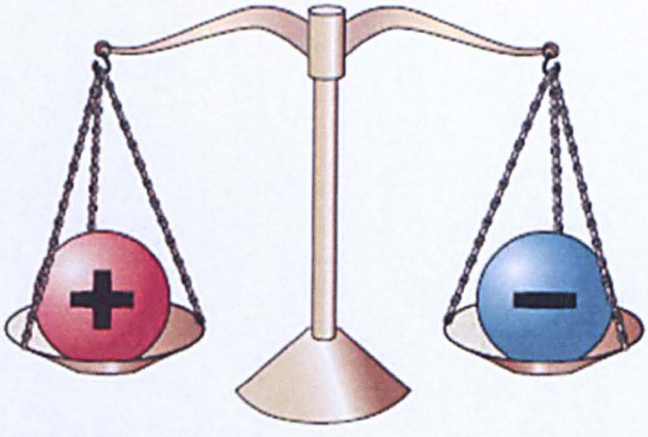

**ACTIVATORS**
Angiogenin
Angiopoietin 1
Basic fibroblast growth factor
Hepatocyte growth factor
Interleukin 8
Placental growth factor
Vascular endothelial growth factor

**INHIBITORS**
Angiostatin
Endostatin
Interferon
Interleukin-12
Tissue-inhibitor of metalloproteinase 1
Thrombospondin 1

**Figure 1.7 Angiogenesis is a balance between pro- and anti-angiogenic factors.** In most tissues, angiogenesis is held in check by tightly regulated amounts of pro- (activators) and anti- (inhibitors) angiogenic factors . From Zetter 2008.

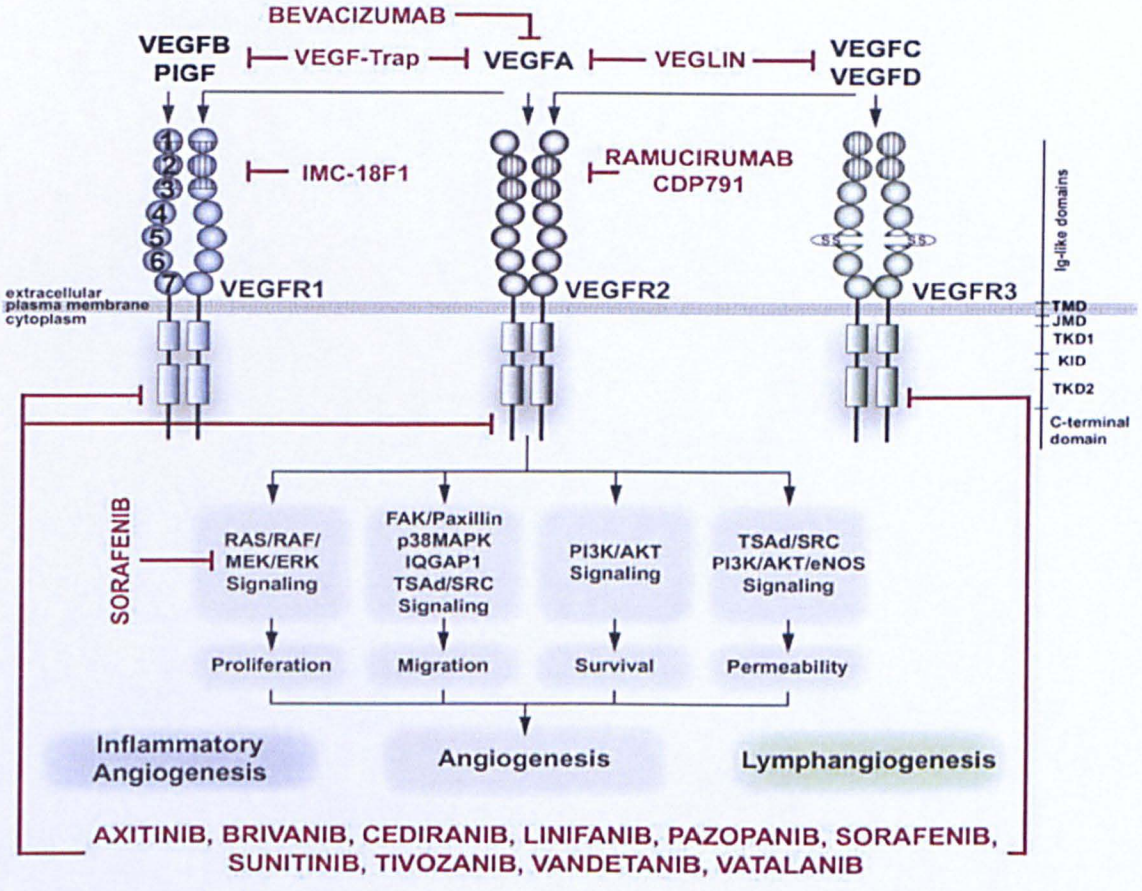


**Figure 1.8 VEGF signaling inhibitors and their targets.** The VEGF family of ligands (VEGFA, PlGF, VEGFB, VEGFC, and VEGFD) bind to their cognate receptors (VEGFR1; blue, VEGFR2; grey, VEGFR3; green) as indicated (arrows). Several different VEGF antagonists interfere with binding of VEGF ligands on the extracellular domain (e.g. Bevacizumab, VEGF-Trap, Veglin, IMC-18F1, Ramuciumab/CDP791), or compete for ATP-binding to the intracellular kinase domain (e.g. axitinib, brivanib, cediranib, linifanib, pazopanib, sorafenib, sunitinib, tivozanib, vandetanib, vatalanib). VEGFRs are shown with their extracellular domain organized in immunoglobulin-like loops (circles, labeled 1–7) and with intracellular split tyrosine kinase domain (squares). From Tugues, Koch et al. 2011.

Chapter 2

# Materials and Methods

## 2.1 Drugs and Reagents

Cediranib (AZD2171, AstraZeneca, Alderley Park, Macclesfield, UK) was dissolved in DMSO (1000X stock solution) for *in vitro* studies and further diluted in test medium immediately before *in vitro* assays (control cells received the same amount of DMSO). For *in vivo* treatments, cediranib was suspended in 1% Tween-80 (Sigma-Aldrich, Milan, Italy) by gentle shaking with 6-mm glass beads at room temperature overnight, and the suspension used within one week of preparation.

Paclitaxel (PTX, Indena S.p.A., Milan, Italy) was dissolved in 50% polyxyethylated castor oil (Cremophor EL, Sigma-Aldrich, Milan, Italy) and 50% ethanol and further diluted with 0.9% saline before use.

Cisplatin (cis-diamminedichloroplatinum, DDP, Sigma-Aldrich, Milan, Italy) was dissolved in 0.9% saline before use.

Recombinant VEGFR3/Fc chimera (R&D Systems, Minneapolis, MN) was reconstituted in PBS 0.1% BSA (20X stock solution).

## 2.2 *In vitro* studies

### *2.2.1 Cell lines and culture conditions*

The human ovarian carcinoma cell line 1A9, a variant derived from the A2780 human ovarian carcinoma cell line (Manenti, Riccardi *et al.* 2005) and IGROV1 (Benard, Da Silva *et al.* 1985) were obtained from National Cancer Institute, Fredrick, MD.

Stocks of cell lines, authenticated by short-tandem repeat profiling (AmpFlSTR Identifiler Plus PCR Amplification Kit; Applied Biosystems, Monza, Italy), were stored frozen in liquid nitrogen.

Cells were resurrected from the cell bank by rapid thawing (to 37°C in a water bath), the vial containing the cells in cryogenic medium (Lonza, Walkersville, MD) and the contents were

counted by Trypan blue exclusion (Fluka Analytical, Sigma-Aldrich, Milan, Italy) and transferred to a fresh tube. About 10 ml of fresh medium containing 10% of heat-inactivated fetal bovine serum (FBS, BioWhittaker, Lonza, Walkersville, MD) was added. After centrifugation, cells were transferred to a T25 tissue culture flask in 5-ml fresh culture medium containing RPMI 1640 (BioWest-Voden Medical, Milan, Italy) supplemented with 10% FBS (BioWhittaker, Lonza, Walkersville, MD) and 2 mM L-Glutamine (L-Glutamine 100X solution, 200 mM, BioWest-Voden Medical, Milan, Italy). Once resurrected from the cell bank, cells were allowed to go through at least 2-4 passages before being used. Cells were maintained in a $CO_2$ incubator at 37°C with 5% $CO_2$ and were passaged routinely twice a week, to maintain logarithmic growth.

Cell culture procedures were carried out aseptically in a class II laminar flow cabinet and the cells were tested for Mycoplasma contamination upon thawing.

Lentivirus-infected cells were cultured as the wild-type cells with the addition of selection antibiotic in culture medium to select infected cells.

Selection antibiotics were:

- Blasticidin for luciferase-infected cells, 5 μg/ml (Invitrogen, Life-Technologies, Monza, Italy);
- Neomycin for VEGFC-infected cells, 500 μg/ml (BioWhittaker, Lonza, Walkersville, MD);
- Zeocin for Katushka-infected cells, 1 μg/ml (Invitrogen, Life-Technologies, Monza, Italy).

The mouse lymphatic endothelial cell line (MELC), expressing VEGFR3 was provided by Annunciata Vecchi (Istituto Clinico Humanitas, Rozzano, Italy) and maintained as previously described (Sironi, Conti *et al.* 2006), in DMEM (BioWest-Voden Medical, Milan, Italy)

supplemented with 1 mM L-Glutamine (BioWest-Voden Medical, Milan, Italy), 1% MEM Non-Essential Amino Acids (NEAA, Sigma-Aldrich, Milan, Italy), 1 mM Sodium Pyruvate (Sigma-Aldrich, Milan, Italy), penicillin-streptomycin (BioWhittaker, Lonza, Walkersville, MD), 10% FBS (BioWhittaker, Lonza, Walkersville, MD), 100 μg/ml ECGS (Harbor Bio-Products, Norwood, MA), 100 μg/ml heparin (Hospira Italia S.r.l., Napoli, Italy), and 10% supernatant from sarcoma 180 cells. All the plastics used for lymphatic endothelial cell culture were pre-coated with 1% gelatin in PBS (37°C for at least 2 h).

The 293FT is a cell line used for lentivirus production. The stable expression of the SV40 large T antigen (Naldini, Blomer *et al.* 1996) makes the 293FT cell line a particularly suitable host for generating lentiviral constructs. The 293FT cell line was kindly provided by Enrico Pesenti (Nerviano Medical Sciences Oncology, Nerviano, Italy) and maintained in high-glucose DMEM (BioWest-Voden Medical, Milan, Italy), supplemented with 10% FBS (BioWhittaker, Lonza, Walkersville, MD), 0.1 mM MEM Non-Essential Amino Acids (NEAA, Sigma-Aldrich, Milan, Italy), 6 mM L-Glutamine (BioWest-Voden Medical, Milan, Italy) and 1 mM MEM Sodium Pyruvate (Sigma-Aldrich, Milan, Italy).

### *2.2.2 Generation of lentivirus-infected cells*

The generation of lentivirus-infected cells was performed in collaboration with Nerviano Medical Sciences Oncology, Nerviano, Italy.

#### *2.2.2.1 Plasmids*

The lentiviral vector carrying the coding sequence of synthetic firefly luciferase gene luc2 (*Photinus pyralis,* kindly provided by Enrico Pesenti, Nerviano Medical Sciences Oncology, Nerviano, Italy) was integrated into a pLenti6.3/V5-DEST destination vector, expressing the Blasticidin resistence gene (Invitrogen, Life-Technologies, Monza, Italy). The expression

clone pLenti-Luc was obtained by Gateway® Technology (Invitrogen, Life-Technologies, Monza, Italy, Figure 2.1). The Gateway® Technology is a universal cloning method based on the site-specific recombination properties of bacteriophage lambda and is a rapid and highly efficient way to move DNA sequences into multiple vector systems for functional analysis and protein expression (Landy 1989).

Using the same technology, the lentiviral vector carrying the coding sequence of Katushka, a far-red mutant of the red fluorescent protein from sea anemone *Entacmaea quadricolor* (Shcherbo, Merzlyak *et al.* 2007) (Evrogen, Moscow, Russia) was integrated into a pLenti6.3/V5-DEST destination vector, modified to express the Zeocin resistence gene (Invitrogen, Life-Technologies, Monza, Italy) and the expression clone pLenti-Kat was obtained.

Finally, the coding sequence of the full-length VEGFC isoform (VEGFCfl, 1290 bp) or its proteolitically activated mature form (VEGFCmf, 490 bp) (Joukov, Sorsa *et al.* 1997; Skobe, Hamberg *et al.* 2001), kindly provided by Michael Detmar (ETH - Institut f. Pharmazeut. Wissenschaften, Zürich, Switzerland), were integrated into pLenti6.3/V5-DEST expression vectors, modified to express the Neomycin resistance gene, using Gateway® technology. The expression clones pLenti-VEGFCfl or pLenti-VEGFCmf were obtained.

*2.2.2.2 Lentivirus stock production*

Replication-incompetent, HIV-1-based lentivirus were created to deliver and express the genes of interest (luciferase, Katushka and VEGFCfl or VEGFCmf) in ovarian cancer 1A9 or IGROV1 cells.

The optimized 293FT producer cell line, that stably expresses the SV40 large T antigen under the control of the human CMV promoter, facilitates optimal production of virus.

239FT cells were plated in a 10 cm tissue culture plate in order to have a 90-95% cell confluence on the day of transfection. The day of transfection culture medium was removed from the 293FT cells and replaced with Opti-MEM medium (Invitrogen, Life-Technologies, Monza, Italy).

A transfection cocktail containing 9 μg of the Packaging Mix (3 μg pLP1, 3 μg pLP2 and 3 μg pLP/VSVG) and 3 μg of pLenti expression plasmid DNA was diluted in 1.5 ml of Opti-MEM medium.

pLP1 contains *gag* and *pol* genes: gag is the viral core proteins required for forming the structure of the lentivirus (Luciw 1996), pol is the viral replication enzyme required for replication and integration of the lentivirus (Luciw 1996). Expression of the *gag* and *pol* genes from pLP1 has been rendered Rev-dependent by virtue of the HIV-1 RRE in the gag/pol mRNA transcript. pLP2 contains the HIV-1 Rev ORF that encodes the Rev protein that interacts with the RRE on pLP1 to induce Gag and Pol expression, and on the pLenti6/V5 expression vector to promote the nuclear export of the unspliced viral RNA for packaging into viral particles. pLP/VSVG contains the gene that encodes the envelope G glycoprotein from Vesicular Stomatitis Virus to allow production of a pseudotyped retrovirus with a broad host range (Emi, Friedmann *et al.* 1991; Burns, Friedmann *et al.* 1993; Yee, Miyanohara *et al.* 1994).

36 μl of Lipofectamine™ 2000 were diluted in 1.5 ml of Opti-MEM medium and after 5 minutes of incubation at room temperature, the diluted Lipofectamine™ 2000 was combined with the diluted DNA.

After 20 minutes of incubation at room temperature the DNA-Lipofectamine™ 2000 complexes were added to 293FT cells. Cells were incubated overnight at 37°C in a humidified 5% $CO_2$ incubator. Recommended guidelines for working with BL-2 organisms as infectious virus were used.

Medium containing the DNA-Lipofectamine™ 2000 complexes was removed after 24 hours, replaced with 10 ml complete culture medium and incubated at 37°C in a humidified 5% $CO_2$ incubator. Virus-containing supernatants were harvest 48–72 hours post-transfection, centrifuged at 3000 rpm for 15 minutes at 4°C and stored at –80°C.

*2.2.2.3 Cells transduction*

1A9 and IGROV1 cells were plated in complete media as described in section 2.2.1. Lentiviral stock was thawed, and after removing the culture medium from the cells, the virus was added. Hexadimethrine bromide (Sigma-Aldrich, Milan, Italy) was added to a final concentration up to 10 μg/ml, as it enhances transduction. After swirling the plate to mix, it was incubated overnight at 37°C. After 24 hours, the medium containing virus was removed and replaced with complete culture medium. After 24 hours, complete medium containing the appropriate amount of Blasticidin, Zeocin or Neomycin was added to select for stably transduced cells selection. Antibiotic-resistant cells were selected after 10–12 days.

The absence of viral particles was verified by ELISA (Alliance HIV-1 P24 Antigen ELISA Kit, Perkin Elmer, Waltham, MA).

*2.2.3 In vitro bioluminescence imaging*

To verify whether bioluminescent signal intensity correlated with the cell number, cells were seeded at increasing concentration, ranging from $1x10^6$ to $3.125x10^4$, in a 96-well black plate. D-Luciferin substrate (150 μg/ml, Caliper Lifescience, Alameda, CA) was added into the cell medium and bioluminescence signal detected 10 min later by eXplore Optix MX2 (ART, Advanced Research Technologies Inc., Saint-Laurent, Canada). Photon emission was recorded as pseudo-color images representing the spatial distribution of detected photon counts emerging from active luciferase within the well and quantified using Optiview

software (version 2.02.00; ART, Advanced Research Technologies Inc., Saint-Laurent, Canada). The mean value of BLI signal detected in each well was plotted against the number of cells seeded in the well.

*2.2.4 Supernatant collection*

Cells were plated in 6-wells culture plates at the concentration of 5 x $10^4$ cells (1A9 cell line variants) or 1 x $10^5$ cells (IGROV1 cell line variants) per well in RPMI 1640 supplemented with 10% FBS. After 48h hours at 37°C, monolayers were washed twice with Ca- and Mg-free PBS (BioWest-Voden Medical, Milan, Italy) and 1 ml of RPMI without FBS was added. Conditioned media were collected after 4, 24 and 48 hours, centrifuged at 1200 rpm for 10 minutes at 4°C, aliquoted and stored at −80°C until use.

*2.2.5 Growth curve*

Cells were plated in 96-wells culture plates (1-2 x $10^3$ cells/well) in RPMI 1640 supplemented with 10% FBS. After 4, 24, 48, 72 or 96 hours cells were fixed and stained with 0.5% crystal violet in 20% methanol. The stain was eluted with a solution 1:1 of 0.1M sodium citrate/ethanol and the absorbance was read at 595 nm. Absorbance was proportional to the number of cells.

Doubling time (DT) was calculated according to the ATCC animal cell culture guide, as DT = T x ln2 / ln (Xe-Xb) where T is the incubation time, Xb is the cell number (Abs) at the beginning of incubation time and Xe is the cell number (Abs) at the end of incubation time.

*2.2.6 Motility assay*

Motility of mouse lymphatic endothelial cells or ovarian carcinoma cells in response to conditioned medium was assayed using modified Boyden chambers and 8 μm pore size polycarbonate polyvinylpyrrolidone-free nucleopore filters (Taraboletti, Belotti *et al.* 1993). Conditioned medium of VEGFC infected cells obtained from an equal cell number was used as attractant.

5 x $10^5$ cells/ml in Dulbecco's modified Eagle's medium (DMEM, BioWest-Voden Medical, Milan, Italy) /0.1% BSA were added to the upper compartment of the chamber. Cediranib (10 nM, section 2.1) or recombinant VEGFR3/Fc chimera (10 μg/ml, section 2.1) were added to the cells and incubated overnight throughout the assay.

Filters were stained with Diff-Quick (Merz-Dade, Düdingen, Switzerland), and the cells migrated in 10 high-power fields were counted. Data are expressed as number of migrated cells (mean ± SD of triplicates).

*2.2.7 Multiplex in situ Epitope Profiling (MiSEP)*

The expression levels of VEGFR1, VEGFR2 and VEGFR3 on cell surfaces were measured by MiSEP technology (LEAP Biosciences, Mountain View, CA, Figure 2.2) that simultaneously detected multiple receptors on living cell surfaces. The receptor expression levels were determined by quantifying antibodies that were bound to their receptors. Antibodies specific to the extracellular domain (ECD) of VEGFR1, VEGFR2 and VEGFR3 were incubated with cells. Receptor-bound antibodies were then eluted from their receptors to derive the receptor-profiled antibody sample and then quantified by ECD array using Luminex xMAP® system. The amount of each antibody in the sample reflected the abundance of each receptor on the cell surface. Assays were conducted according to manufacturer's instructions. All samples were analyzed in duplicate.

*2.2.8 ELISA assay*

The levels of human VEGFC in cell supernatants and in serum and ascites of nude mice bearing human ovarian tumors were determined by ELISA (Quantikine®, R&D Systems, Minneapolis, MN), according to manufacturer's instructions. The sensitivity of the assay was 13,3 pg/ml. Each sample was analyzed in duplicate. The results were expressed in pg/ml.

*2.2.9 Real-Time PCR*

VEGFC, VEGFR3 and VEGFR2 transcripts were analyzed by real-time reverse transcription-PCR (RT-PCR) using *TaqMan® Gene Expression Assay* (Applied Biosystems, Monza, Italy). Briefly, total RNA was extracted from tumor cells and tumor masses snap frozen in liquid nitrogen with Trizol® protocol (Invitrogen, Life-Technologies, Monza, Italy), then purified and reverse-transcribed with Archieve kit (Applied Biosystems, Monza, Italy) to cDNA, according to manufacturer's instructions. Experiments were run in triplicate. Amplification reactions were performed with the 7900HT Fast Real Time PCR System (Applied Biosystems, Monza, Italy). PCR data were analyzed using the Sequence Detection Systems (SDS) version 2.3 (Applied Biosystems, Monza, Italy). VEGFC, VEGFR3 and VEGFR2 mRNA were normalized to HPRT1 or beta-actin housekeeping gene: $\Delta Ct = Ct_{target} - Ct_{housekeeping}$. Data are expressed as $2^{-\Delta Ct} \times 1000$ or $2^{-\Delta Ct} \times 100$ (Schmittgen and Livak 2008), mean ± SD of three replicates from one experiment representative of three.

**2.3 *In vivo* studies**

*2.3.1 Human ovarian cancer xenografts*

Patient-derived human ovarian cancer (HOC) xenografts (high-grade serous HOC8, HOC22, HOC10 and the endometroid-clear cell HOC79) were established and maintained by intraperitoneal transplantation in nude mice (Massazza, Tomasoni *et al.* 1989). These

xenograft models were molecularly, biologically and pharmacologically characterized (Nicoletti, Lucchini *et al.* 1993; Valoti, Nicoletti *et al.* 1998) and stored as frozen stocks at early passages after establishment.

*2.3.2 Animals*

Six- to eight-week-old female NCr-nu/nu mice were obtained from Harlan (Correzzana, Italy). Mice were maintained under specific pathogen-free conditions, housed in isolated vented cages, and handled using aseptic procedures. Procedures involving animals and their care were conducted in conformity with institutional guidelines that comply with national (Legislative Decree 116 of January 27, 1992, Authorization n.19/2008-A issued March 6, 2008, by the Italian Ministry of Health) and international laws and policies (EEC Council Directive 86/609, OJ L 358, 1, December 12, 1987; standards for the Care and Use of Laboratory Animals, United States National Research Council, Statement of Compliance A5023-01, October 28, 2008) and in line with Guidelines for the welfare and use of animals in cancer research (Workman, Aboagye *et al.* 2010).

*2.3.3 Intraperitoneal tumor models*

Patient-derived ovarian cancer cells (described in section 2.3.1) were obtained by harvesting and centrifuging at 1200 rpm for 10 minutes at 4°C the ascites of at least three-five mice. Pellets of cells were pooled, resuspended in HBSS (BioWest-Voden Medical, Milan, Italy) and again centrifuged. Then cells were counted by trypan blue exclusion with the aid of a Bürker chamber and resuspended in HBSS at the concentration of $5 \times 10^7$ cells/ml.

A suspension of 0.2 ml ($10 \times 10^6$ cells) was injected intraperitoneally in the lower right quadrant of abdomen using a syringe with a 21 gauge needle. The day of inoculation was considered to be day 0.

Mice were checked twice a week for tumor formation (abdominal distension) in the peritoneal cavity, and killed when moribund (Garofalo, Naumova *et al.* 2003).

*2.3.4 Intraovarian tumor models*

1A9 and IGROV1 variants were grown to semi-confluence in tissue culture as described in section 2.2.1. Once harvested with trypsine/EDTA (trypsin 0.05% w/v EDTA 0.02% w/v, BioWest-Voden Medical, Milan, Italy), cells were pooled and quantified. Detached cells were resuspended in RPMI 1640 with 10% FBS and washed three times with HBSS (BioWest-Voden Medical, Milan, Italy). Then, the cells were counted by trypan blue exclusion with the aid of a Bürker chamber and resuspended in HBSS at the concentration of $2 \times 10^8$ cells/ml.

Nude mice were anesthetized with isoflurane (Florane, Abbott Laboratories, Chicago, IL) and a single lateral midline incision allowed access to the left ovary. Ovarian cancer cells were implanted orthotopically under the bursa of the ovary of nude mice as a $1 \times 10^6$ cell suspension in 5 µl HBSS using a Hamilton syringe with a 26 gauge needle (Fu and Hoffman 1993; Connolly 2009). The day of inoculation was considered to be day 0.

Mice were checked twice a week for tumor formation in the ovary, and killed when moribund.

*2.3.5 Surgical removal of primary tumor*

Mice were anesthetized in lateral side with isoflurane. A 2-3 cm lateral midline skin incision was made and the ovary and the oviduct were exteriorized. A hemostat was clamped around the uterine vasculature between the oviduct and uterus. Each ovary and part of the oviduct was removed with single cuts through the oviducts near the ovary. After removing the hemostat, the remaining tissue was replaced into the peritoneal cavity. The incision was sutured with wound clips.

*2.3.6 In vivo bioluminescence and fluorescence imaging*

Bioluminescence imaging (BLI) was used to confirm the presence of luciferase-infected tumors in the ovary of nude mice and to monitor tumor progression. Nude mice were anesthetized with isoflurane and scanned ten minutes after the injection of D-luciferin solution (150 mg/kg, i.p.; Caliper Lifescience, Alameda, CA) by eXplore Optix MX2 (ART, Advanced Research Technologies Inc., Saint-Laurent, Canada).

Fluorescence imaging (FLI) was used to confirm the presence of Katushka-infected cells in the ovary of nude mice and to monitor tumor progression. Mice were scanned for fluorescence using the 635 nm excitation wavelength pulse laser by eXplore Optix MX2 (ART, Advanced Research Technologies Inc., Saint-Laurent, Canada).

A region of interest (ROI) was designed over the peritoneal cavity of each animal, and light emission in the selected ROI was quantified as total photon counts using Optiview software (version 2.02.00; ART, Advanced Research Technologies Inc., Saint-Laurent, Canada). Photon emission was recorded as pseudo-color images representing the spatial distribution of detected photon counts emerging from active luciferase of fluorescent cells within the animal. Overlay of the grey-scale (body of reference photograph) and pseudo-color images allowed localization of tumors within the animal. For each group and for each time point, the mean value of BLI or FLI signal detected in the selected ROI was calculated and plotted against days after tumor transplantation in a histogram graph. Tumor burden was expressed as photon counts (Oliva, Decio *et al.* 2012).

*2.3.7 Blood sample collection*

Blood samples were collected at different time points from the superficial temporal vein of mice (Figure 2.3). This technique allows to collect blood sample at different time points during tumor progression from the same animal.

Nude mice were restrained so that the hairless freckle was located on the side of the jaw. Then, the freckle was pricked with a 18 gauge needle and quickly blood drops were collected in a sterile plastic tube. Blood was incubated 30 minutes at 37°C to activate platelets, centrifuged at 3000 rpm for 15 minutes to obtain serum and stored at -80°C until processing.

### *2.3.8 In vivo treatments and preclinical trials*

#### *2.3.8.1 Cediranib as monotherapy in IGROV1 and HOC xenografts*

IGROV1-luc and IGROV1-luc/VEGFCmf tumor-bearing mice were randomized by bioluminescence imaging seven days after tumor transplant (8-10 mice in each group). Patient-derived HOC8, HOC10, HOC22 and HOC79 xenografts were randomized respectively 7, 10, 6, 5 days after tumor transplant, on the basis of representative mice with confirmed tumor burden in the peritoneal cavity by histological analysis. Cediranib was given orally at the dose of 6 mg/kg (for IGROV1-luc and IGROV1-luc/VEGFCmf) or 3 mg/kg (for HOCs), daily for 21 days (Q1x21), or until survival (day 108, maintenance regimen, detailed schedule of treatment in chapter 5, Figure 5.8A). Vehicle was administered following the same schedule as the active compound.

#### *2.3.8.2 Cediranib in combination therapies*

HOC8-bearing mice were randomized seven days after tumor transplant, on the basis of representative mice with confirmed tumor burden in the peritoneal cavity by histological analysis. Mice were treated with standard chemotherapy, PTX and DDP (PTX+DDP, at the dose of 10 mg/kg and 3 mg/kg, respectively), for three cycles (Q7x3) and cediranib (3 mg/kg, daily) was administered according to different schedules:

a) in combination with chemotherapy, started on day 7 (Q1x21), Figure 5.9A;

b) in combination with chemotherapy, started on day 7, and continued until day 90 (Q1x83), Figure 5.9A;

c) alone, or in combination with chemotherapy, started on day 22 (24h after the end of the chemotherapy) and continued until day 90 (Q1x68), Figure 5.10A.

Detailed schedules, doses and lengths of treatment are reported in chapter 5 (Figures 5.9A and 5.10A). Vehicles were administered at the same schedule as the active compounds.

*2.3.9 Treatment evaluation*

For IGROV1-luc and IGROV1-luc/VEGFCmf-bearing mice, tumor burden and progression were monitored by bioluminescence imaging (BLI), as described in section 2.3.6.

Patient-derived xenografts (HOC8, HOC10, HOC22 and HOC79) bearing mice were monitored and checked twice a week for tumor formation (abdominal distention) in the peritoneal cavity.

For ethical reasons, survival was defined as the day of appearance of signs of distress, at which time mice were euthanized (Garofalo, Naumova *et al.* 2003; Oliva, Decio *et al.* 2012). At necroscopy, the peritoneal cavity was macroscopically examined to ascertain the presence of tumor. Survival time was recorded and increment of life span (ILS) was calculated as 100 × [(median survival day of treated group − median survival day of control group) / median survival day of control group]. Results were plotted as the percentage survival against days after tumor transplant. Complete response, confirmed macroscopically at necropsy, was the absence of tumour in animals still alive 60 days after the death of the last mouse in the same group.

*2.3.10 Necroscopy*

Mice were sacrificed and necropsied to establish tumor burden. Macroscopical analysis of the organs of the peritoneal cavity was performed and gross findings were recorded.

Venous blood was collected and serum for soluble VEGFC and VEGFRs analysis was obtained as described in section 2.3.7.

Ascites was harvested, centrifuged at 1200 rpm for 10 minutes and the volume of fluid and number of cells in the pellet (representative of tumor burden) recorded for each mouse. Serum and ascites were stored at -80°C until processing (Manenti, Riccardi *et al.* 2005).

For histopathological and immunohistochemical analysis, organs (para-aortic lymph nodes, ovaries and diaphragms) were formalin-fixed and paraffin-embedded (section 2.4.1).

Pellet of cells after ascites centrifugation and tumor tissues were immediately frozen in liquid nitrogen for mRNA extraction and gene expression analysis (section 2.2.9).

## 2.4 *Ex-vivo* analysis

### *2.4.1 Histological and immunohistochemical analysis*

Histological and immunohistochemical analysis were done in collaboration with Veronica Patton and Rachele Alzani from Nerviano Medical Sciences Oncology, Nerviano, Italy.

Para-aortic lymph nodes, ovaries and diaphragms were collected, fixed in 10% phosphate-buffered formalin (Bio Optica Milano S.p.A., Milan, Italy) and embedded in paraffin with the aid of a microwave rapid tissue processor (Histos5, Milestone S.r.l., Sorisole, Italy). Organs were cut into 5 µm-thick sections and stained with hematoxylin and eosin (H&E).

For immunohistochemistry an anti-human VEGF Receptor 3 rabbit polyclonal antibody (Abcam, Cambridge, UK), an anti-mouse LYVE-1 rabbit polyclonal antibody (Abcam, Cambridge, UK) and anti-mouse CD31 rat monoclonal antibody (Dianova GmbH, Hamburg, Germany) were used. LYVE-1 positive vessels were not labeled with anti-CD31 antibody, confirming their lymphatic identity. For LYVE-1, a morphological analysis of stained

lymphatic vessels was done, considering positive vessels in lymph nodes, ovaries/tumors and diaphragms, and their location and dilation. The presence of neoplastic emboli within lymphatic vessels was recorded. For CD31 five fields/tumor were counted at 400x magnification. Fields were selected in highly vascularized tumor areas. Every lumen lined by positive endothelial cells and/or endothelial clusters clearly stained and separated from adjacent clusters was counted as a single microvessel.

*2.4.2 Mouse soluble VEGF receptors assay*

Murine soluble VEGFR1, VEGFR2 and VEGFR3 were measured in serum of nude mice bearing human ovarian carcinoma tumors by luminex kit (Milliplex® MAP kit, Millipore S.p.A., Vimodrone, Italy), according to manufacturer's instructions. The sensitivity of the assay was 76.2 pg/ml for soluble VEGFR1, 32.6 pg/ml for soluble VEGFR2 and 41.5 pg/ml for soluble VEGFR3. Each sample was analyzed in duplicate. The results were expressed as relative release: [amount VEGFR (pg/ml) at day x] / [amount VEGFR (pg/ml) at randomization].

**2.5 Statistical analyses**

Statistical analyses were done using Prism Software (Prism 5.01; GraphPad Software, La Jolla, CA). Differences in VEGFC levels, in VEGFRs levels, in photon counts and cell migration were analysed by two-way ANOVA followed by Bonferroni post-test. Differences in growth curves were analyzed by Multiple t tests. Correlations between a) VEGFC levels and tumor burden and b) VEGFRs levels and tumor burden and c) photon intensity and the number of cells *in vitro* were assessed using the Pearson's correlation coefficient. Differences in mouse survival time were analyzed by the Log-Rank test.

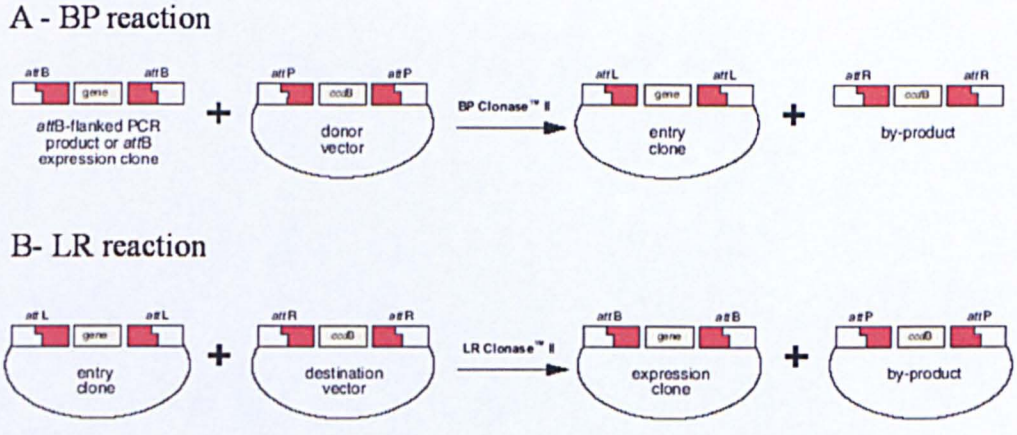


**Figure 2.1 Gateway® technology**. This technology uses the lambda recombination system to facilitate transfer of heterologous DNA sequences (flanked by modified *att* sites) between vectors (Hartley, Temple et al. 2000). Two recombination reaction constitute the basis of the Gateway® Technology. (A) BP reaction: facilitates recombination of an *att*B substrate (*att*B-PCR product or a linearized *att*B expression clone) with an *att*P substrate (donor vector) to create an *att*L-containing entry clone. This reaction is catalyzed by BP Clonase™ enzyme mix. (B) LR Reaction: Facilitates recombination of an attL substrate (entry clone) with an attR substrate (destination vector) to create an attB-containing expression clone. This reaction is catalyzed by LR Clonase™ enzyme mix.

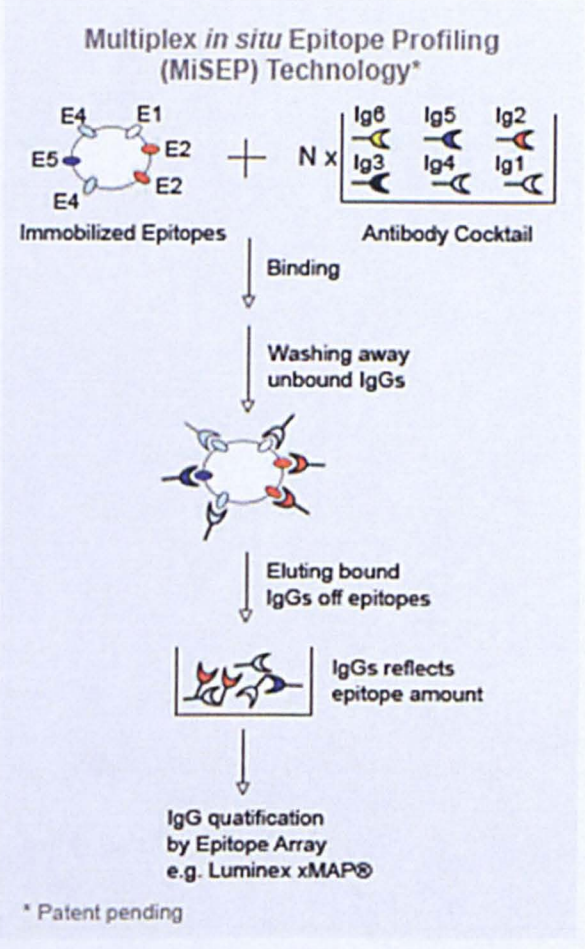


**Figure 2.2** Multiplex in situ Epitope Profiling Technology. Downloaded from http://www.leapbio.com/technology_MiSEP.html

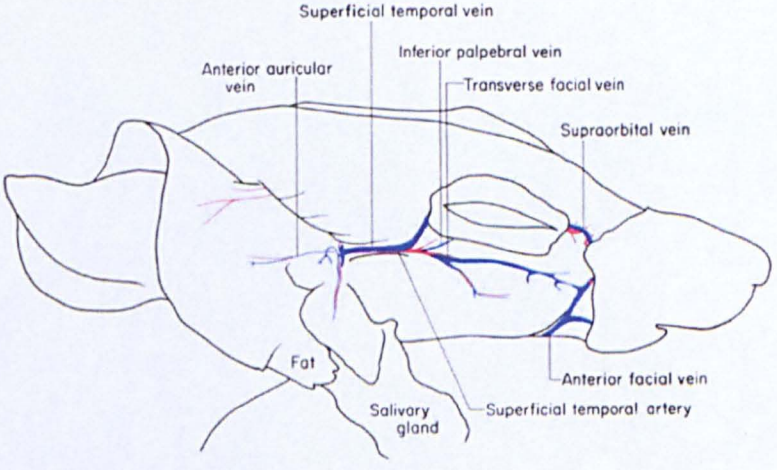


**Figure 2.3** Mouse facial vessels, from Cook 1965.

Chapter 3

# Characterization of *in vivo* models

### 3.1 Introduction and goals

Preclinical animal models of cancer are one of the most important tools to study tumors. In particular, mice are used because they are comparative living systems that allow researchers to discover the underlying basis of how and why cancers arise, why primary tumors metastasize, and how various kinds of preventive interventions and treatments can be used to stop the progression of cancer, or the growth and spread of tumors, and prolong patient lives.

Four main categories of cancer models are generally used in preclinical investigations, namely genetically engineered models (GEMs), syngeneic murine models (both induced or spontaneously arisen), xenografts obtained from human tumor specimens from patients (patient-derived tumor xenografts, PDTX), directly transplanted into immunodeficient mice, without an intermediate *in-vitro* passage, and xenografts derived from well-established and characterized human tumor cell lines cultured *in vitro*.

Each of these models has advantages and disadvantages.

GEMs often concern specific molecular targets highly suited to preclinical assessment of the corresponding targeted compounds, as tumor growth occurs spontaneously in situ and in organspecific sites. This reproduces the situation observed in human cancers and interactions between tumor and stroma, as well as the impact of the immune system, appear to closely mimic human situations. However, assessment of therapeutic efficacy could be hampered in the case of non superficial or delayed tumor growth and by the fact that the GEMs represent only one model of the tumor-specific target, which does not necessarily predict that the target itself will be coupled to the biological 'read-out' in real human cancers (Peterson and Houghton 2004).

Syngeneic murine models provided the first opportunity for large scale screening for antitumor drugs. These models allow to consider the involvement of immune system in cancer

development and progression. A drawback is that these syngeneic models grow so rapidly that their applications are limited (Langdon 2012).

PDTX maintain the molecular and genetic heterogeneity typical of the human tumor of origin (Tentler, Tan *et al.* 2012); the majority of the key genes and global pathway activity in primary tumors is maintained (Jones, Zhang *et al.* 2008; Daniel, Marchionni *et al.* 2009). Furthermore, the original tumor architecture and histological characteristics are preserved (Massazza, Tomasoni *et al.* 1989; Daniel, Marchionni *et al.* 2009).

PDTX have also a good correlation with clinical outcome (Fiebig, Maier *et al.* 2004; Gorelik, Ziv *et al.* 2008), as procedures for assessment of therapeutic efficacy have been well standardized and readily allow evaluation of combined therapies, particularly for the purposes of objective biostatistical assessment (Decaudin 2011). Indeed when combined with mathematical modelling, these results can be applied to individualise treatment for the patients from which these tumours are obtained (Gorelik, Ziv *et al.* 2008).

A drawback of PDTX models is that although the original tumor architecture is maintained the human stroma is replaced by murine stroma with sequential passage (Tentler, Tan *et al.* 2012).

Human tumor cell lines, obtained establishing and culturing *in vitro* cells from tumor tissues from patients, once transplanted in mice in the orthotopic site grow as the original tumor maintaining the same behavior (Moro, Bertolini *et al.* 2012).

Cell lines are widely used to explore new aspects of cancer biology, from the role of individual molecules, to the role of cellular processes involved in invasion and metastasis within animal models. They are easy to use, grow rapidly, produce reproducible results and have a strong track record of use in cancer research. For experimental use or compound screening for a target mechanism it is certainly possible to change the phenotype of cell lines by *ex-vivo* manipulations before xenotranplantation to create variants that reflect better the

biology of their parent lines (Cree, Glaysher *et al.* 2010; Decaudin 2011). Unfortunately, there is increasing recognition that their relevance to human cancer may not be all it seems, and results from cell lines of a particular lineage rarely correlate with the sensitivity of that tumor type to the drugs tested.

Cell lines are adapted to grow in cell culture medium, which provides a very different environment to that which they experienced in their originating tumor (Fernando, Glaysher *et al.* 2006), resulting in genetic changes that are distinct from the genetic stress imposed on tumors in patients (Daniel, Marchionni *et al.* 2009). The expression of these changed genes is not restored when derivative cell line is returned to grow *in vivo* (Daniel, Marchionni *et al.* 2009). Likewise, there is strong evidence that a greater genetic divergence exists between a primary tumor and the corresponding cell line derived from that tumor, versus a direct xenograft after several generations (Daniel, Marchionni *et al.* 2009).

Within tumors, cancer cells are normally capable of independent growth and show reduced attachment to substrate (usually basement membrane proteins) and to other cells. In contrast, cell lines may become dependent on growth factors supplied as serum or other supplements and adherence to plastic. Withdrawal of serum or use of plastics such as polypropylene, which do not encourage cell adherence results in the death of many cell lines (Cree, Glaysher *et al.* 2010).

The highly anaplastic cancer cells cultivated *in vitro* represent the extreme derivates from highly advanced cancers and are not associated with original tumor stroma, which now has been recognized as a crucial factor in the pathogenesis of cancer metastasis (Bhowmick, Neilson *et al.* 2004).

GEM, syngeneic models, PDTX and tumor cell line models are complementary, as each of them gives particular information on the different aspects of cancer growth and dissemination.

In this chapter two different and complementary models used to investigate different features of tumor growth and metastasis induced by the VEGFC/VEGFR3 pathway are described:

1. Patient-derived ovarian carcinoma xenografts established in this laboratory and implanted in the peritoneal cavity of nude mice.
2. Human ovarian carcinoma cell lines implanted orthotopically under the bursa of the ovary of immunodeficient mice.

***Part of the work presented is a manuscript in press in American Journal of Pathology, 2014.***

### 3.2 Patient-derived ovarian carcinoma xenografts

HOC xenografts are high grade serous (HOC8, HOC22, HOC10) and endometroid-clear cell (HOC79) ovarian cancer (Massazza, Tomasoni *et al.* 1989) derived from untreated (HOC8 and HOC10) and treated (HOC22 and HOC79) patient and established intraperitoneally (i.p.) in nude mice (Table 3.1). When transplanted into the peritoneal cavity of nude mice they produce ascites and carcinomatosis, recapitulating the behavior of the original patients' tumors. These xenografts were molecularly and pharmacologically characterized for the response to chemotherapy in this lab.

#### *3.2.1 Correlation between tumor burden and VEGFC*

The expression of VEGFC was analyzed in the four ovarian tumor xenografts. Tumor xenografts were transplanted i.p. in nude mice. Mice were killed with a heavy tumor burden, biological fluids harvested, and the amount of VEGFC measured by ELISA assay. All the four tumor xenografts released soluble VEGFC both in ascites and serum at sacrifice (Figure 3.1). Comparable VEGFC levels were detected in ascites of HOC8, HOC10 and HOC22 (256, 214 and 223 pg/ml, respectively) while VEGFC detected in ascites of HOC79 was lower (69

pg/ml). VEGFC was detectable also in serum of HOC8, HOC10 and HOC22 (66, 68 and 87 pg/ml, respectively). Since the ELISA assay recognized specifically human (not mouse) VEGFC, this VEGFC was certainly produced by the tumor cells.

The relationship between soluble VEGFC levels and tumor progression was investigated in HOC8 xenograft. Nude mice (n=7 for each time point) were transplanted i.p. with HOC8 cells. Ascites was harvested 13, 21, 35, 43 and 55 days after tumor transplantation and the amount of VEGFC was measured by ELISA assay. The levels of VEGFC in ascites rose with time after tumor injection, showing a strong correlation with tumor burden, expressed as number of cells in the peritoneal cavity (Figure 3.2A, $R^2$=0.9082, ***p<0.0005). Serum VEGFC peaked 21 days after transplant (173 pg/ml, Figure 3.2B).

### *3.2.2 Para-aortic lymph nodes invasion*

Tumor infiltration of para-aortic lymph node and ovaries was analyzed 21 and 35 days after tumor transplant by histological analysis. On day 21, HOC8 cells were found outside the lymph nodes (Figure 3.3A) and by 35 days 69% of the lymph nodes (n=14) were massively invaded by neoplastic cells (Figure 3.3B and Table 3.2). The capsule of invaded lymph nodes was intact, suggesting that tumor cells reached the nodes through lymphatic and/or blood vessels rather than directly from the peritoneal cavity. This path of dissemination was also supported by the detection of tumor cells inside diaphragmatic lymphatic vessels (LYVE-1+) and peritoneal blood vessels (CD31+) (Figure 3.3C and 3.3D).

A tendency of lymph nodes to present with enlarged lymphatic vessels before the arrival of metastatic cancer cells was evidenced by LYVE-1 immunostaining 21 days after tumor transplantation (Figure 3.4).

### 3.3 Set up of orthotopic intraovarian models

In order to set up an orthotopic model of human ovarian cancer growing in the ovary of immunodeficient mice, 1A9, a variant derived from A2780 (Manenti, Riccardi *et al.* 2005) and IGROV1 (Benard, Da Silva *et al.* 1985) human ovarian carcinoma cells were injected under the bursa of the ovary. The accuracy of transplant was confirmed by the presence of some ovarian structures (follicles with oocytes) in neoplastic masses (Figure 3.5). 1A9 and IGROV1-transplanted mice were sacrificed and necropsied at day 20 and at day 28, respectively.

Histopathological analysis of ovaries and lymph nodes indicated that the tumor take of 1A9 cells was 3 out of 4 (75%). No metastases were observed in the contralateral ovaries or into the para-aortic lymph nodes (Table 3.3). A tumor take of 4 out of 4 (100%) was observed for IGROV1 cells, 66% of mice with metastasis into the contralateral ovary, while the presence of metastatic cells was not revealed in para-aortic lymph nodes (Table 3.3).

The expression of human VEGFC and its receptor human VEGFR3 in 1A9 and IGROV1 cell lines was analyzed by Real-Time PCR. VEGFC transcript was not detectable in 1A9 nor in IGROV1, while VEGFR3 was expressed in both the cell lines (Figure 3.6).

#### *3.3.1 Surgical removal of primary tumor*

The standard first-line therapy for ovarian cancer patients is cytoreductive surgery followed by chemotherapy (Cannistra, Bast *et al.* 2003). In order to reproduce a more accurate model of ovarian cancer, surgical removal of primary tumor in the ovary was performed and tumor dissemination and mice survival evaluated.

Specifically, 1A9 tumor cells were injected under the bursa of the ovary. Fourteen days after tumor cell injection, primary tumor was surgically removed from half of the mice.

Increased survival was observed in mice undergoing surgery, with an ILS of 37% (Median survival time - MST control 41 days, MST Surgery 56 days, Figure 3.7).

However, histopathological analysis of ovaries and lymph nodes indicated that the 100% of tumors relapsed. As observed in control mice, no metastases were observed in the contralateral ovaries or into the para-aortic lymph nodes (Table 3.4).

Removal of the primary tumor resulted in increased mice survival, although the tumor regrew rapidly and no differences in the metastatic pattern were observed.

## 3.4 Summary of results

The data presented in this chapter can be summarized as follows:

HOCs

- Patient-derived xenografts transplanted in nude mice release soluble VEGFC which circulates at high levels in the serum and ascites of mice bearing the xenografted tumors.
- In the HOC8 model the amount of VEGFC released in ascites correlates with tumor burden
- Peak of VEGFC is observed in serum 21 and 35 days after transplant and correlates with lymph nodes invasion.
- Lymphatic vessels from tumor bearing mice are enlarged in lymph nodes before the arrival of metastatic cancer cells.

Intraovarian models

- 100% tumor take is observed after 1A9 and IGROV1 cells transplantation.
- 1A9 and IGROV1 cells do not express human VEGFC, but do express human VEGFR3.
- No metastasis in lymph nodes are observed.

- Surgical removal of intraovarian primary tumor increases mice survival but does not influence tumor growth and metastasis.

## 3.5 Discussion

Mouse models recapitulate many aspects of the genesis and progression of human cancers, thus they are valuable resources to investigate the mechanisms of cancer and to predict clinical behavior.

In this chapter, models of human ovarian carcinoma xenografts were set up and characterized. To study a correlation between tumor progression and VEGFC expression, VEGFC was measured in patient-derived HOC xenografts, that produce ascites and carcinomatosis to the organs of the peritoneal cavity.

Circulating VEGFC has been recently shown to correlate with ovarian carcinoma progression (Cheng, Liang *et al.* 2013). In the current study, it was shown that VEGFC is released in serum and ascites of all four human ovarian carcinoma bearing mice. Furthermore, in the HOC8 xenograft VEGFC levels correlated with tumor burden and lymph node invasion, suggesting that VEGFC released in biological fluids might serve as an indicator of tumor burden and invasion. Particularly interesting was the fact that capsules in invaded lymph nodes were intact; the location of tumor cells in the subcapsular sinus just beneath the capsule suggests that they reached the lymph nodes from afferent lymphatic vessels and/or blood vessels, not directly from the peritoneal cavity. This was supported by immunohistochemical findings of tumor cells in lymphatic and blood vessels of the diaphragm and peritoneum. In addition, consistent with recent reports (Qian, Berghuis *et al.* 2006; Alitalo and Detmar 2012; Liersch, Hirakawa *et al.* 2012) observing that VEGFC secreted by primary skin tumors induced lymphangiogenesis and enlargement of lympatic vessels within the draining lymph nodes before tumor metastasis (Qian, Berghuis *et al.* 2006; Hirakawa, Brown *et al.* 2007),

there was a tendency to pre-metastatic lymphatic vessel dilation in para-aortic lymph nodes. These results indicate lymphatic vasculature reorganization in sentinel lymph nodes before tumor cells arrival and provide clues to the active role of lymphatics in ovarian cancer dissemination.

The limit of patient-derived tumors is that they only grow *in vivo* by serial propagation in mice not allowing genetic manipulation.

On the contrary, tumor cells lines have the advantage to grow *in vitro*, they are easily infectable with specific genes in order to investigate their functions, or with reporter genes, to visualize cells with imaging instruments.

Given that neither 1A9 nor IGROV1 cells expressed VEGFC, it was decided to stably infect these cells with VEGFC to study its role in ovarian cancer progression, comparing the behavior of the infected cell lines with the wild type cells. The characterization of VEGFC overexpressing cell lines is described in the next chapter.

Intraovarian transplant was set up by injecting the cells directly under the bursa of the ovary of immunodeficient mice. The orthotopic model reproduces the appropriate tumor microenvironment, and mimic tumor-stroma interaction typical of the target organ, allowing the emergence of the biological features of ovarian cancer progression, angiogenic process, metastatic phenotype, resistance and therapeutic response to therapies similar to those observed in patients. A very important limit is the testing of mouse stroma and more important, the use of immunocompromised mice that does not allow to consider the involvement of immune system in cancer development and progression.

Usually, ovarian cancer patients undergo surgery to remove primary tumor and later are treated with chemotherapy. We therefore reproduced cytoreductive surgery of primary tumor in 1A9 model, to verify if surgery modified tumor behavior and metastasis, and to explore if the model was more representative of the clinical situation. Our results indicated a survival

advantage of cytoreduced mice, without any differences in the metastatic pattern compared to not surgical mice. For this reason, in the following experiments, it was decided not to remove the primary tumors from mice.

In summary, the models described in this chapter are complementary tools that have been used to analyze the role of VEGFC and VEGFR3 in tumor progression and metastasis and to study the efficacy of VEGFC/VEGFR3 inhibitors (Chapters 4 and 5 of this thesis).

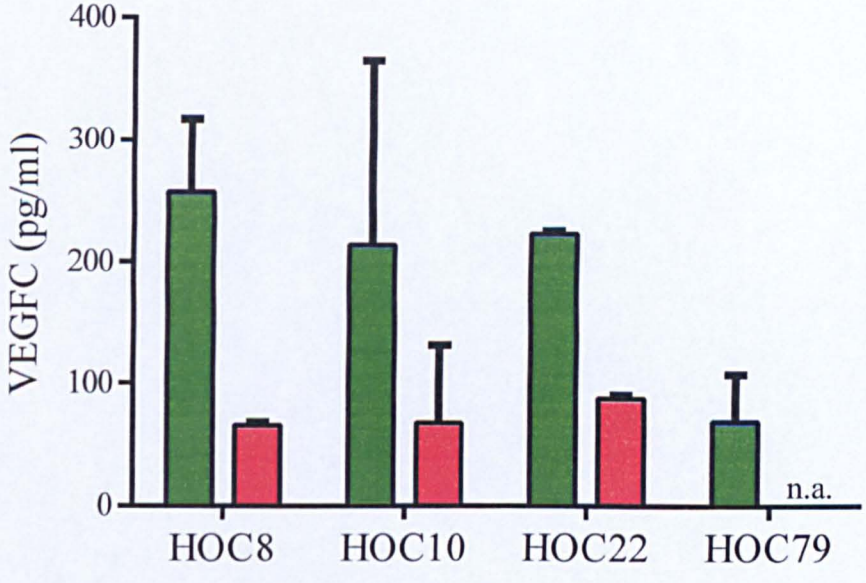


**Figure 3.1 VEGFC levels in patient-derived EOC-xenografts transplanted in nude mice.** Nude mice were transplanted intraperitoneally with the indicated HOC xenografts. VEGFC levels in ascitic fluids (green columns) and serum (red columns) were assayed by ELISA. Results are the mean ± SD of three mice per group. n.a. = not available.

A

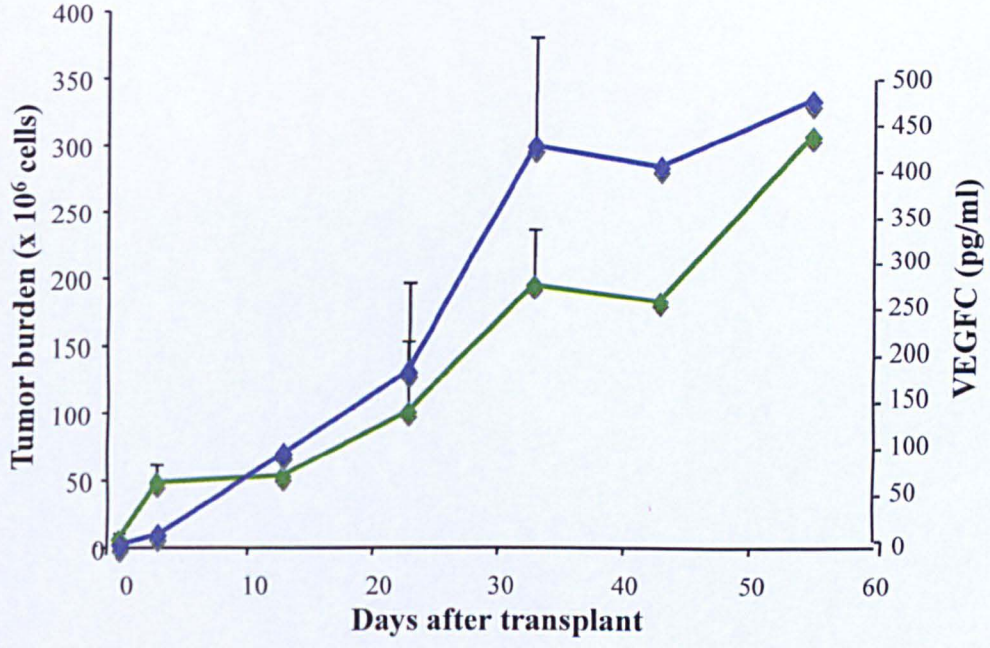


B

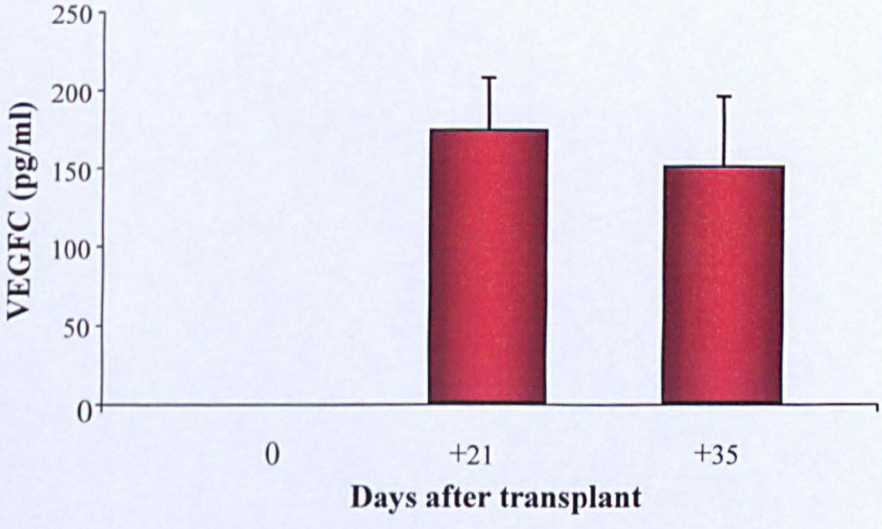


**Figure 3.2 Correlation between VEGFC levels and tumor progression in HOC8 xenograft.** (A) Nude mice were transplanted intraperitoneally with HOC8. Tumor burden (number of cells harvested from the peritoneal cavity, blue) and VEGFC (green) were measured in ascitic fluids by ELISA. Results are the mean ± SD of three mice per group for each time point. (B) Serum VEGFC was measured at the indicated time after tumor transplant. Results are the mean ± SD of seven mice per group for each time point.

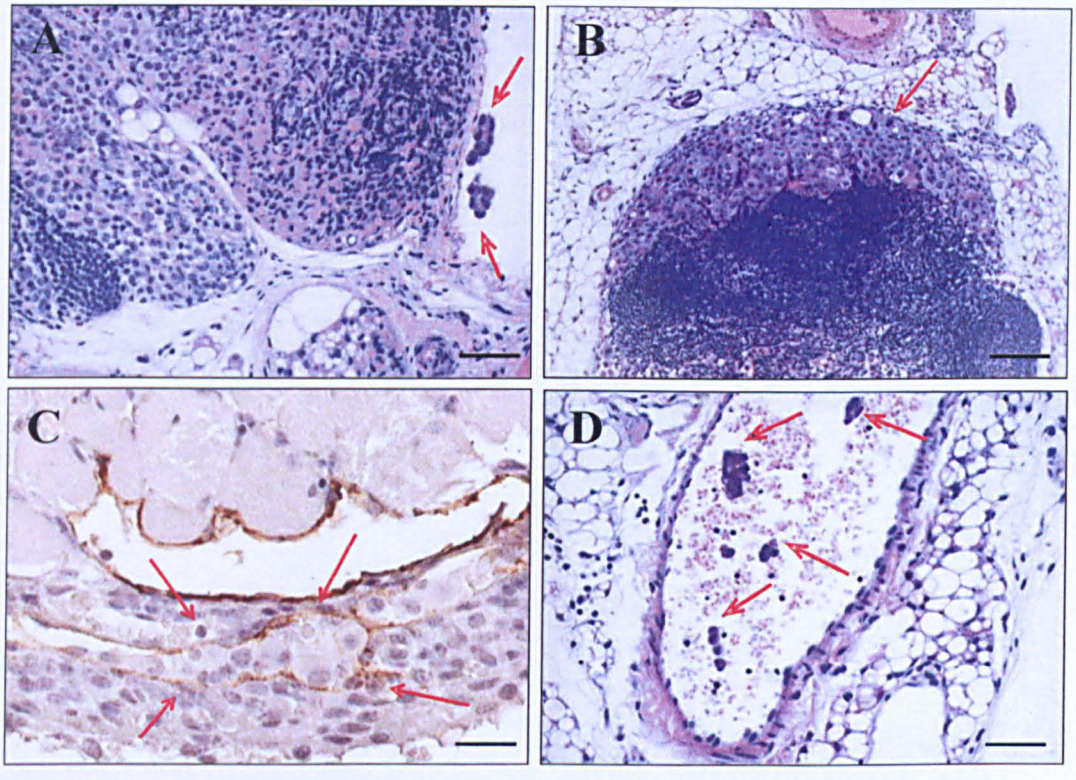


**Figure 3.3. Tumor cells invasion and localization.** (A-B) Representative histological images of lymph nodes. Histological analysis at different times after tumor transplant showed tumor cells (red arrows) outside (A) and inside (B) para-aortic lymph nodes on days +21 and +35 respectively. Tumor cells (red arrows) in diaphragmatic LYVE-1 positive lymphatic vessel (C) and a peritoneal blood vessel (D) 21 days after tumor transplant. (A,B,D) Scale bars represent 100 μm; (C) Scale bar represents 50 μm.

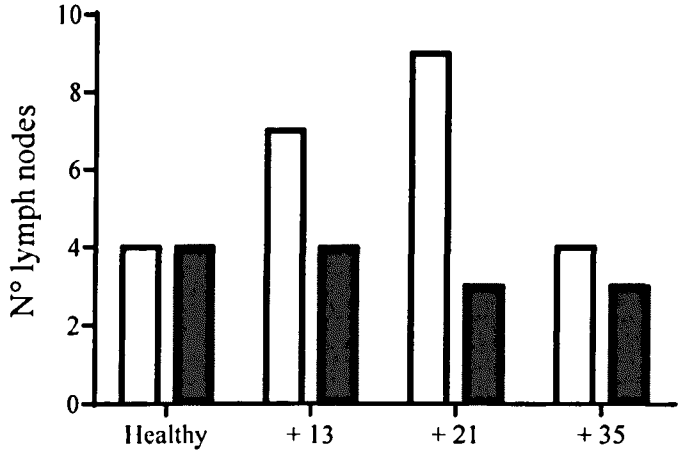


**Figure 3.4. Enlarged lymphatic vessels are present before the arrival of metastatic cancer cells.** An increased number of lymph nodes presenting enlarged lymphatic vessels was observed at days 13 and 21 after transplant. White and black columns indicated enlarged and not enlarged lymphatic vessels, respectively. n= 4-6 mice for each time point.

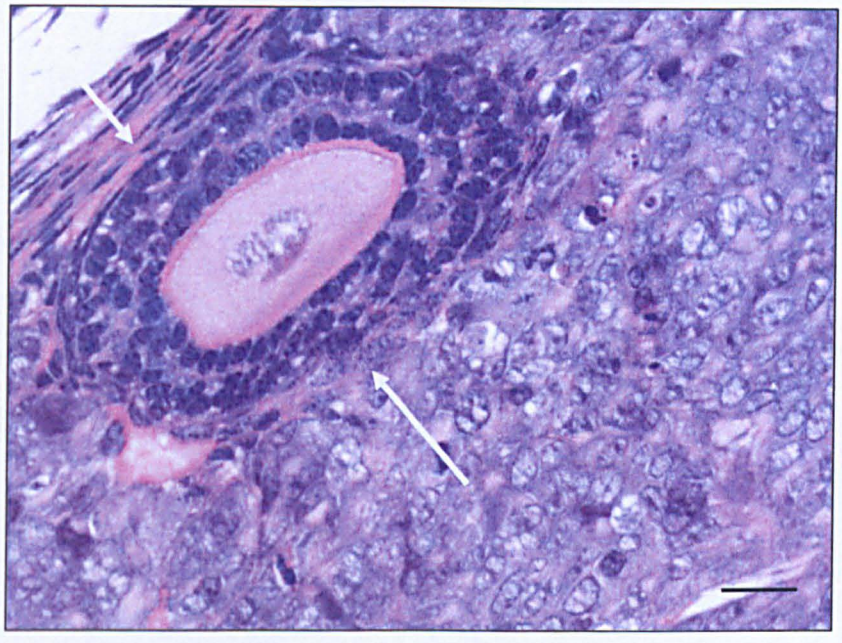

**Figure 3.5. Accuracy of injection.** Representative histological image of some ovarian structures (follicles with oocytes, white arrows) recognizable in some neoplastic masses thus indicating the accuracy of injection. Scale bar respresents 50 μm.

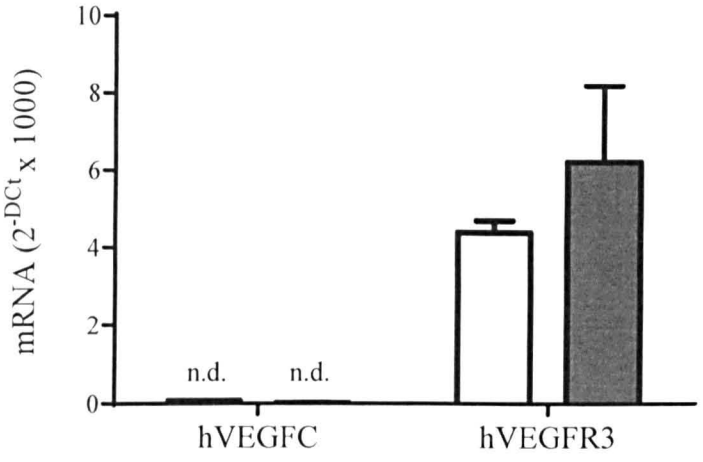


**Figure 3.6. Expression of hVEGFC and hVEGFR3 in 1A9 and IGROV1 cell lines.** RT-PCR. hVEGFC and hVEGFR3 mRNAs were normalized to HPRT1 housekeeping gene: $\Delta Ct = Ct_{target} - Ct_{HPRT1}$. Data are expressed as $2^{-\Delta Ct}$ x 1000 (mean and SD from one experiment representative of three). Experiments were run in triplicate. 1A9 = white columns; IGROV1 = grey columns. n.d. = not detectable.

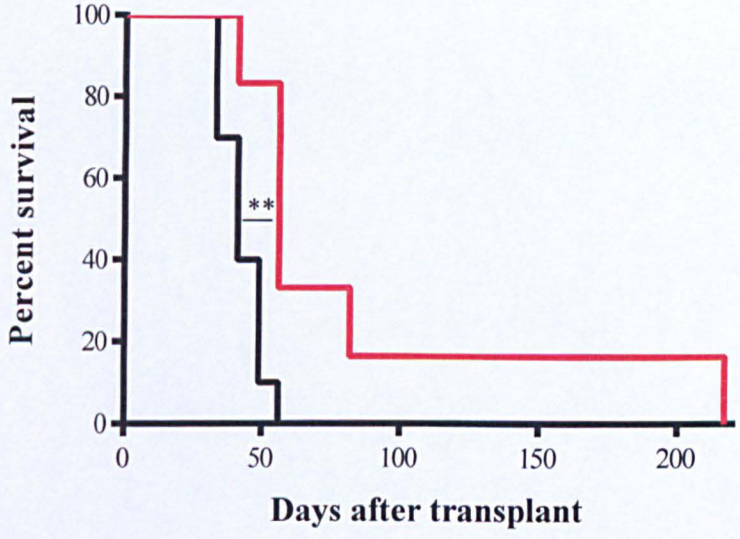


**Figure 3.7. Survival curve.** Effect of primary tumor surgically removal on the lifespan of mice bearing 1A9 intraovarian tumor. Control mice = black curve; surgical mice = red curve. n=6-10, **p<0.001.

| Xenograft | Histological type | Grade | Stage | Treated |
|---|---|---|---|---|
| HOC8 | serous | G3 | IV | NO |
| HOC10 | serous | G3 | IIIC | NO |
| HOC22 | serous | G3 | IIIC | YES |
| HOC79 | Endometroid + clear cell | G3 | IIIC | YES |

**Table 3.1. Panel of patient-derived EOC-xenografts transplanted in nude mice.** Clinicopathological characteristics of the tumors from ovarian cancer patients.

| Lymph nodes | | | | | |
|---|---|---|---|---|---|
| Days after transplant | N° mice | LN[1] | TC intra[2] (%) | TC extra[3] (%) | neg[4] (%) |
| + 21 | 7 | 14 | 0 (0%) | 10 (71%) | 4 (29%) |
| + 35 | 7 | 13 | 9 (69%) | 3 (23%) | 1 (8%) |

**Table 3.2. Para-aortic lymph nodes invasion of HOC8 transplanted mice.** (1) Number of lymph nodes (LN) analyzed. Lymph nodes with tumor cells (TC) located inside (2, intranodal) or outside (3, extranodal). (4) Lymph nodes negative for the presence of tumor cells.

| Presence of tumor cells | 1A9 | IGROV1 |
|---|---|---|
| Tumor take (left ovary) | 3/4 (75%) | 3/3 (100%) |
| Contralateral ovary | 0% | 2/3 (66%) |
| Para-aortic lymph nodes | 0% | 0% |

**Table 3.3. Metastatic behaviour of 1A9 and IGROV1 cells transplanted orthotopically under the bursa of the ovary of nude mice.** Histopathological analysis of transplanted left ovaries, contralateral right ovaries and para-aortic lymph nodes was done at day 20 for 1A9 and at day 28 for IGROV1. Data are the number (and percentage) of mice with metastatis over total mice.

| Presence of tumor cells | Control | Surgery |
|---|---|---|
| Tumor take (left ovary) | 9/9 (100%) | 6/6 (100%) |
| Relapse | - | 6/6 (100%) |
| Contralateral ovary | 0% | 0% |
| Para-aortic lymph nodes | 1/9 (11%) | 0% |

**Table 3.4. Metastatic behaviour of 1A9 intraovarian bearing mice undergoing surgery for the removal of primary tumor.** Histopathological analysis of transplanted left ovaries, relapsed tumor, contralateral right ovaries and para-aortic lymph nodes was done at sacrifice. Data are the number (and percentage) of mice with metastatis over total mice.

Chapter 4

# Characterization of VEGFC over-expressing cell lines

### 4.1 Introduction and goals

The studies presented in this chapter are aimed to study how VEGFC affects ovarian carcinoma progression.

In the previous chapter, it was shown that neither 1A9 nor IGROV1 cells expressed VEGFC. This fact makes both cell lines good candidates to be manipulated to over-express VEGFC by infection and thus studying and clarifying its role in ovarian cancer.

This chapter is also aimed to establish cell lines over-expressing reporter genes. As one of the limits of orthotopic transplant is the difficulty to follow tumor growth and progression, especially when tumors are small, infecting cells with reporter genes allows to facilitate the visualization of cancer cells *in vivo* by non-invasive optical imaging.

Two widely used non-invasive optical imaging techniques are bioluminescence imaging (BLI) or fluorescence imaging (FLI).

BLI utilizes native light emission from one of several organisms which naturally bioluminesce, for example the firefly. The DNA encoding the luminescent protein (the luciferase enzyme) is incorporated in the target (e.g. tumor cells) and then the substrate (D-luciferin) is required to be injected to the luciferase carrying target. The chemical reaction that occurs is this: D-luciferin + ATP + $O_2$ $\xrightarrow{\text{Luciferase}}$ Oxyluciferin + Light (photons).

As the reaction involves ATP, only viable cells can produce light after administration of the substrate.

FLI is based on the integration of an engineered fluorescent protein, essentially a fluorochrome, into a target recipient (e.g. tumor cells). This protein fluoresces, emitting photons of light after being excited from its ground state to a higher quantum state by a source of energy, for example a laser.

Thus, these two imaging techniques enable visualization of physiological and pathophysiological processes at the cellular and molecular level in different mouse models

with high specificity. Furthermore, in oncology preclinical research, optical imaging allows to visualize tumors, *in vivo*, and to follow tumor growth and progression in the same mice at different time points, avoiding killing animals, thus reducing the number of mice used in the experimentation.

The aims of this chapter are:

- To establish cell lines over-expressing reporter genes +/- VEGFC.
- To test VEGFC paracrine and autocrine activities, *in vitro*, on lymphatic and infected ovarian tumor cells respectively.
- To characterize the VEGFC over-expressing cell behavior *in vivo*, analyzing tumor growth and metastasis.

***Part of the work presented is a manuscript in press in American Journal of Pathology, 2014.***

### 4.2 Generation of cell lines over-expressing reporter genes

Both, 1A9 and IGROV1 cells were infected with lentiviral vector carrying the coding sequence for luciferase or for Katushka, a far-red mutant of the red fluorescent protein from sea anemone *Entacmaea quadricolor* (Shcherbo, Merzlyak *et al.* 2007) and bioluminescence and fluorescence compared in order to select the best model.

Luc2 gene was integrated into a pLenti6.3/V5-DEST destination vector using Gateway® technology. Then a lentiviral stock was produced co-transfecting the pLenti-luc and the viral vectors packaging mix into the 293FT cell line, and finally the lentiviral stock was used to transduce 1A9 and IGROV1 cells to obtain stably infected cell lines (1A9-luc and IGROV1-luc). The evaluation of the luciferase expression is described in the section 4.2.1 of this chapter.

A portion of 1A9-luc and IGROV1-luc cells were also infected with Katushka, to direct compare BLI and FLI in the same mice.

Katushka gene was integrated into a pLenti6.3/V5-DEST destination vector, using Gateway® technology. Then a lentiviral stock was produced co-transfecting the pLenti-Kat and the viral vectors packaging mix into the 293FT cell line, and finally the lentiviral stock was used to transduce 1A9-luc and IGROV1-luc cells, previously infected with luciferase, to obtain stably infected cell lines (1A9-Kat-luc and IGROV1-Kat-luc). The evaluation of the Katushka expression is described in the section 4.2.2 of this chapter.

Thus, 1A9-luc, 1A9-Kat-luc, IGROV1-luc and IGROV1-Kat-luc cells were obtained.

*4.2.1 Evaluation of the luciferase expression and the sensitivity of BLI detection system*

To verify the expression of luciferase by 1A9-luc and IGROV1-luc cells and so as to evaluate the sensitivity of BLI detection system, cells were seeded at increasing concentration, ranging from $1x10^6$ to $3.125x10^4$, in a 96-well black plate. Bioluminescence signal was detected 10 min after the addition of D-Luciferin substrate into the cell medium (Figure 4.1A) with eXplore optix MX2. Images analyzed with Optiview software showed that light intensity of infected cells, expressed as photon counts, strongly correlated with cell number both in 1A9-luc (Figure 4.1B, $r^2=0.9708$, ***$p<0.0001$) and IGROV1-luc (Figure 4.1C, $r^2=0.9973$, ***$p<0.0001$) cells.

*4.2.2 Evaluation of Katushka expression*

Cells were analysed for the expression of Katushka using a FACSTAR (Becton Dickinson, Mountain View, CA) in collaboration with Sergio Bernasconi, IRCSS - Istituto di Ricerche Farmacologiche Mario Negri, Milan, Italy.

The percentage of infected cells were calculated measuring the fluorescence through a 620 nm band pass filter after illumination with the 488 nm line of an argon ion laser. The percentage of 1A9-Kat-luc cells expressing the red fluorescent protein was 97.62%, and the percentage of IGROV1-Kat-luc cells was 89.32%.

To evaluate cell viability and proliferation of the infected cells, growth curve and doubling time were determined.

A significant difference in growth rate and doubling time between 1A9-luc and 1A9-kat-luc cells was observed (Figure 4.2A). The doubling time was 13 hours and 19.6 hours for 1A9-luc and 1A9-Kat-luc, respectively. On the contrary, growth rate was not significantly different between IGROV1-luc and IGROV1-Kat-luc (Figure 4.2B). The median of the doubling time of three independent experiments was 18 hours for both cell line variants.

The shape of the 1A9 Katushka infected cells (Figure 4.2D) was different from 1A9-luc cells (Figure 4.2C), while no differences were observed between IGROV1-luc variants (Figures 4.2F and 4.2G).

*4.2.3 Comparison between bioluminescence (BLI) and fluorescence imaging (FLI) in vivo*

In order to understand whether the two techniques were useful *in vivo*, in detecting tumors at very early stage (this point was very important, considering that the imaging would be used in the following experiments to verify tumor take and to randomize mice before therapy), 1A9-Kat-luc and IGROV1-Kat-luc cells were transplanted under the bursa of the ovary of nude mice. At days 2, 7, 10 and 16 mice were imaged with eXplore Optix MX2 for both bioluminescence and fluorescence emission. Briefly, mice were placed on the ventral or lateral side onto the warmed stage inside the camera box and then were scanned for fluorescence using the 635 nm excitation wavelength pulse laser. After image acquisition

mice were injected intraperitoneally with D-luciferin substrate and, after 10 minutes, imaged for bioluminescence production.

The images obtained with FLI were not very specific, background was evident in both cell lines, especially in correspondence of scars (due to surgery for intraovarian transplant) (Figures 4.3A and 4.3B). Only at day 16, a small signal was visible in IGROV1-kat-luc mice (Figure 4.3B).

On the contrary, BLI was very specific: tumor cells were already detected at day 7 for 1A9-Kat-luc and at day 2 for IGROV1-Kat-luc, and it was possible to follow tumor growth (the photon counts scale increased with time, indicating that also the signal was becoming brighter and thus the tumor bigger) and progression. As already observed *in vitro*, 1A9-Kat-luc cell growth was very slow. Indeed, photon counts measured by BLI in 1A9-Kat-luc tumor only reached a peak of 362 photon counts at day 16. On the contrary, IGROV1-Kat-luc reached a peak of $1.42 \times 10^4$ photon counts.

On the basis of these results, further experiments were carried on using the 1A9-luc and IGROV1-luc cell lines, infected with luciferase only, instead of the luciferase+Katushka-infected ones.

## 4.3 *In vitro* characterization of VEGFC over-expressing ovarian cancer cell lines

### *4.3.1 Establishment of VEGFC over-expressing cell lines*

To investigate the role of VEGFC in ovarian carcinoma progression, 1A9-luc and IGROV1-luc cells, which do not express VEGFC, were lentivirally infected to over-express the gene.

In particular, two different isoforms of VEGFC with different grade of processing (full-length and mature form of VEGFC) were used. The full-length VEGFC binds only to VEGFR3 and can undergo a series of proteolytic processes to become the mature form of VEGFC that has higher affinity to VEGFR3 and can also bind to VEGFR2.

Briefly, the coding sequence of the full-length VEGFC isoform (VEGFCfl, 1290 bp) or its proteolitically activated mature form (VEGFCmf, 490 bp), were integrated into pLenti6.3/V5-DEST destination vectors, using Gateway® technology. Then lentiviral stocks were produced co-transfecting the pLenti-VEGFCfl or pLenti-VEGFCmf and the viral vectors packaging mix into the 293FT cell line, and finally the two lentiviral stocks were used to transduce 1A9-luc and IGROV1-luc cells to obtain stably infected cell lines (1A9-luc/VEGFCfl, 1A9-luc/VEGFCmf, IGROV1-luc/VEGFCfl and IGROV1-luc/VEGFCmf).

*4.3.2 Evaluation of VEGFC expression and release*

The expression of VEGFC was investigated in 1A9 and IGROV1 cell variants by quantitative Real Time PCR using Taqman® technology.

Gene expression analysis confirmed that VEGFC was undetectable in wild type and luciferase infected cells, while a high expression of the gene was observed in the VEGFC-infected cells (Figure 4.4). In particular, the relative gene expression calculated as $2^{-\Delta Ct}$ x 100 was higher in VEGFC full length-infected cells (76 and 23 for 1A9-luc/VEGFCfl and IGROV1-luc/VEGFCfl, respectively) than in cells expressing the mature form of VEGFC (25 and 11 for 1A9-luc/VEGFCmf and IGROV1-luc/VEGFCmf, respectively).

Soluble VEGFC was also analyzed by ELISA in serum-free conditioned medium collected after 4, 24 and 48 hours. VEGFC was not detected in the conditioned media of either 1A9-luc or IGROV1-luc cells (Figure 4.5), confirming the specificity of the assay. The release of VEGFC in conditioned medium was time dependent. In particular the amount of VEGFC released by 1A9luc/VEGFCfl and 1A9-luc/VEGFmf increased with time and reached 7664 pg/ml and 5005,8 pg/ml, respectively, after 48 hours (Figure 4.5A). Similar increasing trend was observed after 48 hours in the conditioned medium of IGROV1-luc/VEGFCfl and

IGROV1-luc/VEGFCmf, where VEGFC reached 3129 and 728,8 pg/ml, respectively (Figure 4.5B).

*4.3.3 Biological activity of secreted VEGFC*

The biological activity of VEGFC released by tumor cells was verified as the ability to stimulate mouse lymphatic endothelial cell (MELC) migration. Conditioned medium of 1A9-luc cells over-expressing VEGFC induced greater MELC migration than medium conditioned by 1A9-luc control cells (Figure 4.6A). Increased MELC migration was observed also with conditioned medium of IGROV1-luc/VEGFCfl and IGROV1-luc/VEGFCmf compared to medium conditioned by IGROV1-luc control cells (Figure 4.6B). Conditioned medium of the two tumor variants secreting different amounts of VEGFC stimulated MELC migration equally, suggesting greater activity of mature VEGFC on cell motility. The specificity of the effect was shown on IGROV1-luc/VEGFCmf-induced migration by the activity of the recombinant VEGFR3/Fc chimera. The structure of the human VEGFR3/Flt-4 Fc chimera is a fusion between the N-terminus of Flt-4 protein and the C-terminus of the human IgG1 antibody, thus the chimera specifically binds to VEGFC and VEGFD, and consequently inhibits their activity. It was observed that the chimera inhibited 70% of migration (Figure 4.6B), whereas an irrelevant antibody (IgG1) did not cause any significant inhibition.

*4.3.4 Cell proliferation*

To evaluate whether cell proliferation and doubling time were affected by the infection with VEGFC, the growth curve was determined. Briefly, tumor cells were plated in 96-wells culture plates in complete medium and after 4, 24, 48, 72 or 96 hours cells were stained with crystal violet and the absorbance, proportional to the number of cells, read at 595 nm.

Neither daily growth rates nor total growth after 96 hours were significantly different between VEGFC wild-type and VEGFC-overexpressing cells (Figure 4.7). The media of the doubling time of three independent experiments was 16, 15 and 15.9 hours respectively for 1A9-luc, 1A9-luc/VEGFCfl and 1A9-luc/VEGFmf (Figure 4.7A). IGROV1-luc, IGROV1-luc/VEGFCfl and IGROV1-luc/VEGFCmf doubled respectively in 18, 18.4 and 19.7 hours (Figure 4.7B).

*4.3.5 Autocrine activity: VEGFR3 gene and protein expression*

Besides the paracrine activity of VEGFC through VEGFR3 located on lymphatic endothelial cells, the VEGFC/VEGFR pathway has been reported to influence tumor progression also through autocrine mechanisms (Su, Yang *et al.* 2006; Kodama, Kitadai *et al.* 2008) through VEGFRs expressed by the tumor cells.

VEGFR3 and VEGFR2 tumor cell expression was analyzed. 1A9 and IGROV1 expressing VEGFC or not, constitutively expressed comparable levels of VEGFR3 mRNA (Figure 4.8A). VEGFR2 mRNA was detectable at very low levels in 1A9 variants, while it was not detectable in any of the variants of IGROV1 cells (data not shown).

The expression level of VEGFR3 on cell surfaces was measured by MiSEP technology.

VEGFR3 protein was expressed at comparable levels in 1A9-luc, 1A9-luc/VEGFCfl and 1A9-luc/VEGFCmf (Figure 4.8B). Comparable levels of VEGFR3 were also measured in IGROV1 variants (Figure 4.8B).

*4.3.6 Autocrine activity: migration*

To demonstrate that VEGFC released by infected cells acted in an autocrine manner, cell migration was analysed. Medium conditioned by VEGFC-over-expressing 1A9-luc induced greater cell migration than medium conditioned by control 1A9-luc (Figure 4.9A). Similarly,

an increment of cell migration was observed on IGROV1-luc cells stimulated with IGROV1-luc/VEGFCfl or IGROV1-luc/VEGFCmf conditioned medium compared to control IGROV1-luc medium (Figure 4.9B), suggesting that VEGFC may directly influence tumor cell dissemination through an autocrine mechanism. VEGFCmf conditioned medium stimulated tumor cell motility significantly more than VEGFCfl conditioned medium in both cell lines, confirming the greater activity of mature VEGFC as chemoattractant. Migration induced by the conditioned medium of VEGFC expressing cells, but not of control cells, was completely prevented by the VEGFR3/Fc chimera, demonstrating the specificity of the effect (Figures 4.9C and 4.9D). Similarly, cediranib (10 nM), a tyrosine kinase receptor inhibitor of VEGF receptors, significantly inhibited 1A9-luc migration in response to the conditioned medium of 1A9-luc/VEGFCmf cells (Figure 4.9E), and IGROV1-luc migration in response to the conditioned medium of IGROV1-luc/VEGFCmf cells (Figure 4.9F), confirming the autocrine activity of the VEGFC/VEGFR3 pathway on tumor cell motility and suggesting that the compound might potentially affect VEGFC-induced tumor dissemination also by directly acting on the tumor cells.

## 4.4 *In vivo* characterization of VEGFC over-expressing ovarian cancer cell lines

Having demonstrated that VEGFC has both paracrine and autocrine activities on lymphatic endothelial cell and tumor cell migration, the effect of the overexpression of VEGFC was investigated *in vivo*, comparing the behavior of wild type tumors to tumors infected with VEGFCfl or VEGFCmf.

### *4.4.1 Tumor growth and progression*

The three 1A9 tumor variants (1A9-luc, 1A9-luc/VEGFCfl and 1A9-luc/VEGFCmf) were injected orthotopically under the bursa of the ovary of nude mice and tumor growth followed

by BLI. Tumor growth was more rapid in 1A9-luc/VEGFCmf than 1A9-luc control tumors at day 30, although not significantly (Figure 4.10A).

IGROV1-luc over-expressing VEGFC, either the proform or its proteolytically activated form, grew faster than control tumors, when injected othotopically into the ovary of immunodeficient mice. Twenty-four and twenty-eight days after tumor cell injection, mice bearing IGROV1-luc/VEGFCmf and IGROV1-luc/VEGFCfl, respectively, had a significantly higher tumor burden than mice with the respective control tumors (Figure 4.10B).

Differences in tumor burden did not reflect survival of mice bearing luciferase or VEGFC over-expressing cells. Indeed, the MST of 1A9-luc, 1A9-luc/VEGFCfl and 1A9-luc/VEGFCmf-bearing mice were 29, 23.5 and 30 days, respectively (Figure 4.10C). MST of mice bearing IGROV1-luc, IGROV1-luc/VEGFCfl and IGROV1-luc/VEGFCmf tumors were 28, 35 and 28 days, respectively (Figure 4.10D).

As differences in tumor growth were more evident in IGROV1-luc, we selected IGROV1-luc infected variants (instead of 1A9-luc) to investigate more deeply the effect of VEGFC over-expression on this tumor model.

### *4.4.2 VEGFC release*

The release of VEGFC into the serum of mice transplanted with IGROV1-luc, IGROV1-luc/VEGFCfl and IGROV1-luc/VEGFCmf was analyzed by ELISA assay. As expected, only mice with VEGFC infected cells had detectable VEGFC in their serum (Figure 4.11A). VEGFC levels increased with time in both IGROV1-luc/VEGFfl and IGROV1-luc/VEGFCmf-bearing mice and correlated positively with tumor burden expressed as photon counts in both IGROV1-luc/VEGFCfl (***p=0.0043, $R^2$=0.9914, Figure 4.11B) and IGROV1-luc/VEGFCmf (***p=0.0004, $R^2$=0.9992, Figure 4.11C) tumors.

*4.4.3 Metastasis and lymphangiogenesis*

Organs of the periotoneal cavity and para-aortic lymph nodes of mice bearing IGROV1-luc, IGROV1-luc/VEGFfl or IGROV1-luc/VEGFCmf were analysed by histopathology.

Histopathological analysis indicated that the VEGFC-infected variants, particularly the over-expressing mature VEGFC, metastasized more efficiently to the diaphragm, the retroperitoneal space and the contralateral ovary than control cells. Ninety-two percent of mice transplanted with IGROV1-luc/VEGFCmf presented neoplastic masses to the diaphragm, 67% to the retroperitoneal space and 27% to the contralateral ovary (Table 4.1).

To verify whether tumor metastasis was associated with induction of lymphangiogenesis and/or angiogenesis, immunohistochemical staining of primary tumors with anti-LYVE-1 and anti-CD31 antibodies was done on IGROV1-luc and IGROV1-luc/VEGFCmf. Lymphatic vessels were detected only at the periphery of primary tumors, in the ovarian septa and capsule (Figures 4.12A and 4.12B). There was no real difference in lymphatic vessel number between tumors releasing VEGFC or not. In a few cases LYVE-1 stained vessels invaded by tumor cells were observed but exclusively in tumors expressing the mature form of VEGFC (Figure 4.12B inset).

CD31-positive blood vessels were located inside the primary tumor parenchyma, as well as in the ovarian capsule and septa (Figures 4.12C and 4.12D). The number of blood vessels was higher, though not significantly, in VEGFC-over-expressing tumors (median 6.0, range 4-10) than in control tumors (median 3.9, range 3-6). The difference in blood vessel number between the tumor variants was not due to any difference in their capability to recruit inflammatory cells, since F4-80+/LYVE-1+ (a mature macrophage specific antigen) cells were present in both variants without noteworthy differences (data not shown).

### 4.5 Summary of results

The data presented in this chapter can be summarized as follows:

- Bioluminescent and fluorescent cell lines are established: light intensity strongly correlates with cell number.
- Bioluminescent cell lines are chosen because of more specific signal *in vivo*.
- VEGFC over-expressing cells are established.
- VEGFC is expressed and released in conditioned medium of infected cells.
- Secreted VEGFC is biologically active and stimulates mouse lymphatic endothelial cell migration.
- VEGFC does not affect cells proliferation *in vitro*.
- Soluble VEGFC has autocrine activity: it induces the migration of VEGFR3-expressing tumor cells. The migration is prevented by VEGFR3/Fc chimera or cediranib.
- VEGFC over-expressing cells grow faster than wild-type cells when transplanted orthotopically under the bursa of the ovary of nude mice, without effect in mouse survival.
- VEGFC is released in serum of mice bearing VEGFC over-expressing cells and it correlates with tumor burden.
- Mice transplanted with VEGFCmf cells present increased metastasis in the organs of the peritoneal cavity (e.g. diaphragm, retroperitoneal space and contralateral ovary).
- Lymphangiogenic activity is apparently not present, though presence of tumor cells in LYVE-1 stained vessels is observed exclusively in tumors expressing VEGFCmf.
- Angiogenic activity is present as there is a tendency to develop more intratumoral blood vessels (CD31+) in VEGFC-over-expressing tumors.

## 4.6 Discussion

Non-invasive optical imaging techniques, such as BLI and FLI, have emerged as important tools in biomedical research.

In this chapter, it was noted that Kathuska was toxic in 1A9-Kat-luc cells, as a slower cell growth (both *in vitro* and *in vivo*) was observed compared to control cells. And also the shape of 1A9-Kat-luc cells was different from the 1A9-luc. Indeed, limits of fluorescent proteins that emit in the red orange are the unsuitable subcellular localization and protein-induced toxicity, especially if proteins tend to aggregate (Shaner, Steinbach *et al.* 2005; Shemiakina, Ermakova *et al.* 2012). The same toxicity was not observed in IGROV1-Kat-luc cells. This different behavior between 1A9-Kat-luc and IGROV1-Kat-luc cells could be explained by the different amount of Katushka protein expressed by the cells: 1A9-Kat-luc cells expressed more Katushka (cells were brighter) than IGROV1-Kat-luc. Thus, more integration of Katushka gene is reflected in more toxicity for cells.

VEGFC, the main promoter of lymphangiogenesis, is expressed in a number of tumors and has regulatory functions in their progression and dissemination. Whereas some early studies reported a role in the invasive phenotype of ovarian carcinoma, its contribution in the pathophysiology of ovarian cancer is far from be clear.

In this chapter it was demonstrated that VEGFC may significantly promote the growth and dissemination of ovarian cancer and that an autocrine effect through VEGFR3 on tumor cells might be a critical mechanism for this activity.

The effect of VEGFC in ovarian tumor progression was investigated in a model of ovarian cancer cells over-expressing VEGFC growing orthotopically in the mouse ovary. This model presents several advantages over subcutaneous or intraperitoneal injection of tumor cells as it reproduces the primary site of tumor growth where tumor cells interact with the appropriate

microenvironment and reproduces the pattern of dissemination observed in patients. The limit of the orthotopic transplant is that is not possible to check tumor take and to follow tumor progression, especially for tumors that grow deeply into the peritoneal cavity of mice. Ovarian tumor cells stably expressing luciferase overcome this limit enabling to track growth and dissemination of ovarian tumors in real time.

In this chapter it was shown that VEGFC promotes *in vivo* tumor growth and metastatic spread of ovarian cancer cells to the diaphragm and the retroperitoneal space, the most common sites of ovarian tumor dissemination (Sehouli, Senyuva *et al.* 2009). VEGFC is considered to drive the spread of tumor cells to lymph nodes in some tumors, such as breast cancer and melanoma (Skobe, Hamberg *et al.* 2001; Skobe, Hawighorst *et al.* 2001). However, over-expression of VEGFC in IGROV1-luc ovarian cancer cells was not sufficient to induce para-aortic lymph node colonization, suggesting that other factors are involved in driving nodal metastasis in this pathology. Accordingly, in human gastric (Kodama, Kitadai *et al.* 2008), lung carcinoma models (He, Kozaki *et al.* 2002) and human soft-tissue sarcoma (Lahat, Lazar *et al.* 2009), VEGFC was described as not being the only rate-limiting factor for metastasis.

VEGFC detected in serum of mice bearing VEGFC-overexpressing cells correlated with tumor burden, supporting also in these models the possible use of VEGFC released in biological fluids as an indicator of tumor burden and invasion.

Although similar amounts of VEGFC were detected in serum of mice, mature VEGFC had a greater effect in inducing metastasis. These findings are in agreement with the fact that stepwise proteolytic processing of VEGFC proforms generates several VEGFC forms with greater activity and affinity towards VEGFR3 (Joukov, Sorsa *et al.* 1997). The stronger biological activity of VEGFC mature form compared to proforms was confirmed by the finding that the conditioned medium of IGROV1-luc infected with mature VEGFC stimulated

lymphatic endothelial cell motility as efficiently as the conditioned medium of IGROV1-luc infected with full-length VEGFC, despite the smaller amounts of mature VEGFC in the conditioned medium. The same effect was observed in another cell line, the 1A9-luc, where 1A9-luc/VEGFCmf and 1A9-luc/VEGFCfl stimulated MELC motility with the same efficiency, even if higher amount of VEGFC were released by 1A9-luc/VEGFCfl.

The mechanism by which the mature form of VEGFC increased metastasis in these models might depend on autocrine or paracrine VEGFC activities. It was shown that the VEGFC/VEGFR3 autocrine loop can potentially enhance ovarian cancer progression. This was demonstrated by the autocrine stimulation of cell motility by VEGFC on both IGROV1-luc and 1A9-luc tumor cells expressing VEGFR3.

The specificity of VEGFR3/Fc chimera for VEGFC blocking motility served as an additional confirmation that VEGFC is involved in IGROV1 cell motility.

The expression and role of VEGFR3 in tumor cells has been debated. Some studies restricted the expression of VEGFR3 to blood and lymphatic vessels (Petrova, Bono *et al.* 2008), while others showed that VEGFR3 is expressed in a wide variety of malignant cells, including melanoma (Mouawad, Spano *et al.* 2009), prostatic cancer (Kaushal, Mukunyadzi *et al.* 2005), non-small cell lung cancer (Arinaga, Noguchi *et al.* 2003), neuroblstoma (Beierle, Dai *et al.* 2004) and colorectal adenocarcinoma (Witte, Thomas *et al.* 2002). It is therefore apparent that many tumor cells express VEGFR3 and the responses induced by the VEGFC/VEGFR3 pathway vary with the tumor type. Although VEGFC released by the infected IGROV1-luc cells was biologically active and stimulated mouse lymphatic endothelial cell migration *in vitro,* it apparently did not have lymphangiogenic activity in the ovarian tumor *in vivo*. It was noted that lymphatic vessel staining in the primary tumor was peritumoral rather than intratumoral, as previously described (Fadare, Orejudos *et al.* 2008), with no differences in lymphatic microvessel density between VEGFC-over-expressing and

control tumors. However, tumor cells were detected in lymphatics in VEGFC-over-expressing tumors only, indicating that lymphatic vessels were somehow activated by VEGFC, favoring tumor cell entry. Results from Issa *et al.* support this, demonstrating that VEGFC promotes tumor invasion toward lymphatics by increasing lymphatic secretion of CCL21 which, in turn, drives CCR7-dependent chemotactic tumor invasion (Issa, Le *et al.* 2009).

VEGFC stimulated the tumor growth rate *in vivo*, but not tumor cell proliferation *in vitro*. This can be explained by the complex interaction between tumor cells, host cells and the *in vivo* microenvironment. The tendency to develop more intratumoral blood vessels in VEGFC-overexpressing IGROV1 tumors compared to control tumors indicates that VEGFC-stimulated angiogenesis might contribute to the enhanced growth of IGROV1-luc over-expressing VEGFC.

In conclusion, the mature form of VEGFC contributes to ovarian carcinoma progression by directly acting on tumor cells, at the same time inducing angiogenesis and lymphatic vessel activation. Blocking the VEGFC/VEGFR3 pathway might improve the outcome of patients with ovarian cancer through direct antitumor activity in addition to anti-lymphangiogenic and anti-angiogenic effects (Chapter 5).

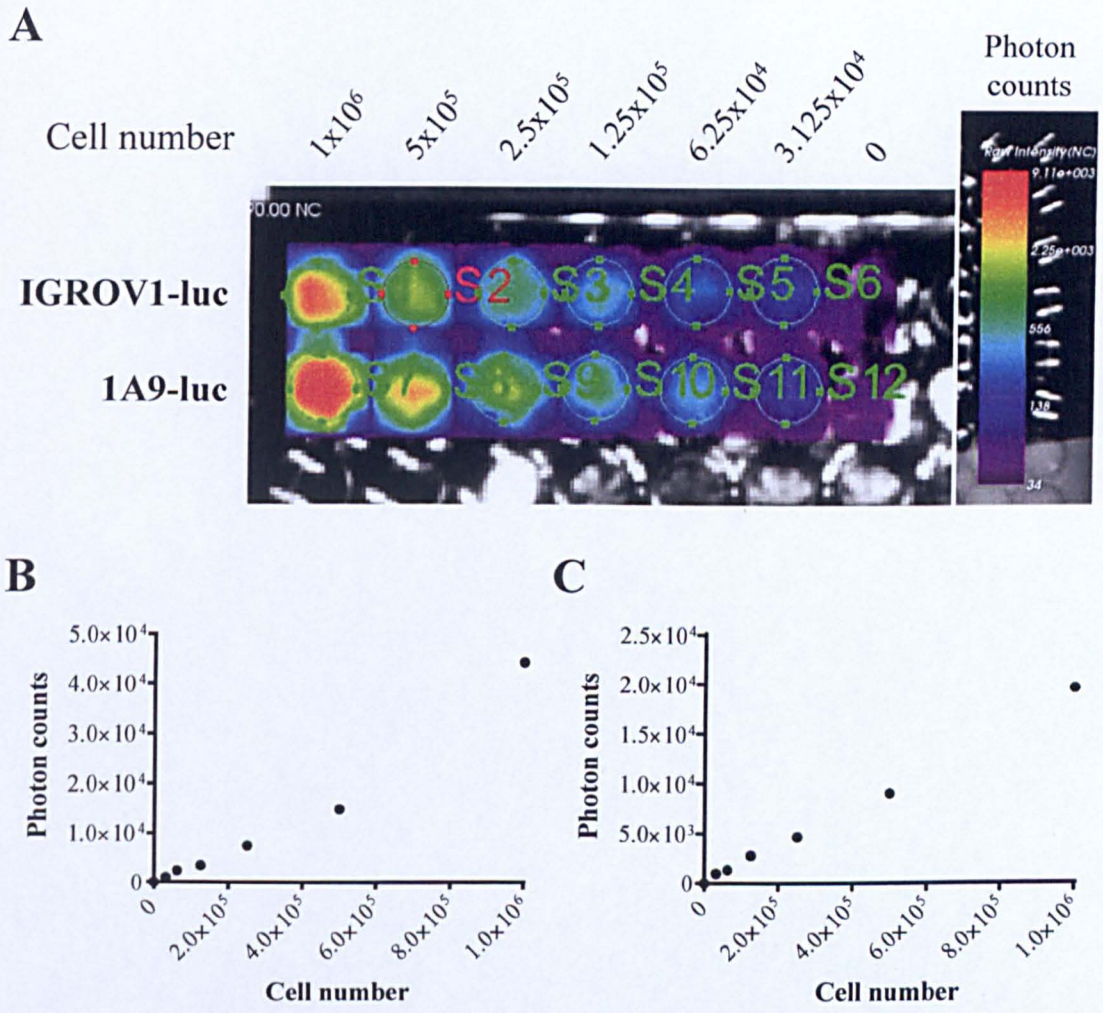


**Figure 4.1 Correlation between cell number and bioluminescence (BL).** (A) A representative image of infected cells in vitro. 1A9-luc and IGROV1-luc cells were seeded at densities of 1 X $10^6$ to 3.125 X $10^4$ and imaged 10 minutes after adding D-luciferin. The experiment was repeated twice. (B) Number of 1A9-luc cells per well plotted against photon counts. Number of cells correlated with amount of emitted light ($r^2$=0.9708, ***p<0.0001). (C) Number of IGROV1-luc cells per well plotted against photon counts. Number of cells correlated with amount of emitted light ($r^2$=0.9973, ***p<0.0001).

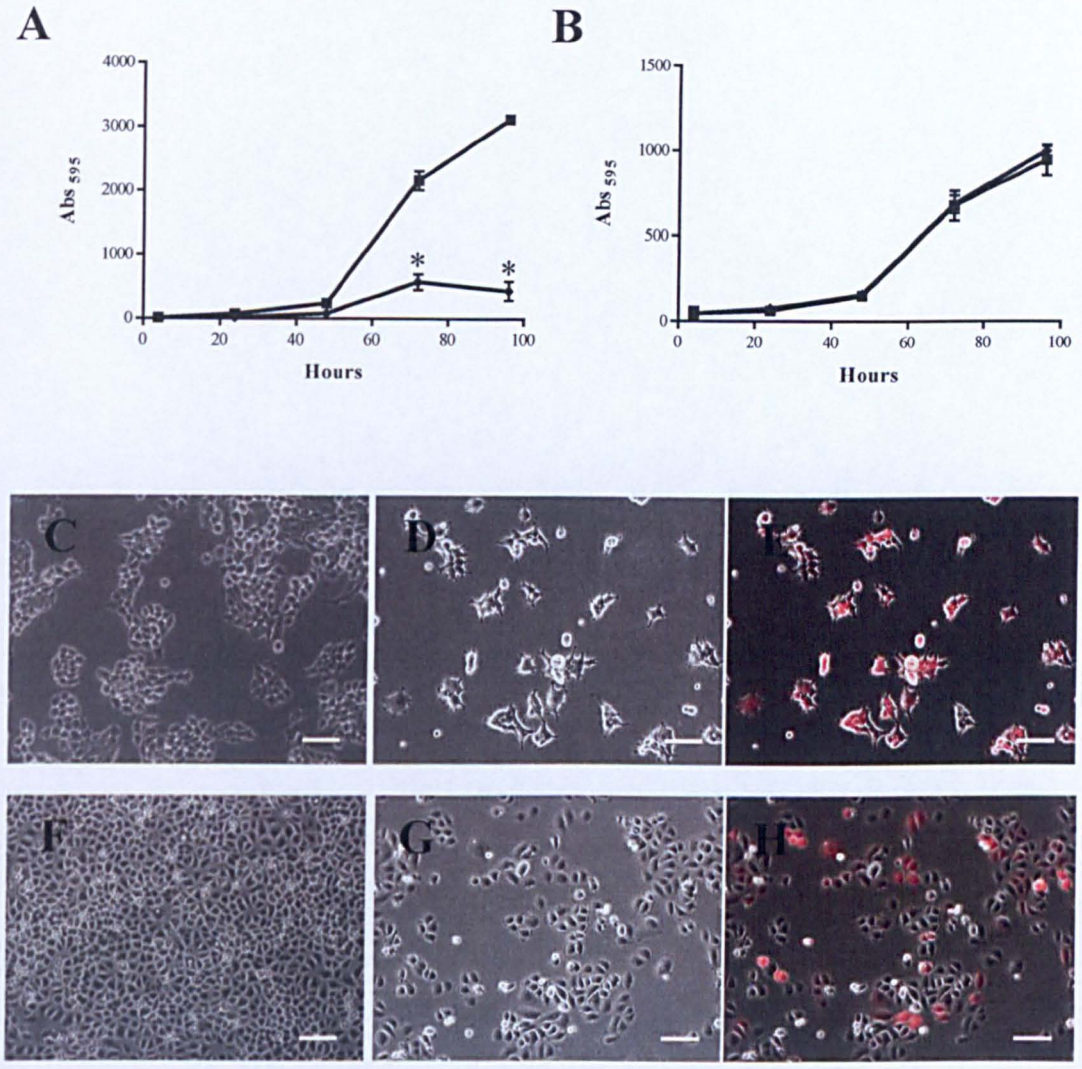


**Figure 4.2 Behaviour of Katushka-expressing cells.** (A-B) Growth curves. Proliferation capacity measured by absorbance at 595 nm *(Abs595)* every 24 hours. Data are mean of five replicates representative of three experiments. (A) 1A9-luc (squares) and 1A9-Kat-luc (diamonds). *$p<0.05$. (B) IGROV1-luc (squares) and IGROV1-Kat-luc (diamonds). (C) Brightfield image of 1A9-luc. (D-E) Brightfield (D) and fluorescence (E) images of 1A9-Kat-luc. (F) Brightfield image of IGROV1-luc. (G-H) Brightfield (G) and fluorescence (H) images of IGROV1-Kat-luc. Scale bars represent 100 μm.

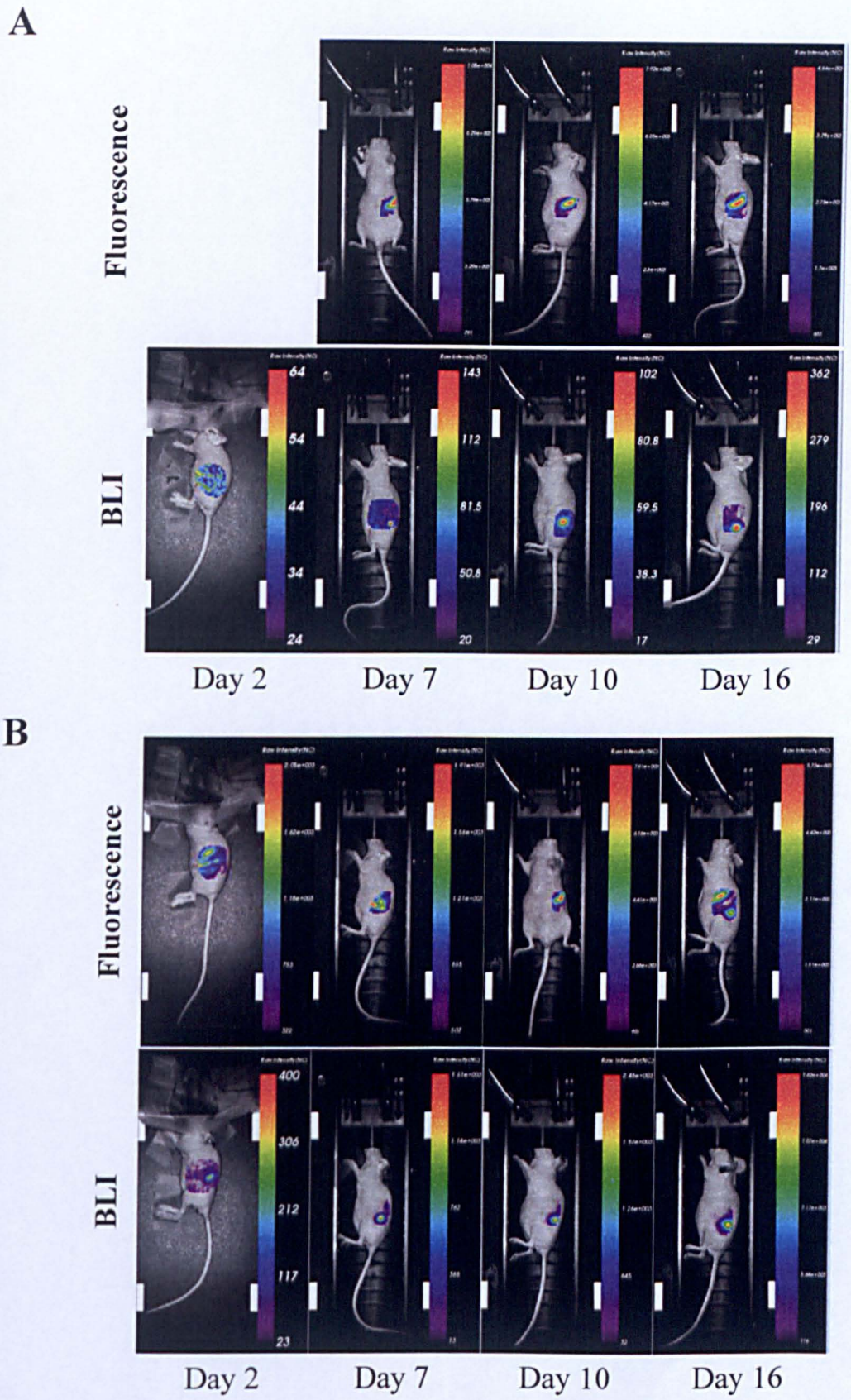


**Figure 4.3 Comparison between FLI and BLI techniques in vivo.** Representative images of the same mouse transplanted under the bursa of the ovary with (A) 1A9-Kat-luc or (B) IGROV1-Kat-luc and imaged ate day 2, 7, 10 and 16 for fluorescence and bioluminescent imaging.

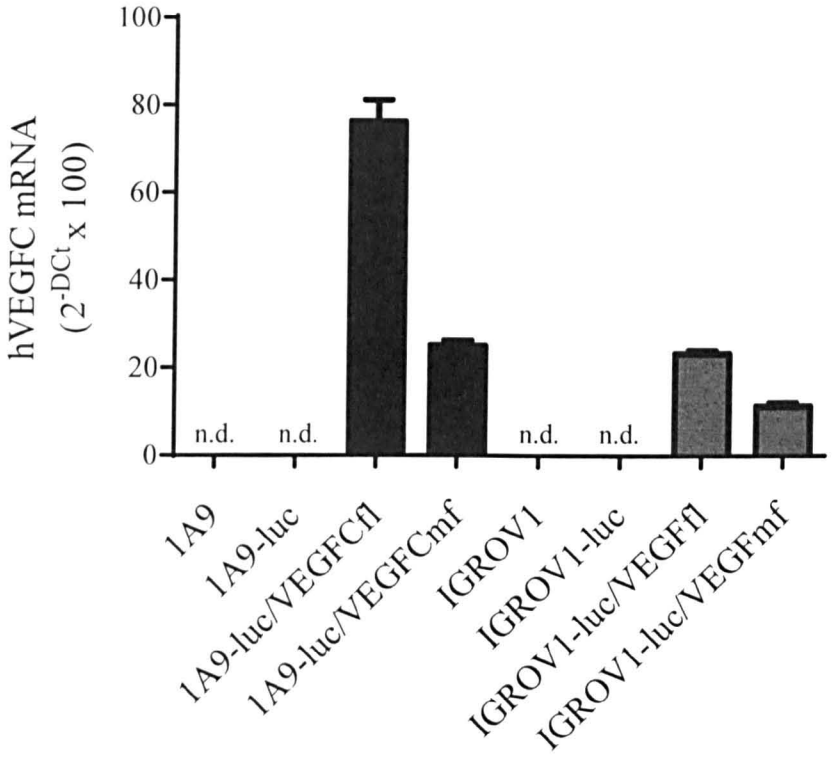


**Figure 4.4 Expression of hVEGFC transcript in 1A9 and IGROV1 infected cells.** RT-PCR. hVEGFC mRNA was normalized to HPRT1 housekeeping gene: $\Delta Ct = Ct_{target} - Ct_{HPRT1}$. Data are expressed as $2^{-\Delta Ct}$ x 100 (mean and SD from one experiment representative of three). Experiments were run in triplicate. n.d. = not detectable.

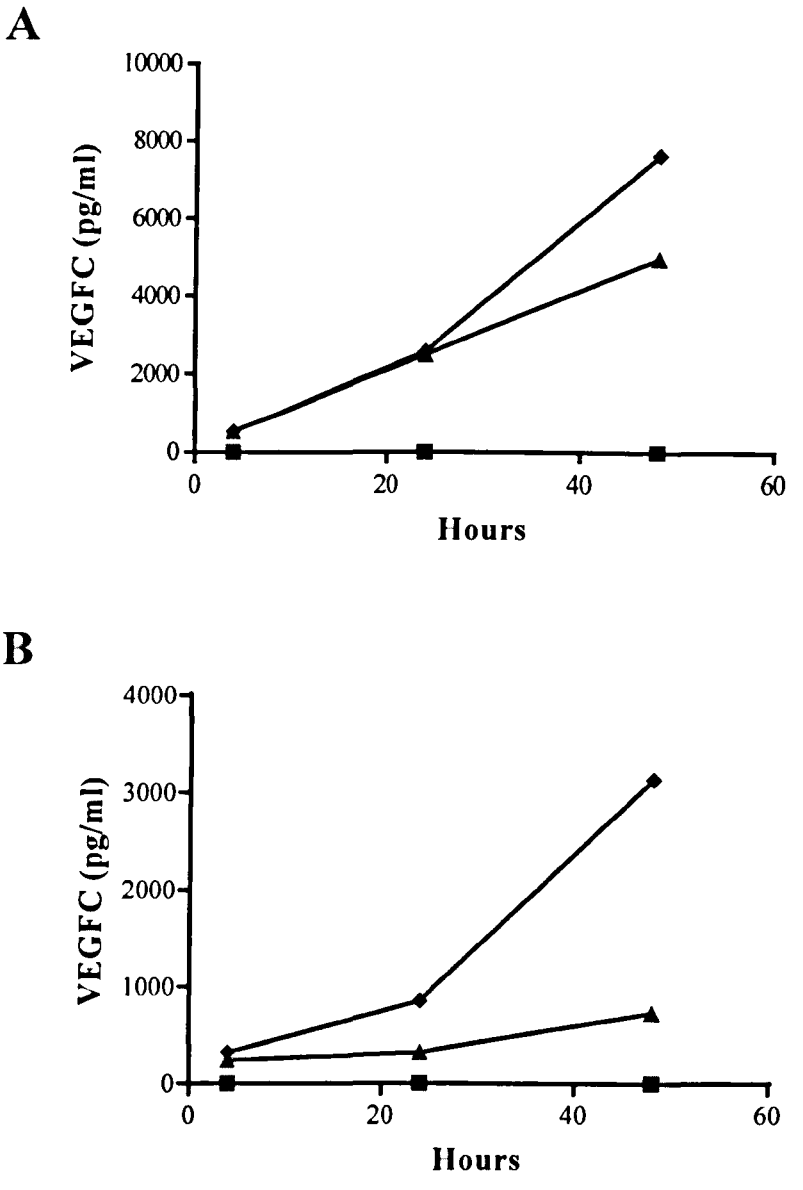


**Figure 4.5 Release of soluble VEGFC in 1A9-luc and IGROV1-luc infected cells.** ELISA analysis. (A) VEGFC (pg/ml) released in the conditioned medium of 1A9-luc (squares), 1A9-luc/VEGFCfl (diamonds) and 1A9-luc/VEGFCmf (triangles). Data are mean of two replicates representative of three experiments. (B) VEGFC (pg/ml) released in the conditioned medium of IGROV1-luc (squares), IGROV1-luc/VEGFCfl (diamonds) and IGROV1-luc/VEGFCmf (triangles). Data are mean and SD of two replicates representative of three experiments.

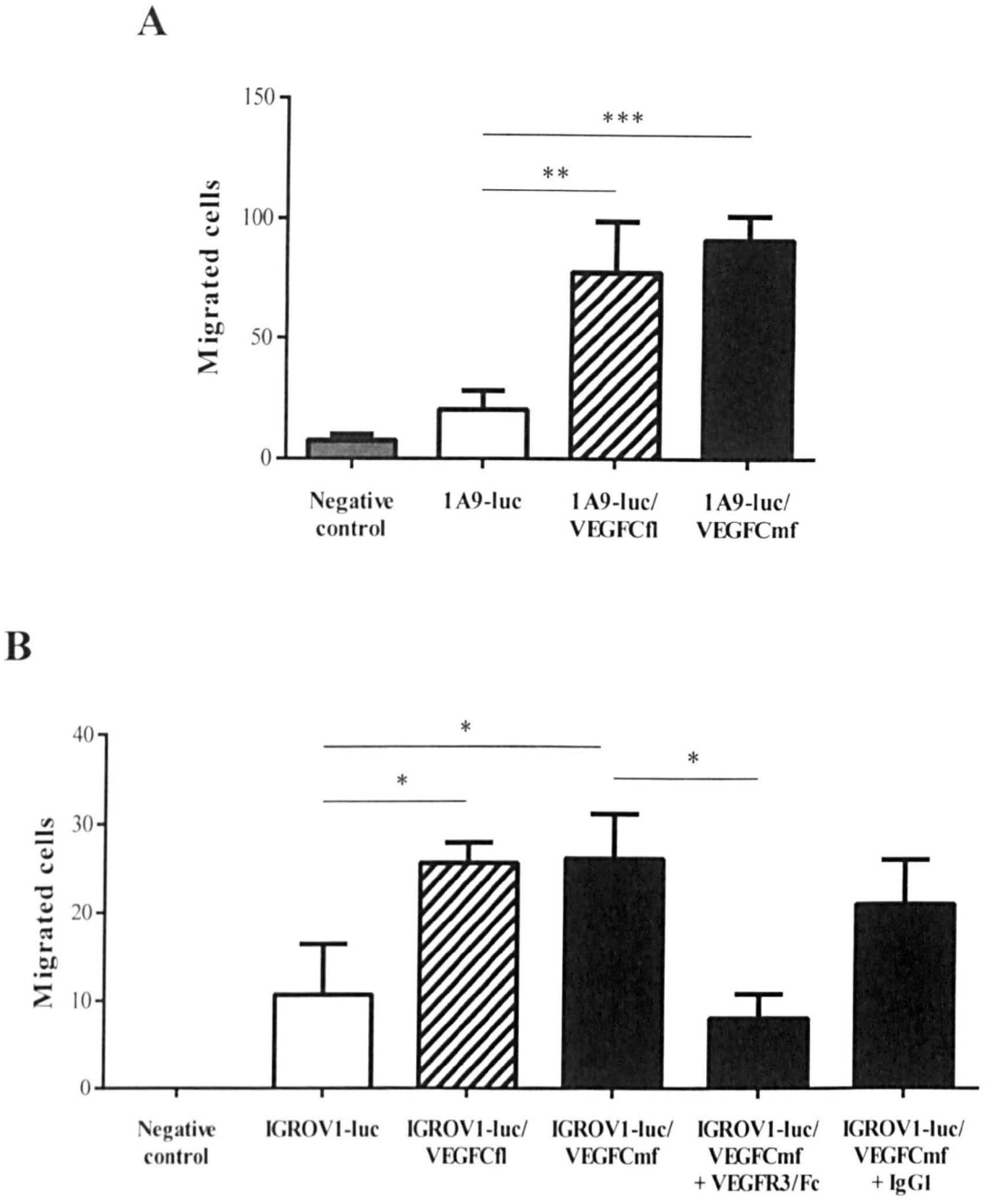


**Figure 4.6 Biological activity of secreted VEGFC.** (A) Lymphatic endothelial cell motility in response to conditioned media of 1A9-luc, 1A9-luc/VEGFCfl and 1A9-luc/VEGFCmf. Results are the number of migrated cells (means and SD of at least three values from one experiment representative of two). **$p<0.01$, ***$p<0.001$. (B) Lymphatic endothelial cell motility in response to conditioned media of IGROV1-luc, IGROV1-luc/VEGFCfl and IGROV1-luc/VEGFCmf, with or without VEGFR3/Fc chimera or irrelevant antibody (IgG1). Results are the number of migrated cells (means and SD of at least three values from one experiment representative of two). *$p<0.05$.

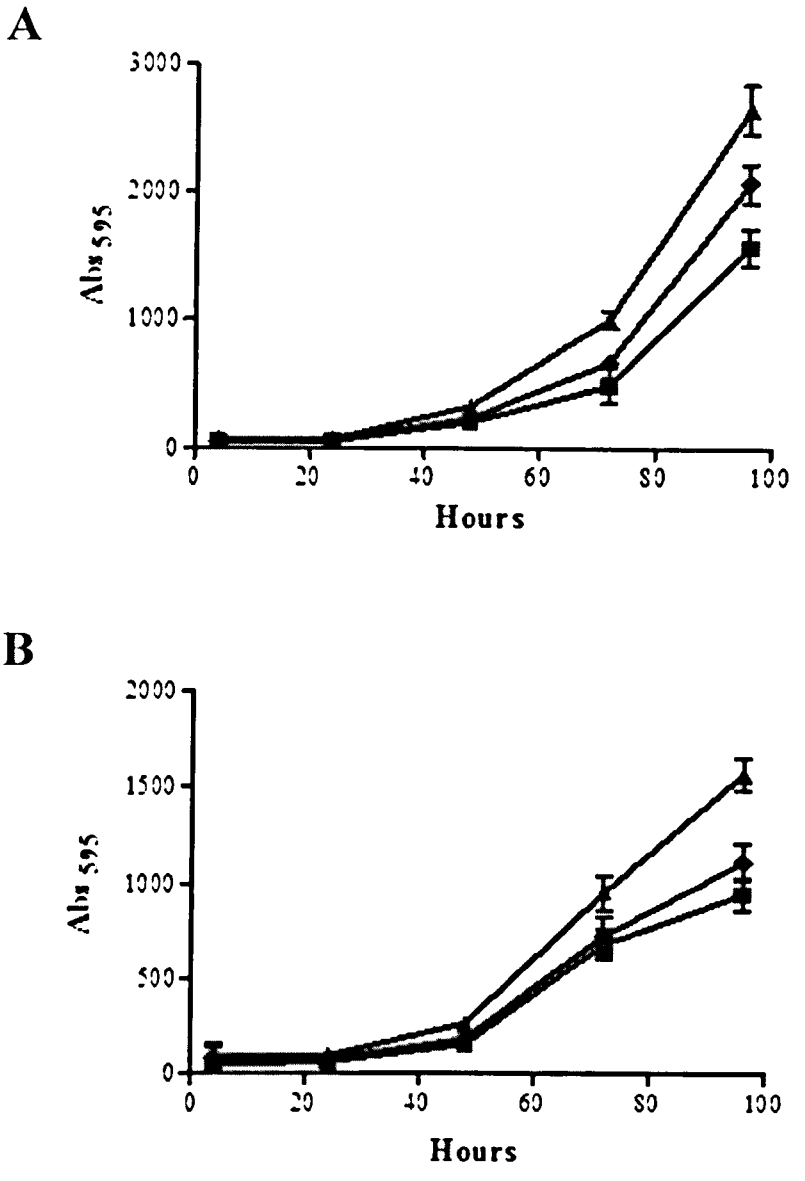


**Figure 4.7 VEGFC-infected cells proliferation.** Growth curves. Proliferation capacity measured by absorbance at 595 nm (*Abs595*) every 24 hours. (A) 1A9-luc (squares), 1A9-luc/VEGFCfl (diamonds) and 1A9-luc/VEGFCmf (triangles). Data are mean of five replicates representative of three experiments. (B) IGROV1-luc (squares), IGROV1-luc/VEGFCfl (diamonds) and IGROV1-luc/VEGFCmf (triangles). Data are mean of five replicates representative of three experiments.

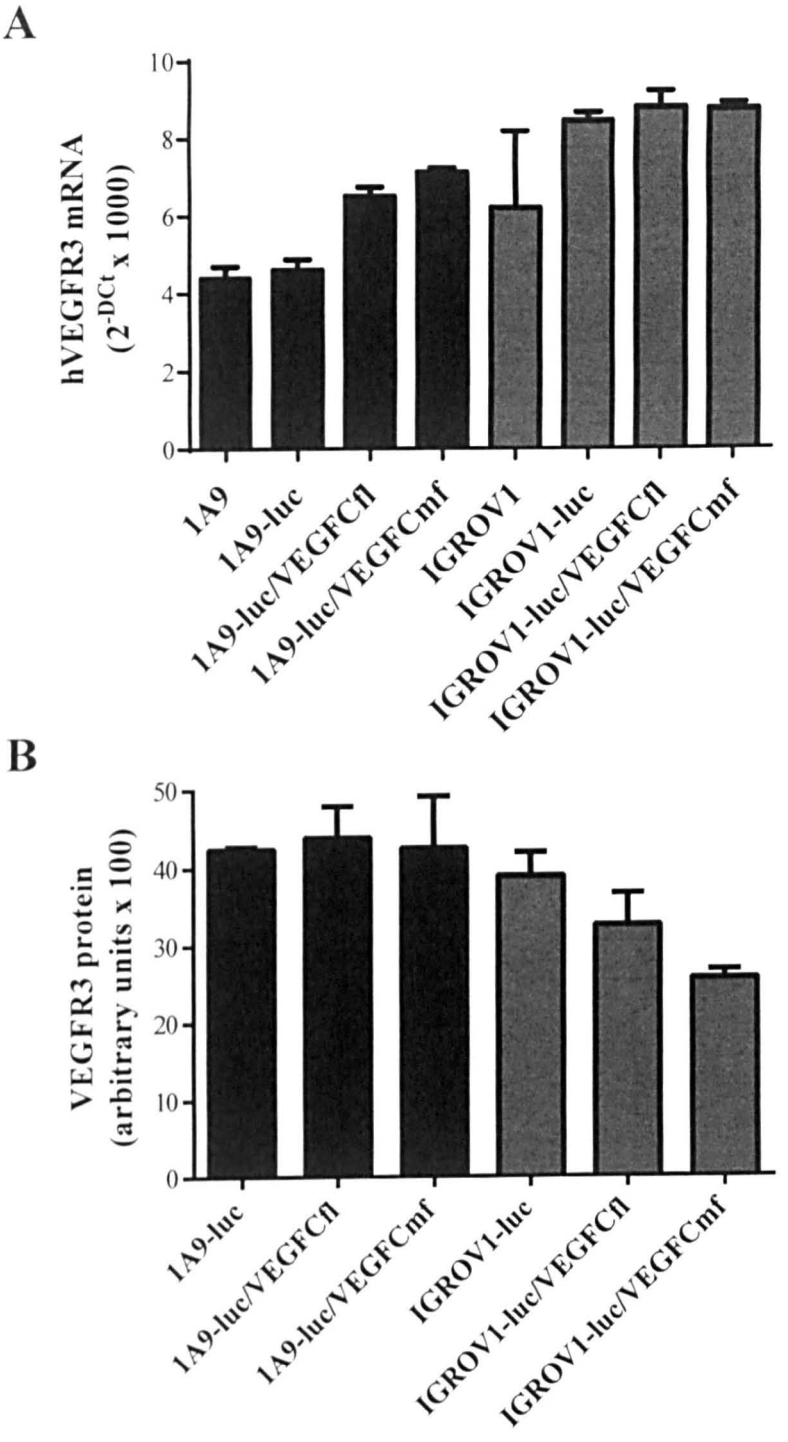


**Figure 4.8 Expression of VEGFR3 transcript in infected cells.** VEGFR3 expression was analyzed in each 1A9 and IGROV1-infected variant *in vitro*. (A) RT-PCR. VEGFR3 mRNA was normalized to the HPRT1 housekeeping gene: $\Delta Ct = Ct_{target} - Ct_{HPRT1}$ and expressed as $2^{-\Delta Ct}$ x 1000 (mean and SD of three replicates from one experiment representative of three). (B) VEGFR3 expression on the cell surface was analyzed by Multiplex *in situ* Epitope Profiling (MiSEP) and expressed as arbitrary units (mean and SD of two values).

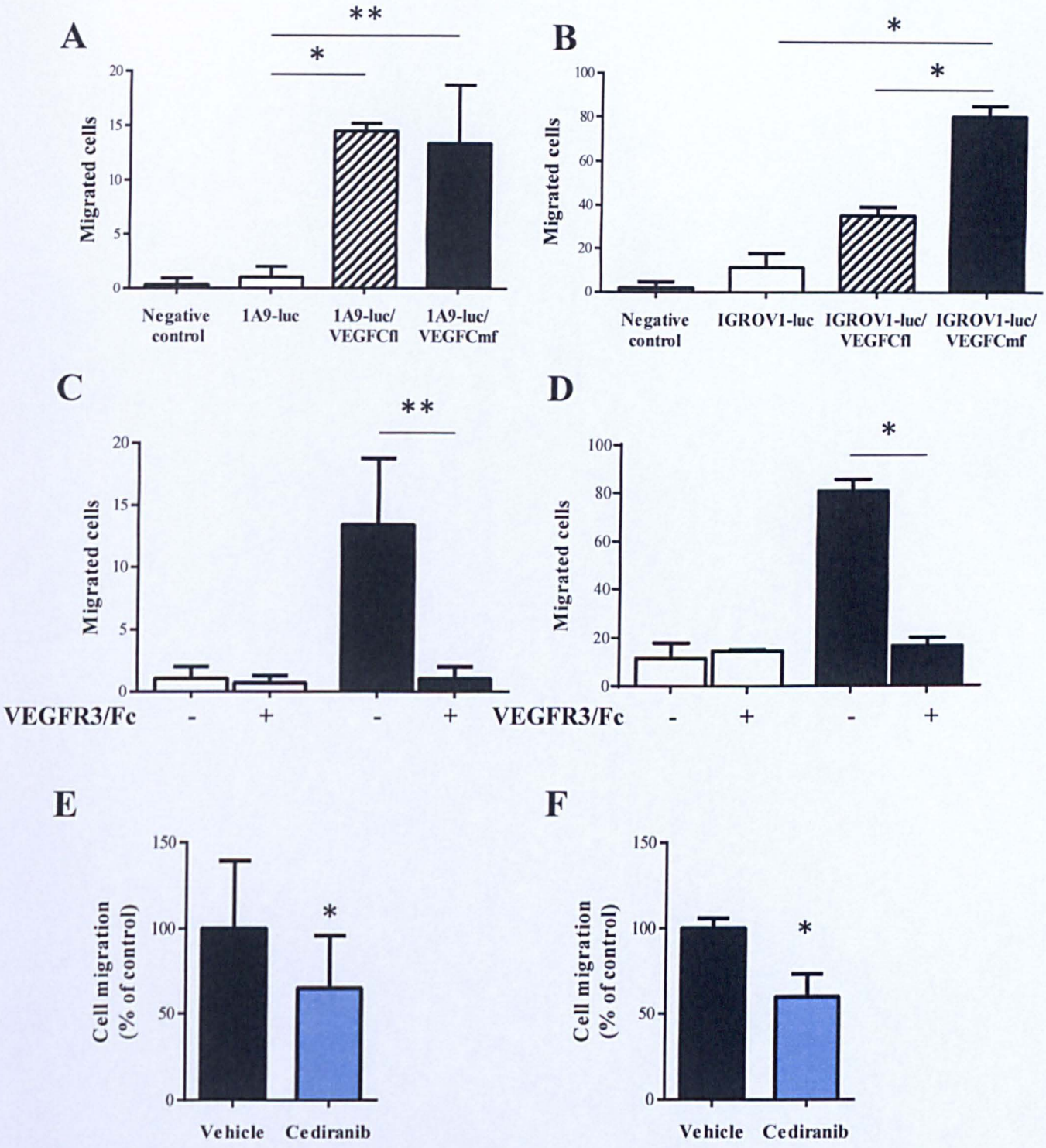


**Figure 4.9 Autocrine activity of VEGFC.** (A) Effect of conditioned medium of 1A9-luc, 1A9-luc/VEGFCfl and 1A9-luc/VEGFCmf on 1A9-luc cell motility. (B) Effect of conditioned medium of IGROV1-luc, IGROV1-luc/VEGFCfl and IGROV1-luc/VEGFCmf on IGROV1-luc cell motility. * $p<0.05$, **$p<0.01$. (C-D) VEGFR3/Fc chimera (10 µg/mL) was added to 1A9-luc cells together with conditioned medium of 1A9-luc (white) or 1A9-luc/VEGFCmf (black, C) or to IGROV1-luc cells together with conditioned medium of IGROV1-luc (white) or IGROV1-luc/VEGFCmf (black, D). Results are the number of migrated cells (means and SD of at least three values from one experiment representative of two). * $p<0.05$, **$p<0.01$. (E-F) Effect of cediranib (10 nM) on 1A9-luc (E) or IGROV1-luc (F) migration induced by conditioned medium of 1A9-luc/VEGFCmf (E) or IGROV1-luc/VEGFCmf (F). Results are expressed as the migrated cells as a percentage of controls (vehicle treated cells). * $p<0.05$.

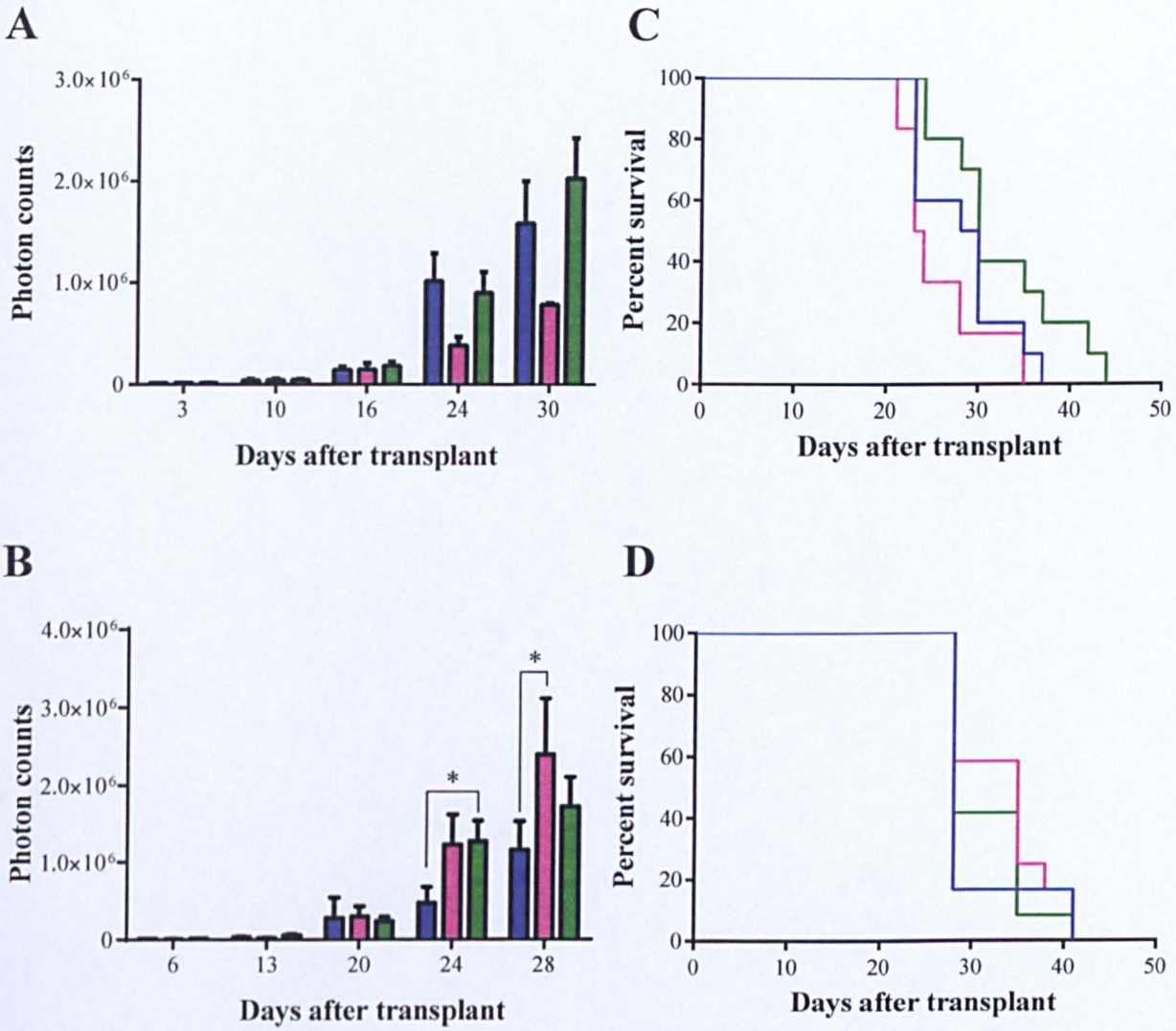


**Figure 4.10 *In vivo* tumor growth and survival of tumors over-expressing VEGFC.** (A,C) 1A9-luc (blue), 1A9-luc/VEGFCfl (pink) and 1A9-luc/VEGFCmf (green) cells, and (B,D) IGROV1-luc (blue), IGROV1-luc/VEGFCfl (pink) and IGROV1-luc/VEGFCmf (green) cells were transplanted orthotopically under the bursa of the ovary of nude mice. (A-B) Tumor growth was checked by BLI at the times indicated. Photon counts, indicative of tumor burden, are expressed as mean ± SEM. n= 6-12. *$p<0.05$. (C-D) Survival curves of mice bearing wild-type or VEGFC over-expressing cells. n= 6-12.

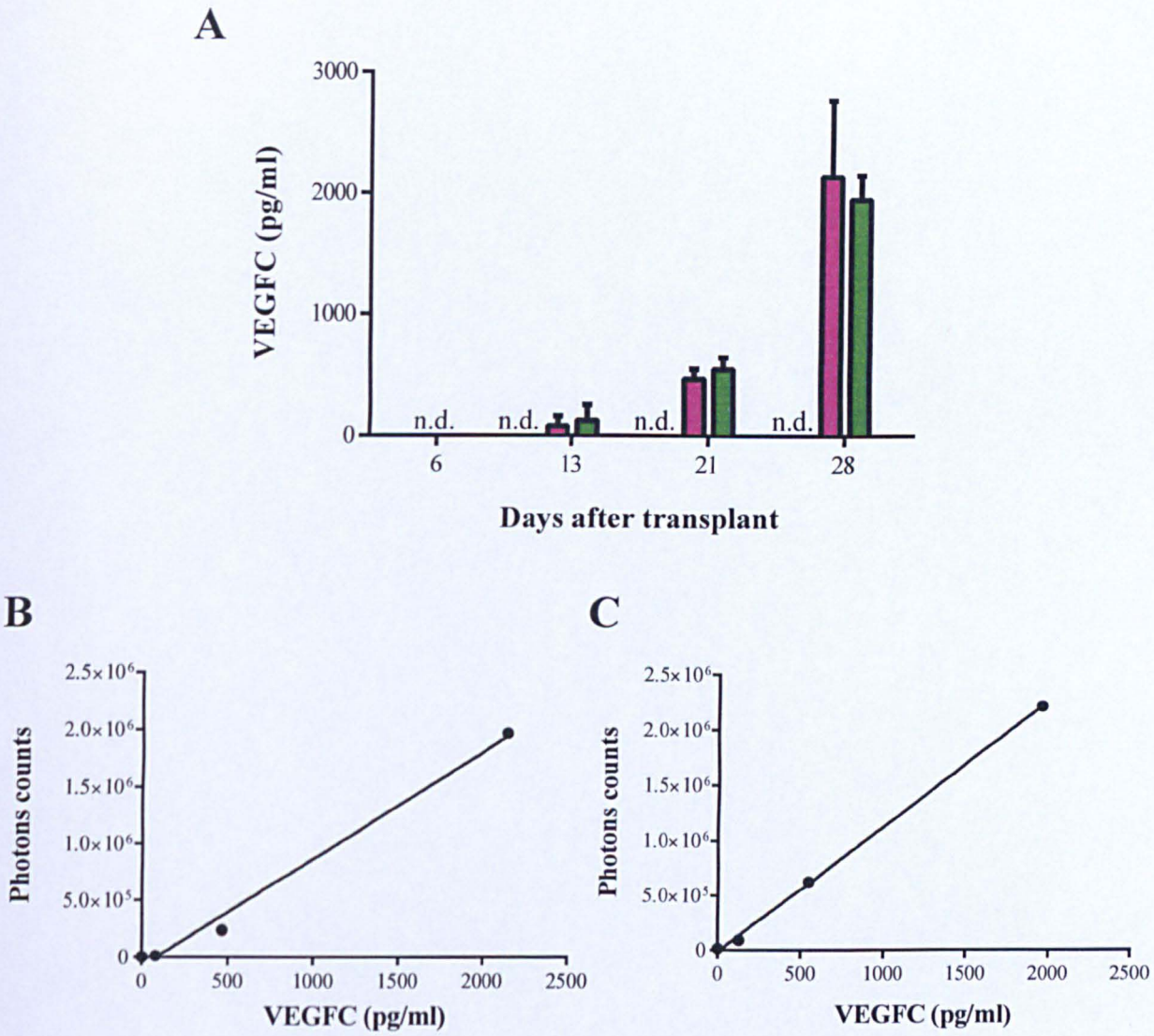


**Figure 4.11 VEGFC released in serum.** (A) IGROV1-luc (blue), IGROV1-luc/VEGFCfl (pink) and IGROV1-luc/VEGFCmf (green) cells were transplanted orthotopically under the bursa of the ovary of nude mice and serum VEGFC was assayed by ELISA. There was no detectable VEGFC in mice bearing the control variant IGROV1-luc. Bars, mean of three samples for each time point ± SEM. n.d.= not detectable. (B) VEGFC levels correlated positively with tumor burden ($p=0.0043$, $R^2=0.9914$) in IGROV1-luc/VEGFCfl tumors. (C) VEGFC levels correlated positively with tumor burden ($p=0.0004$, $R^2=0.9992$) in IGROV1-luc/VEGFCmf-bearing mice.

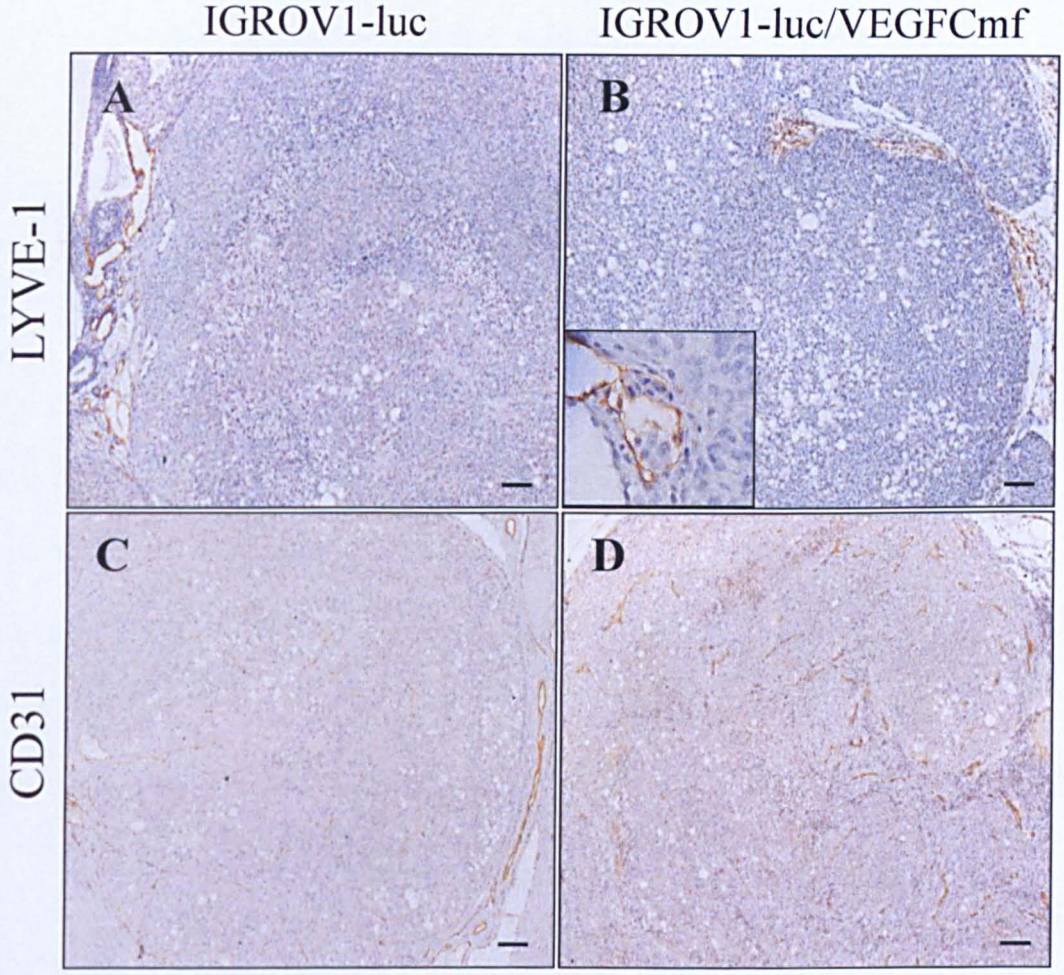


**Figure 4.12 Lymphatic and blood vasculature in IGROV1 tumors over-expressing VEGFC.** IGROV1-luc variants expressing mature VEGFC or not were implanted in the ovary of immunodeficient mice. (A-B) LYVE-1 immunostaining revealed lymphatic vessels at the periphery of primary tumors, and in the septa and capsule of the ovary. Tumor cells (B inset) were observed in lymphatic vessels of tumors over-expressing VEGFC. (C-D) CD31 immunostaining revealed blood vessels inside the tumor parenchyma and the in ovarian capsule and septa. Scale bars represent 200 μm.

| IGROV1 variant | Para-aortic LNs | Contralateral Ovary | Diaphragm | Retroperitioneal tumor |
|---|---|---|---|---|
| IGROV1-luc | 0/6 | 1/6 (**17%**) | 3/6 (**50%**) | 1/6 (**17%**) |
| IGROV1-luc/VEGFCfl | 1/28 (**3.5%**) | 0/11 | 5/12 (**42%**) | 7/12 (**58%**) |
| IGROV1-luc/VEGFCmf | 0/12 | 3/11 (**27%**) | 11/12 (**92%**) | 8/12 (**67%**) |

**Table 4.1 Metastatic behaviour of IGROV1-luc cells expressing VEGFC.** IGROV1-luc, IGROV1-luc/VEGFCfl expressing full-length VEGFC or IGROV1-luc/VEGFCmf expressing the mature form were transplanted orthotopically in the ovary of nude mice. Histopathological analysis of para-aortic lymph nodes, contralateral ovary, diaphragm and retroperitoneal space was done at killing. Data are the number (and percentage) of mice with metastasis over total mice.

Chapter 5

# Inhibition of VEGFC/VEGFR3 pathway with Cediranib

## 5.1 Introduction and goals

In the previous chapters it was shown that VEGFC released in serum and ascites of nude mice correlated with tumor burden and VEGFCmf over-expression induced increased metastasis to diaphragm and retroperitoneal space. Furthermore it was demonstrated that VEGFC not only has a paracrine activity on lymphatic endothelial cells, but it has also an autocrine effect on the tumor cells. Thus, it was interesting to evaluate the therapeutic potential of the blockade of VEGFC/VEGFR3 pathway. For this purpose, since specific inhibitors for VEGFR3 *in vivo* were not available, cediranib, a VEGF receptor tyrosine kinase inhibitor, effective in blocking VEGFR3 and VEGFR2 and preventing the formation of lymphatic metastasis was used (Padera, Kuo *et al.* 2008).

Aims of this chapter are:

- To evaluate the efficacy of cediranib on *in vivo* IGROV1-luc/VEGFCmf growth, metastasis and survival.
- To evaluate the efficacy of cediranib on the survival of patient-derived human ovarian carcinoma xenografts.
- To evaluate the efficacy of cediranib in combination with chemotherapy, reproducing the ongoing ICON 6 clinical trial.

Clinically relevant doses were used throughout these studies.

***The work presented is part of a manuscript in preparation.***

## 5.2 Response to Cediranib of IGROV1-luc over-expressing VEGFC

The efficacy of cediranib on tumor progression, survival and invasion induced by VEGFC was tested on the IGROV1-luc (control variant) and IGROV1-luc/VEGFCmf intraovarian orthotopic models. IGROV1-luc xenograft allowed us to observe the activity of the compound independently from VEGFC (background activity), while the VEGFC-

overexpressing xenograft permitted us to focus on the inhibition of the VEGFC/VEGFR3 pathway.

### *5.2.1 Tumor progression and survival*

IGROV1-luc/VEGFCmf and IGROV1-luc cells were transplanted under the bursa of the ovary of immunodeficient mice. On day 7 mice were randomized in two groups with the aid of BLI on the basis of photon counts. One group (13 mice/group) received cediranib 6 mg/kg, per os (p.o.), every day for 3 weeks (Q1x21); the control group received vehicle, at the same schedule. Mice were monitored by BLI, and at day 28, 24 hours after the end of the treatments, 5 mice per group where sacrificed, in order to analyze the early metastasis pattern by histology. Metastasis analysis will be described in section 5.2.2 of this chapter.

Cediranib was effective on tumor progression of IGROV1-luc/VEGFCmf bearing mice. At the end of the treatment (day 28) photon counts were 95.5% lower in mice treated with cediranib than in vehicle-treated mice (Figure 5.1A and 5.1C, $^{**}p<0.01$). Survival reflected the progression of the tumor in the peritoneal cavity (Figure 5.1E): vehicle-treated mice rapidly developed tumors and had a median survival time (MST) of 33.5 days; cediranib significantly prolonged survival (MST 45 days, ILS 34%, $^{**}p<0.005$).

Similarly, cediranib inhibited tumor growth in IGROV1-luc bearing mice (Figures 5.1B and 5.1D). However, at day 28 the effect was less pronounced compared to IGROV1-luc/VEGFCmf (58% of reduction compared to vehicle-treated mice, $^{*}p<0.05$). The effect on mice survival (Figure 5.1F) was comparable to the one observed on VEGFC over-expressing cells, with a significant increment of life span (ILS 35%, $^{*}p<0.05$; MST vehicle 32.5 days, MST Ced 44 days).

### *5.2.2 Metastasis*

Five mice per group were sacrificed and necropsied at day 28, at the end of treatment for interim analysis.

Histopathological analysis confirmed that the VEGFCmf-infected cells metastasized more efficiently to the diaphragm than control cells, with almost all mice presenting neoplastic masses (Table 5.1). Interestingly, cediranib affected only metastasis formed by IGROV1-luc/VEGFCmf and not by IGROV1-luc: only 60% of IGROV1-luc/VEGFCmf transplanted mice treated with cediranib showed neoplastic masses (Table 5.1). On the contrary, 50% of both cediranib treated and untreated mice transplanted with IGROV1-luc presented metastasis to the diaphragm (Table 5.1).

Furthermore, 40% of mice bearing the IGROV1-luc/VEGFCmf presented with ascites (Table 5.1), while ascites was not present in mice transplanted with the wild-type cells. Cediranib was able to inhibit the formation of ascites, as none of cediranib-trated IGROV1-luc/VEGFCmf-bearing mice presented ascites (Table 5.1).

*5.2.3 Soluble VEGFC*

In the previous chapter, section 4.4.2, it was demonstrated that VEGFC released in serum of IGROV1-luc/VEGFCmf bearing mice correlated with tumor burden, thus pointing to VEGFC as a possible indicator of tumor burden and invasion.

The levels of VEGFC released in serum of mice transplanted with IGROV1-luc/VEGFCmf and treated with vehicle or cediranib (described in section 5.2.1 of this chapter) were analysed by ELISA.

As expected, the amount of VEGFC detected in the serum of mice of the two groups at randomization (day 7) were comparable (Figure 5.2A). At day 28, vehicle-treated mice reached 790 pg/ml of VEGFC, while the levels of VEGFC from mice of the cediranib group were significantly lower (227 pg/ml, $^{**}p<0.01$, Figure 5.2A), confirming that VEGFC

correlated positively with tumor burden both in vehicle ($R^2$=0.8863, Figure 5.2B) and in cediranib-treated mice (p=0.0063, $R^2$=0.9873, Figure 5.2C).

*5.2.4 VEGFRs as biomarkers of tumor burden and response*

The analysis of soluble VEGF receptors (host-derived) released in biological fluids, that could be associated to or predict the response to antiangiogenic drugs in mice with patient-derived human ovarian xenografts, was carried out.

Firstly, the presence of soluble VEGFRs was analyzed in serum of mice bearing IGROV-luc variants by luminex Milliplex® MAP kit. Soluble VEGFR1 was detected in the serum of mice and its levels increased with time after tumor transplant (Figure 5.3A). In particular, it was observed that soluble VEGFR1 positively correlated with tumor burden in both VEGFC over-expressing and control tumors (Table 5.2). However, the correlation was significant only in IGROV1-luc over-expressing VEGFC. On the contrary, in both VEGFC over-expressing and control tumors, soluble VEGFR2 (Figure 5.3B) and soluble VEGFR3 (Figure 5.3C) decreases with time and they significantly inversely correlated with tumor burden (Table 5.2). No differences in soluble VEGFR2 and VEGFR3 were observed among the three IGROV1-luc variants.

To test whether VEGFRs were associated with response to cediranib, soluble VEGFRs were detected in the serum of mice transplanted with IGROV-luc or IGROV-luc/VEGFCmf and treated with vehicle or cediranib (section 5.2.1 of this chapter). As observed above, mice transplanted with IGROV1-luc/VEGFCmf and treated with vehicle showed increasing level of soluble VEGFR1 (Figure 5.4A), that positively and significantly correlated with tumor burden (Table 5.3). On the contrary soluble VEGFR2 decreased with time (Figure 5.4C) and inversely correlated with tumor burden (Table 5.3). Soluble VEGFR3 had a decreasing trend (Figure 5.4E) and showed an inverse correlation with tumor burden (Table 5.3).

As shown above in section 5.2.1, tumor burden, expressed as photon counts, was lower in IGROV1-luc/VEGFCmf bearing mice treated with cediranib than vehicle (Figure 5.1C). Analyzing soluble VEGFRs, it was observed that cediranib-treated mice had significantly lower amounts of soluble VEGFR1 than vehicles (Figure 5.4A). Similarly, the decrease of soluble VEGFR2 was slower in mice treated with cediranib than with vehicle (Figure 5.4C). Soluble VEGFR3 seemed to decrease in the same way as in vehicle-treated mice (Figure 5.4E). Positive correlation between tumor burden and soluble VEGFR1 and inverse correlation between tumor burden and soluble VEGFR2 or soluble VEGFR3 were observed (Table 5.3).

Similar results were obtained also in the IGROV1-luc bearing mice treated with cediranib (Figures 5.4B, 5.4D, 5.4F and Table 5.3).

### 5.3 Response to cediranib of patient-derived xenografts

The efficacy of cediranib was investigated on a panel of patient-derived ovarian cancer xenografts (HOC8, HOC10, HOC22 and HOC79), described in chapter 3, section 3.2.1. As described before, all the four tumor xenografts released soluble VEGFC both in ascites and serum, with lower amount of VEGFC detected in the ascites of HOC79 xenograft (Figure 3.1).

As we have demonstrated that VEGFC acts in paracrine and autocrine fashion in the process of tumor progression and metastasis, patient-derived xenografts were characterized for the expression of VEGFR2 and VEGFR3 transcripts by Real-Time PCR.

VEGFR2 mRNA was expressed in 3 out of 4 xenografts: HOC8 showed the higher expression, while VEGFR2 was undetectable in HOC79 (Figure 5.5A).

VEGFR3 transcript was detectable in all the xenografts, with higher levels for HOC22 and lower levels for HOC8 xenografts (Figure 5.5B). The expression of VEGFR3 protein was confirmed by immunohistochemistry (Figure 5.6).

The presence of both VEGFR2 and VEGFR3 suggested that VEGFC can act also through an autocrine mechanism in these models.

Then, the efficacy of cediranib was tested. Immunodeficient mice bearing human ovarian xenografts were randomized (10 mice/group) on day considered ¼ of the median survival time for each model (advanced tumor), on the basis of representative mice with confirmed tumor burden in the peritoneal cavity. Cediranib was administered per os (p.o.) at a dose of 3 mg/kg once a day for 3 weeks (Q1x21). Vehicle treatment was administered following the same schedule of the active compound.

Cediranib significantly prolonged the survival of mice transplanted with HOC8 and HOC10 xenografts, that released comparable levels of VEGFC and also expressed both VEGFR2 and VEGFR3 (HOC8, vehicle, MST 32 days, Ced, MST 44.5 days, ILS 39%, Figure 5.7A; HOC10, vehicle, MST 114.5 days, Ced, MST 142.5 days, ILS 62%, Figure 5.7B).

Interestingly, cediranib showed a stronger effect in the HOC22 model, that released comparable amount of VEGFC than HOC8 and HOC10, but expressed the highest amount of VEGFR3 (vehicle, MST 20 days, Ced MST 37 days, ILS 85%, Figure 5.7C).

On the other hand, cediranib showed a minimal effect on survival of mice transplanted with HOC79 xenograft, that expressed the lowest levels of VEGFC, did not express VEGFR2 and express low amount of VEGFR3 (Vehicle, MST 22 days, Ced, MST 26 days, ILS 18%, Figure 5.7D).

### 5.4. Maintenance therapy on HOC8 xenograft

Maintenance schedule for antiangiogenic therapy is becoming an issue in current clinical trials. Since one of the arms of the ICON6 trial (a phase III clinical trial evaluating the combination of chemotherapy plus cediranib in women with platinum-sensitive relapsed ovarian cancer) contemplated cediranib maintenance (Raja, Griffin *et al.* 2011), cediranib was administered in maintenance therapy on HOC8 model and the efficacy on tumor survival was analyzed.

This model was chosen because it was well described for correlation of VEGFC and tumor burden (chapter 3, section 3.2.1) and lymph nodes invasion (chapter 3, section 3.2.2). Furthermore it was sensitive to cediranb given daily for 21 days (section 5.3 of this chapter).

Nude mice bearing HOC8 were randomized on day seven (ten mice/group), on the basis of representative mice with confirmed tumor burden in the peritoneal cavity, and dosed once-daily orally with cediranib (3 mg/kg) either for twenty-one days or until survival (treatment was stopped at day 108, when only 3 mice were alive). Control mice were treated with vehicle, following the same schedule and route of active compound, until survival. Detailed schedule of the trial is shown in Figure 5.8A.

As already described in section 5.3 of this chapter, cediranib given for twenty-one days significantly increased survival of mice bearing HOC8 tumor xenograft (vehicle, MST 32 days, Ced, MST 44.5 days, ILS 39%, Figure 5.8B). An added benefit of taking cediranib for a longer time was observed. Maintenance treatment further prolonged mice survival compared to cediranib interrupted after three weeks (Ced→Ced, MST 79 days, ILS 147% vs vehicle, ***$p<0.0001$, ILS 77.5% vs Ced, #$p<0.0001$, Figure 5.8B).

## 5.5 Combination therapy: chemotherapy plus cediranib on HOC8 model

### *5.5.1 Paclitaxel/cisplatin and cediranib induction versus maintenance regimen*

The effect of cediranib added to PTX+DDP, the standard chemotherapeutics used for ovarian carcinoma patients, was tested in the HOC8 model. It was investigated whether cediranib enhanced tumor response to chemotherapy. Focusing on the problem of antiangiogenic therapy duration, the triple combination of PTX+DDP+Ced was compared with the triple combination with maintenance of cediranib (PTX+DDP+Ced→Ced90). This trial reproduces the arms of ICON6 clinical trial (Raja, Griffin *et al.* 2011).

Briefly, nude mice bearing HOC8 were randomized (ten mice/group) on day 7, on the basis of representative mice with confirmed tumor burden in the peritoneal cavity, and treated with PTX+DDP as single agent or in combination regimens with cediranib. Detailed schedules of the trial are shown in Figure 5.9A.

At the doses and schedules used, PTX+DDP significantly increased survival (vehicle, MST 33 days, PTX+DDP, MST 170 days, ILS 415%, 4/10 tumor-free mice on day 180, Figure 5.9B). Survival was further increased with the addition of cediranib (21 administrations) to the chemotherapy (PTX+DDP+Ced), with 6/10 tumor-free mice on day 180 (MST not evaluable). Maintaining the treatment with cediranib until day 90 (PTX+DDP+Ced→Ced90) equally prolonged the survival with 7/9 tumor-free mice on day 180 (MST not evaluable, Figure 5.9B; 1 mouse was excluded from the study because it developed a strain-related lymphoma on day 173). As the triple combination (PTX+DDP+Ced) was already very effective, no significant differences with cediranib maintenance were observed.

### *5.5.2 Cediranib concomitantly or after induction with chemotherapy*

Finally, it was investigated whether it was advantageous to give cediranib concomitantly with chemotherapy or sufficient to start the treatment after induction with chemotherapy, in order to reduce the stress and discomfort of patients, while maintaining the efficacy of the therapy.

Cediranib administered as monotherapy starting from day 22 and maintained until day 90 (→Ced90) significantly prolonged the survival (MST 103 days, ILS 212%), suggesting that this TKRI is effective as monotherapy also on advanced tumor.

The survival of the group treated with chemotherapy and subsequently with cediranib (PTX+DDP→Ced90) was significantly prolonged (MST 122 days, 3/8 tumor-free mice on day 180, ILS 270% vs vehicle, ***p<0.0001, ILS 18% vs →Ced90, ***p=0.0002, Figure 5.10B), although an increment of survival was not observed in respect to chemotherapy alone (PTX+DDP, MST 170 days, ILS 415%, 4/10 tumor-free mice on day 180, Figure 5.10B).

These data suggested that cediranib administered as monotherapy is very effective on advanced tumors; on the other hand the compound administered after chemotherapy is not better than chemotherapy alone (PTX+DDP).

### 5.6 Summary of results

The results presented in this chapter can be summarized as follows:

- Cediranib inhibits tumor growth of both IGROV1-luc and IGROV1-luc/VEGFmf tumors.
- The effect of cediranib is more pronounced on VEGFC over-expressing tumors.
- Cediranib is effective in reducing diaphragm metastasis-VEGFC dependent and ascites formation.
- The levels of VEGFC are reduced in cediranib-treated mice compared to controls: VEGFC levels correlated with tumor burden (photon counts) in cediranib treated-mice.
- Soluble VEGFR1 positively correlates with tumor burden in both IGROV1-luc/VEGFCmf and IGROV1-luc and in both vehicle and cediranib-treated mice.
- Soluble VEGFR2 and VEGFR3 inversely correlate with tumor burden.

- Cediranib is effective on the survival of all the four patient-derived ovarian cancer xenografts analyzed.
- Maintenance regimen of cediranib further increases the survival of HOC8 xenograft.
- Cediranib combined with chemotherapy (PTX+DDP) significantly increases the survival compared to monotherapies.
- Cediranib as montherapy is effective on advanced HOC8 tumors.

**5.7 Discussion**

VEGFC and VEGFR3 are interesting novel targets for tumor therapy (Sopo, Anttila *et al.* 2012).

The results of VEGFR3 expression in ovarian tumor cells suggest that agents that interfere with the VEGFC/VEGFRs axis would have a dual effect on tumor growth and invasion, by directly targeting the tumor cells and by inhibiting lymphatic activation and blood vessel formation. To confirm this hypothesis, the TKRI cediranib, which inhibits VEGFR3 but also VEGFR1, VEGFR2 and c-kit was used. The use of cediranib was due to the lack of inhibitors selective for VEGFR3.

However, it cannot be ruled out that the activity of cediranib against VEGFR1, VEGFR2 and c-Kit contributed to the effect.

The results described in this chapter confirmed that VEGFC enhances diaphragm invasion and induces ascites production. It cannot be excluded that the inhibition of tumor dissemination is secondary to the effect of cediranib on primary tumor growth. On the other hand, cediranib efficacy in counteracting these processes only in VEGFC over-expressing tumors suggested the specificity of the inhibition of VEGFC. Nevertheless, its significant effect on VEGFC-stimulated IGROV1-luc migration *in vitro* indicates that VEGFR3 present on ovarian tumor cells might offer an effective therapeutic target for ovarian carcinoma.

One interesting point of this study was the search of predictive biomarkers of treatment response.

In particular, VEGFC expression was associated with a better response to cediranib. Indeed, greater inhibition of tumor burden was observed in IGROV1-luc over-expressing VEGFC-bearing mice, and cediranib was more effective in patient-derived ovarian carcinoma xenografts releasing VEGFC in serum and ascites.

Furthermore, HOC xenografts that differentially express VEGFR3 and VEGFR2 showed different response to cediranib. It was shown that cediranib was more effective on tumor expressing VEGFR3.

The different expression levels of VEGFR3 and VEGFR2 in HOC xenografts supported VEGFC autocrine activity observed *in vitro* in IGROV1 and 1A9 cells (Chapter 4). In addition, the presence of both VEGFC autocrine and paracrine activity, suggest an increased efficacy of compounds targeting the VEGFC/VEGFR3 pathway.

The effect of VEGFC on VEGFR2 must be taken into account, as 3 out of 4 xenografts used express VEGFR2 in addition to VEGFR3 and the mature form of VEGFC can exert angiogenic activity through VEGFR2 (Witzenbichler, Asahara *et al.* 1998; Kodama, Kitadai *et al.* 2008) Thus, the effect of cediranib observed in the xenografts might also be due by inhibition of VEGFC/VEGFR2 pathway on both endothelial cells (antiangiogenic activity) and also tumor cells themselves (autocrine effect).

Beyond the predictive role as biomarker of response to therapy, VEGFC was confirmed as a possible indicator of tumor burden. Indeed, the correlation between tumor burden and VEGFC, already described in chapters 3 and 4, was now described to occur in mice treated with cediranib.

Then, soluble VEGFRs were analysed and the data obtained indicated that soluble VEGFR1 positively and significantly correlated with tumor burden, while on the contrary soluble VEGFR2 and soluble VEGFR3 showed an opposite trend. These correlations were not dependent on the over-expression of VEGFC. All together these results suggested that soluble VEGFR1 and VEGFR2 are possible candidates as biomarkers of tumor burden, and thus of response to therapy.

The use of soluble VEGFRs as biomarkers of antitumor activity, modulated in response to antiangiogenic treatments is far from being clear and the data in the literature are conflicting. In some studies, soluble VEGFRs are principally considered pharmacodynamic markers that increase after antiangiogenic therapy (Denduluri, Yang *et al.* 2008; Wong, Buckman *et al.* 2010). On the contrary, in other studies VEGFRs are described as decreasing (Deprimo, Bello *et al.* 2007; Rini, Michaelson *et al.* 2008; Medinger, Esser *et al.* 2009 ; Hanrahan, Lin *et al.* 2010; Pena, Lathia *et al.* 2010).

Among antiangiogenic agents, bevacizumab, that is the most studied, demonstrated activity on ovarian cancer in a maintenance regimen in terms of both response and progression free survival (PFS) (Aghajanian, Finkler *et al.* 2011; Burger, Brady *et al.* 2011; Perren, Swart *et al.* 2011; Pujade-Lauraine, Hilpert *et al.* 2012). Data with cediranib on ovarian cancer are lacking.

Different regimens of cediranib were compared on xenograft models mainly to study the relevance of maintenance therapy with this compound. In line with other antiangiogenic drugs, cediranib maintenance regimen was more effective than cediranib given for 3 weeks (Ced) and significantly prolonged the survival of mice transplanted with HOC8.

Surprisingly a strong effect was observed with cediranib single therapy on advanced tumor suggesting that cediranib could represent an important therapeutic opportunity for patients with advanced tumors for which conventional therapies are not effective (75% patients are diagnosed at advanced stage).

A huge reduction of abdominal distention was observed after cediranib administration, suggesting that the efficacy of this TKI on advanced tumor is also due by decrease in ascites formation.

Treatment benefits might be improved combining these treatment strategies with the standard first-line treatment for ovarian cancer patients after cytoreductive surgery (Cannistra, Bast *et al.* 2003). Thus, cediranib was combined with PTX+DDP in the HOC8 model. In agreement with a recent study (Kendrew, Odedra *et al.* 2013), the combination was very effective and prolonged the survival, resulting in 6/10 tumor-free mice (on day 180). The same efficacy was observed when treatment with cediranib was maintained after chemotherapy until day 90.

This result prompts us to investigate whether cediranib treatment after chemotherapy was sufficient to obtain the same outcome. This would be important to reduce the stress and discomfort for ovarian cancer patients. Surprisingly, the triple combination of cediranib starting after the induction of PTX+DDP, was not advantageous. These results suggest that in HOC8 model the concomitance of chemotherapy and cediranib is necessary. Further studies on different ovarian tumor xenografts are necessary to confirm these data.

In conclusion, overall efficacy of cediranib as monotherapy was found in all the xenograft models, consistent with the data observed in the two phase II single-agent studies (Hirte, Vidal *et al.* 2008; Matulonis, Berlin *et al.* 2009). Furthermore these results suggested long-term treatment of cediranib to improve the efficacy of the compound. These findings on the

combination of cediranib and chemotherapy showed the efficacy of the triple combination, anticipating the results of the ICON6 trial.

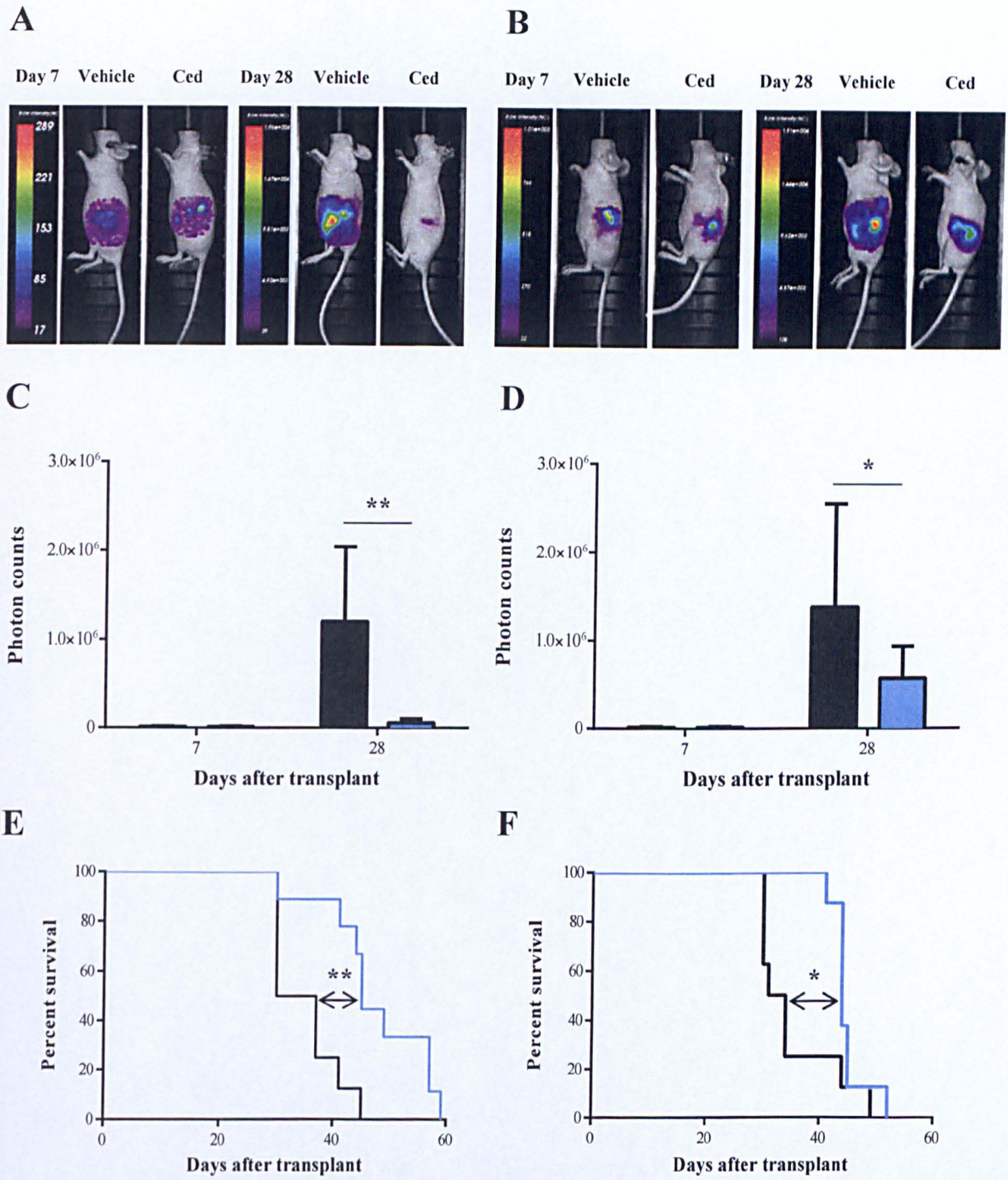


**Figure 5.1 Effect of cediranib on tumor progression and survival.** Nude mice were transplanted with IGROV1-luc variants under the bursa of the ovary and randomized at day 7 on the basis of photon counts. Cediranib was administered every day for 21 days (Q1x21) at the dose of 6 mg/kg, p.o. (A-B) One representative mouse bearing IGROV1-luc/VEGFCmf (A) or IGROV1-luc (B) treated with vehicle or cediranib (Ced) imaged on day 7 and on day 28. (C-D) Mice were monitored by BLI on day 7 (randomization) and day 28 (tumor progression) and tumor burden expressed as photon counts. Vehicle = black bars, Ced = light-blue bars. n=8 (C) IGROV1-luc/VEGFCmf bearing mice. $^{**}p<0.01$. (D) Mice transplanted with IGROV1-luc cells. $^{*}p<0.05$. (E-F) Effect of cediranib on the lifespan of the mice bearing IGROV1-luc/VEGFCmf (E, $^{**}p<0.005$) or IGROV1-luc (F, $^{*}p<0.05$). Vehicle = black lines, Ced = light-blue lines. n=8.

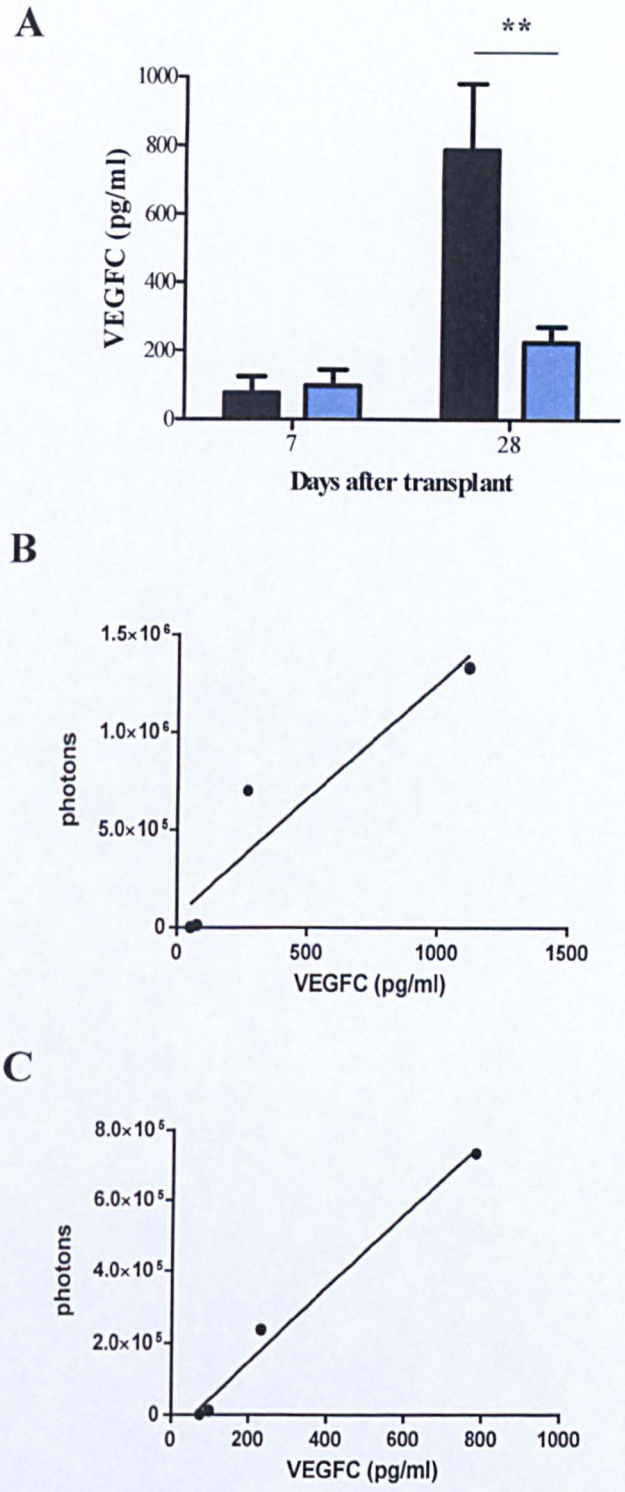


**Figure 5.2 Correlation between tumor burden and VEGFC released in serum of mice bearing IGROV1-luc over-expressing mature form of VEGFC.** (A) Serum VEGFC levels in vehicle (black bars) and cediranib-treated mice (light-blue bars) at randomization (day 7) and at the end of treatment (day 28). n=4. **p<0.01. (B-C) Correlation between tumor burden expressed as photon counts and VEGFC levels in serum of vehicle (B, $R^2$=0.8863) and cediranib (C, p=0.0063, $R^2$=0.9873) treated mice. n=4.

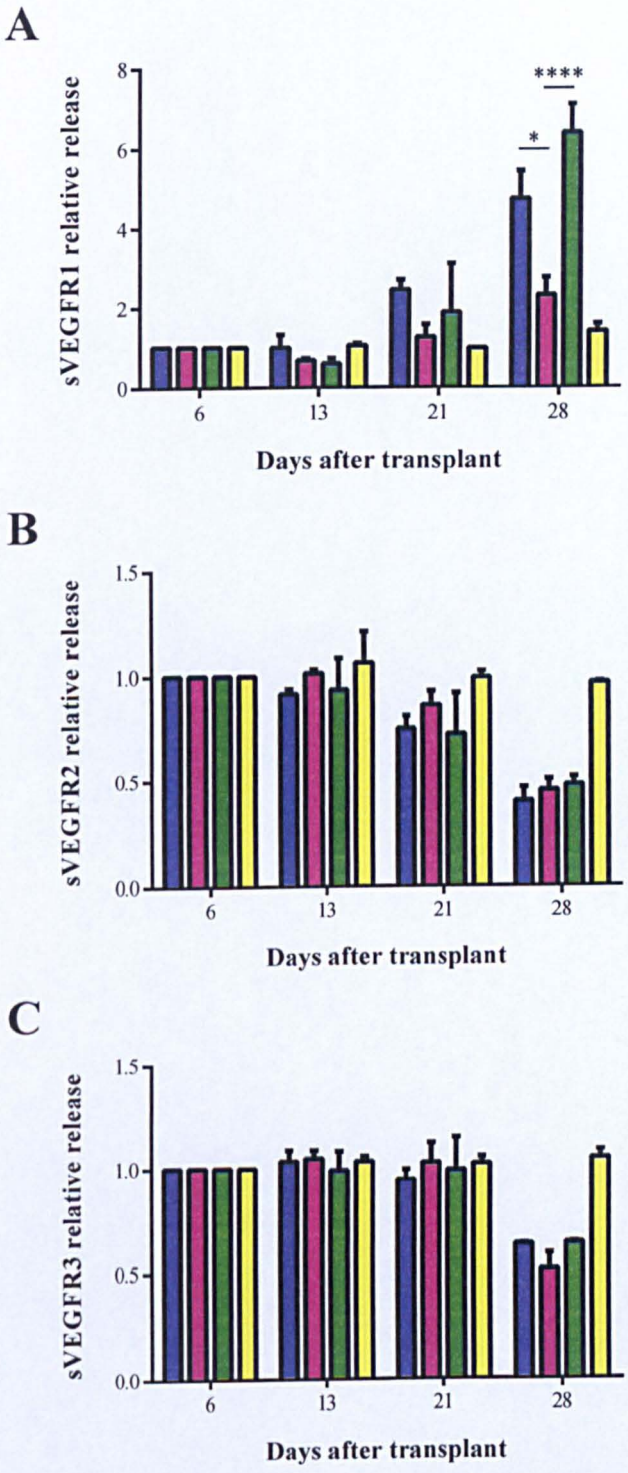


**Figure 5.3 Soluble VEGFR receptors in serum of IGROV1-luc variants.** Soluble VEGFR1 (A), VEGFR2 (B) and VEGFR3 (C) were detected in the serum of IGROV1-luc (blue), IGROV1-luc/VEGFCfl (pink), IGROV1-luc/VEGFCmf (green) bearing mice and healthy mice (yellow). *$p<0.05$, ****$p<0.0001$. n=3.

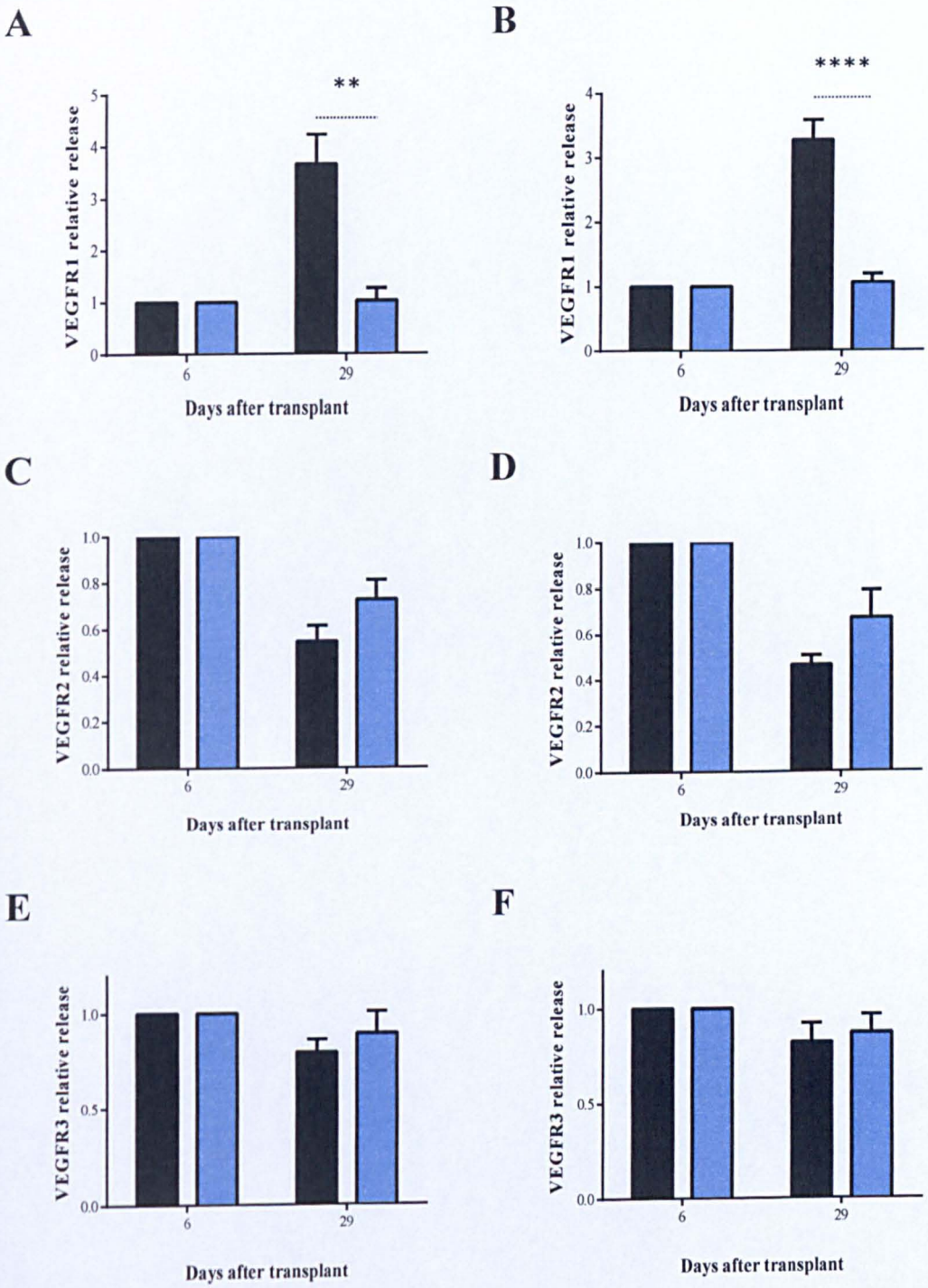


**Figure 5.4 Soluble VEGFR receptor levels in serum of cediranib-treated mice.** Serum of nude mice transplanted with IGROV1-luc/VEGFCmf (A, C, E) or IGROV1-luc (B, D, F) was collected and soluble VEGFR1 (A-B), VEGFR2 (C-D) and VEGFR3 (E-F) were measured. Vehicle = black bars, cediranib = light-blue bars. n=3-6. **p<0.005, ****p<0.0001.

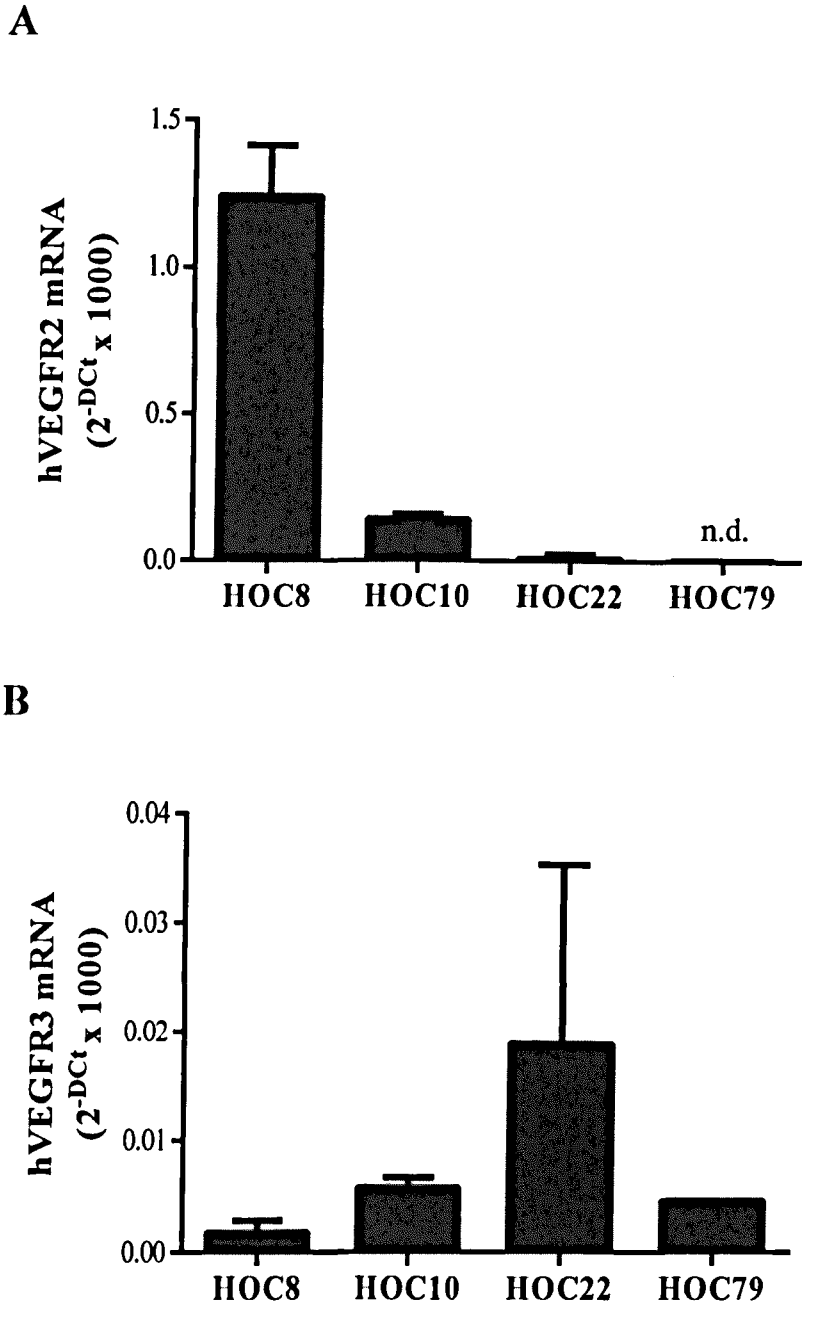


**Figure 5.5 Expression of hVEGFR2 and hVEGFR3 in patient-derived xenografts.** Human VEGFR2 (A) and human VEGFR3 (B) transcripts expression was analyzed in the four patient-derived xenografts HOC8, HOC10, HOC22 and HOC79 by Real-Time PCR. Target mRNA was normalized to the human beta-actin housekeeping gene: $\Delta Ct = Ct_{target} - Ct_{beta\text{-}actin}$ and expressed as $2^{-\Delta Ct} \times 1000$ (mean and SD of three replicates from one experiment representative of three). n.d. = not detectable.

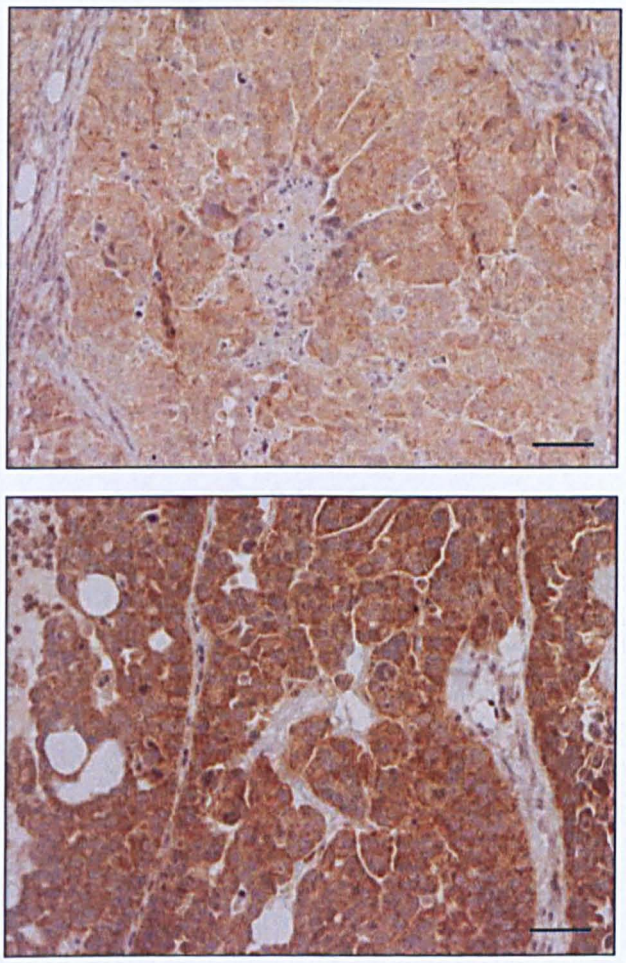

**Figure 5.6 VEGFR3 protein expression in HOC8 xenograft.** Representative immunohistochemical images of HOC8 tumors expressing human VEGFR3. Scale bars represents 100 μm.

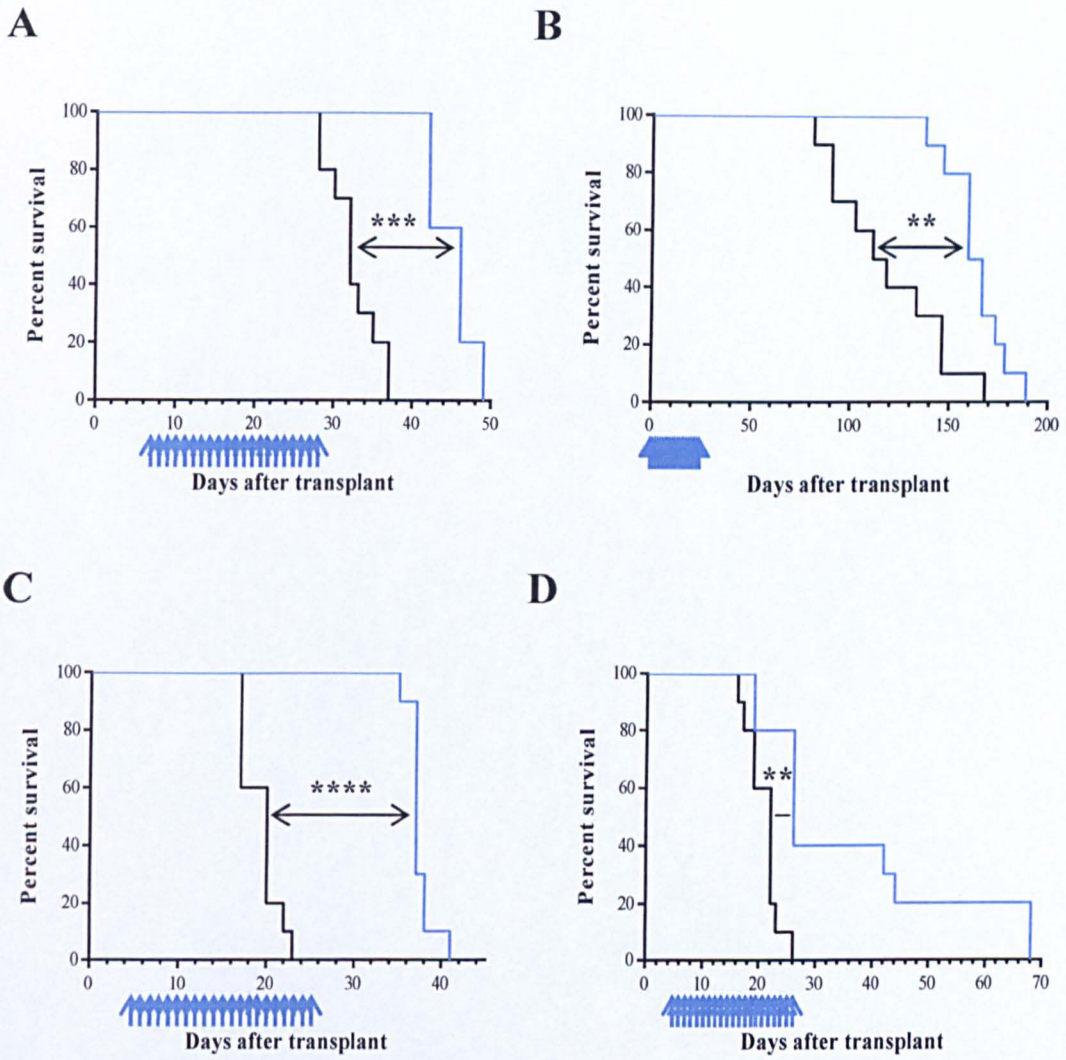


**Figure 5.7 Antitumor activity of cediranib in a panel of patient-derived ovarian carcinoma xenografts.** Effect of cediranib on the lifespan of HOC8 (A), HOC10 (B), HOC22 (C) and HOC79 (D). Cediranib (light-blue lines) was given at the dose of 3 mg/kg, p.o., daily for 21 days (Q1x21). Black lines represent mice treated with vehicles. The light-blue arrows indicated the days at which cediranib was administered. n=10. **p<0.01, ***p<0.001, ****p<0.0001.

A

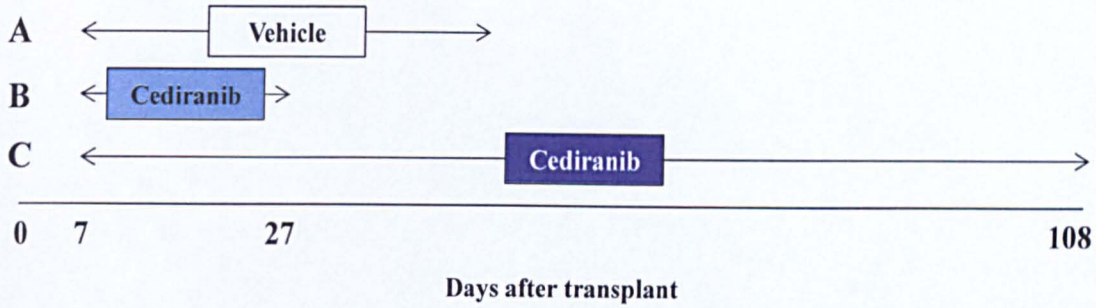


B

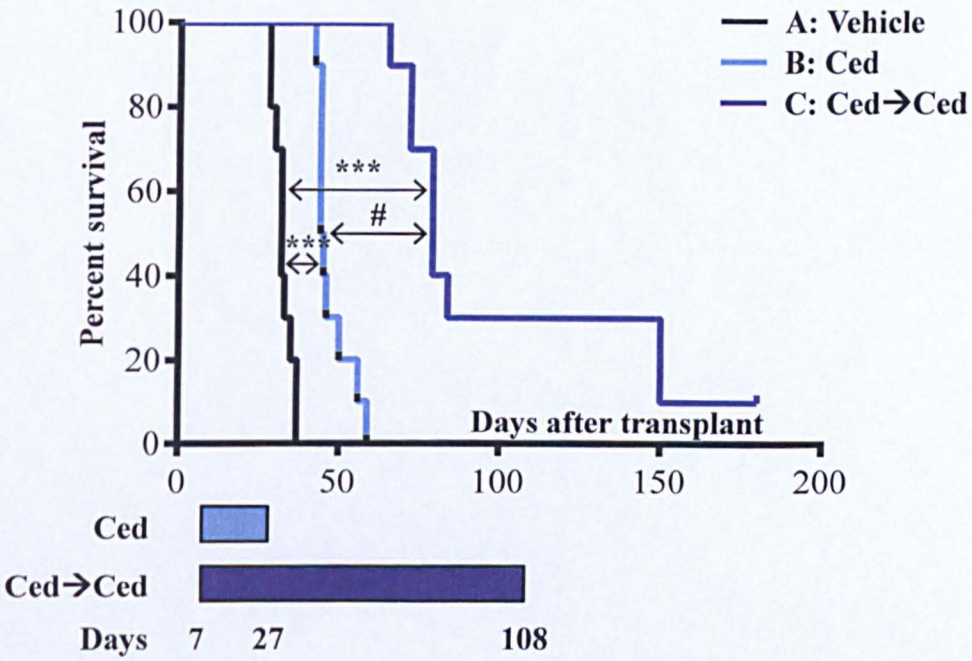


**Figure 5.8 Antitumor activity of cediranib on HOC8 xenograft.** (A) Protocol of the study: treatment started seven days after intraperitoneal HOC8 transplantation in nude mice and given daily by oral gavage. Cediranib was used at the dose of 3 mg/kg, p.o., and was given for 21 days (Ced) or continued until day 108 (Ced→Ced). (B) Effect of cediranib on the lifespan of mice bearing HOC8 (n=10, ***$p<0.0001$ vs vehicle, #$p<0.0001$ vs Ced). The light-blue and blue bars indicated the time at when Ced and Ced→Ced were administered, respectively. This graph is from the same trial of graph in Figure 5.7A, referring to the same vehicle and Ced. Abbreviation: Ced= cediranib.

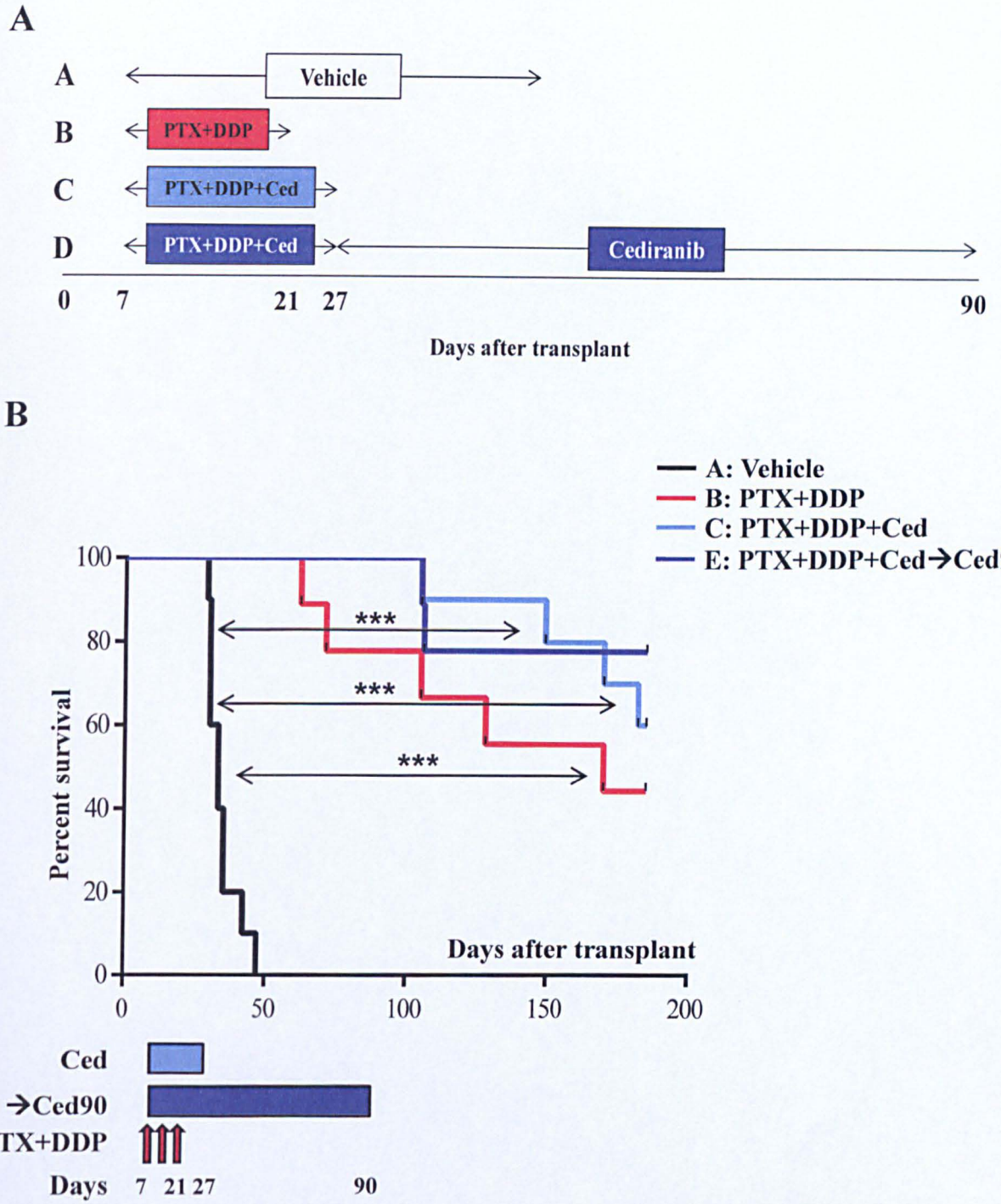


**Figure 5.9 Antitumor activity of paclitaxel plus cisplatin combined with cediranib on HOC8 xenograft**. (A) Protocol of the study: treatments started seven days after HOC8 transplanted intraperitoneally in nude mice. PTX (10 mg/kg) + DDP (3 mg/kg) were injected i.v. every seven days for 3 cycles. Cediranib (3 mg/kg, p.o.) was stopped after three chemotherapy cycles (day 21, Ced), or maintained until day 90 (Ced→Ced90). (B) Effect of PTX+DDP alone or in combination with cediranib on the lifespan of mice bearing HOC8 (n=10). All the groups were significantly different from vehicle group (***$p<0.0001$). The light-blue and blue bars indicated the time at when Ced and Ced→Ced90 were administered, respectively. The arrows indicated the time at when PTX+DDP was given. Abbreviation: Ced= cediranib.

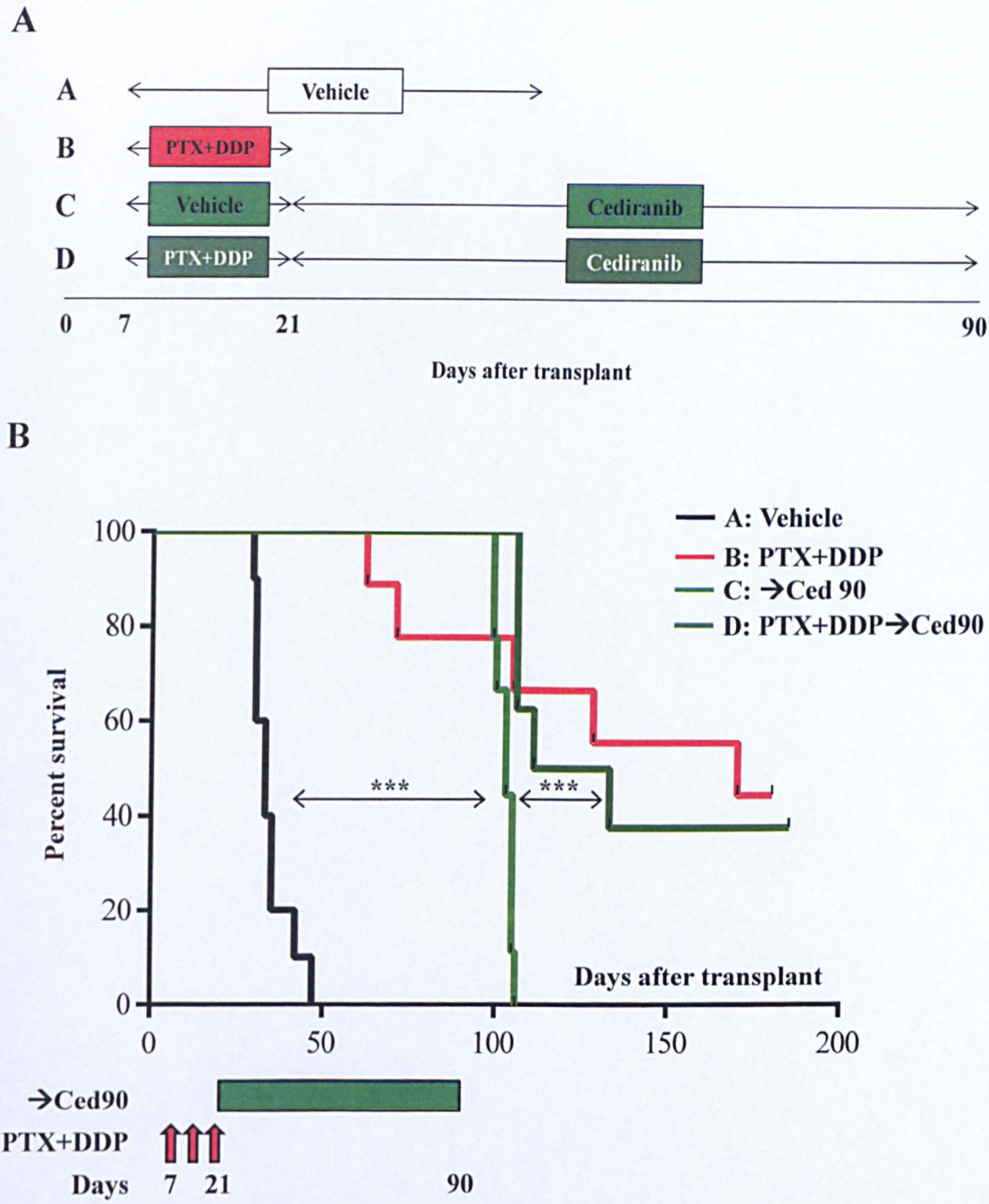


**Figure 5.10 Antitumor activity of cediranib administered after induction with chemotherapy on HOC8 xenograft.** (A) Protocol of the study: chemotherapy treatments started seven days after HOC8 transplanted intraperitoneally in nude mice. PTX (10 mg/kg) + DDP (3 mg/kg) were injected i.v. every seven days for 3 cycles. Cediranib (3 mg/kg, p.o.) started at day 22, at the end of the three cycles of chemotherapy (→Ced90) and continued daily until day 90. (B) Effect of the different treatments on the lifespan of mice bearing HOC8 (n=10, ***p<0.0001 vs vehicle and ***p=0.0002 vs PTX+DDP→Ced90). The green bar indicated the time at when →Ced90 was administered. The arrows indicated the time at when PTX+DDP was given. This graph is from the same trial of graph in Figure 5.9, reffering to the same Vehicle and PTX+DDP. Abbreviation: Ced= cediranib.

| IGROV1 variant | IGROV1-luc/VEGFCmf | | IGROV1-luc | |
|---|---|---|---|---|
| **Treatment** | **Vehicle** | **Cediranib** | **Vehicle** | **Cediranib** |
| Primary tumor take | 5/5 (100%) | 5/5 (100%) | 5/5 (100%) | 5/5 (100%) |
| Presence of ascites | 2/5 (**40%**) | 0/5 | 0/5 | 0/5 |
| Diaphragm metastasis | 4/4 (**100%**) | 3/5 (**60%**) | 2/4 (**50%**) | 2/4 (**50%**) |

**Table 5.1 Effect of cediranib on ascites and diaphragm metastasis.** IGROV1-luc or IGROV1-luc/VEGFCmf were transplanted orthotopically in the ovary of nude mice. At day 28 presence of primary tumor and ascites were verified and histopathological analysis of diaphragm was done. Data are the number (and percentage) of positive mice over total mice.

| IGROV1 variant | sVEGFR1 | | sVEGFR2 | | sVEGFR3 | |
|---|---|---|---|---|---|---|
| | $R^2$ | p | $R^2$ | p | $R^2$ | p |
| IGROV1-luc | 0.8969 | ns | 0.9308 | 0.352 | 0.9832 | 0.0084 |
| IGROV1-luc/ VEGFCfl | 0.9353 | 0.0329 | 0.97 | 0.0151 | 0.9840 | 0.008 |
| IGROV1-luc/ VEGFCmf | 0.992 | 0.004 | 0.9139 | 0.044 | 0.9495 | 0.0256 |

**Table 5.2 Pearson's correlation between tumor burden and soluble VEGFRs.** Tumor burden, expressed as photon counts and showed in Figure 4.10B, had been correlated to soluble VEGFRs detected in the serum of IGROV1-luc, IGROV1-luc/VEGFCfl or IGROV1-luc/VEGFCmf-bearing mice (Figure 5.3). VEGFR1 positively correlated with tumor burden, while VEGFR2 and VEGFR3 showed an inverse corrleation with tumor burden. ns = not significant.

| IGROV1 variants | Treatment | sVEGFR1 | | sVEGFR2 | | sVEGFR3 | |
|---|---|---|---|---|---|---|---|
| | | $R^2$ | p | $R^2$ | p | $R^2$ | p |
| IGROV1-luc | **Vehicle** | 0.9162 | 0.0428 | 0.9796 | 0.010 | 0.9460 | 0.0274 |
| | **Cediranib** | 0.9467 | 0.0270 | 0.8938 | ns | 0.7831 | ns |
| IGROV1-luc/ VEGFCmf | **Vehicle** | 0.9097 | 0.0462 | 0.8723 | ns | 0.8064 | ns |
| | **Cediranib** | 0.9256 | 0.0379 | 0.8864 | ns | 0.9340 | 0.0336 |

**Table 5.3 Pearson's correlation between tumor burden and soluble VEGFRs.** Tumor burden, expressed as photon counts and showed in Figure 5.1, had been correlated to soluble VEGFRs detected in the serum of IGROV1-luc/VEGFCmf and IGROV1-luc bearing mice, treated with vehicle or cediranib (Figure 5.4). VEGFR1 positively correlated with tumor burden, while VEGFR2 and VEGFR3 showed an inverse corrleation with tumor burden. ns = not significant.

Chapter 6

# Conclusions and Future directions

## 6.1 Conclusions

This project was aimed to investigate the role of VEGFC and VEGFR3 in ovarian cancer progression, as it is an interesting targetable pathway to inhibit ovarian cancer.

To this purpose, two different models of human ovarian carcinoma xenografts were described in chapter 3. Firstly, a panel of patient-derived ovarian carcinoma xenografts maintaining the histopathological and molecular features of ovarian cancer patients was investigated, and circulating VEGFC in serum and ascites of human ovarian carcinoma bearing mice demonstrated. Furthermore, for one of these xenografts, the HOC8, it was shown that VEGFC levels correlated with tumor burden and lymph node invasion, suggesting that VEGFC released in biological fluids might serve as an indicator of tumor burden and invasion and confirming the data obtained in patients (Cheng, Liang *et al.* 2013).

The second model was the intraovarian orthotopic xenograft obtained by transplanting human ovarian tumor cells (1A9 and IGROV1) under the bursa of the ovary of immunodeficient mice. The orthotopic model reproduces the appropriate tumor microenvironment and allows the emergence of biological features of cancer progression, angiogenic process, metastatic phenotype and therapeutic response to therapies with patterns more similar to those observed in human cancer.

These models were used in the next chapter to study the interaction VEGFC/VEGFR3.

In chapter 4, the behavior of VEGFC over-expressing ovarian cancer cells was studied.

It was shown that the VEGFC released in the conditioned medium of both IGROV1-luc/VEGFCmf and 1A9-luc/VEGFCmf cells is biologically active, as it stimulated lymphatic endothelial cell motility.

VEGFC is the main promoter of lymphangiogenesis, and it is expressed in a number of tumors with regulatory functions in their progression and dissemination. Here it was demonstrated that VEGFC promoted *in vivo* tumor growth and metastatic spread of ovarian cancer cells to the diaphragm and the retroperitoneal space of experimental mice, although it was not sufficient to induce the colonization of para-aortic lymph node from the intraovarian orthotopic growing tumors. VEGFC detected in serum of mice bearing VEGFC-overexpressing cells correlated with tumor burden, confirming the possible use of VEGFC released in biological fluids as an indicator of tumor burden and invasion.

The increased dissemination in the VEGFC over-expressing xenografts might depend on both autocrine and paracrine VEGFC activities. Indeed, it was shown that VEGFC released by tumor cells enhanced the autocrine stimulation of cell motility on both IGROV1-luc and 1A9-luc tumor cells expressing VEGFR3; on the contrary, the addition of VEGFR3/Fc chimera (specifically inhibiting VEGFC) to the conditioned medium of VEGFC over-expressing cells blocked the induction of cell motility. These data strongly support the involvement of VEGFC in tumor cell migration and dissemination.

In conclusion, VEGFC contributes to ovarian carcinoma progression by directly acting on tumor cells. Moreover, lymphatic dissemination is primarily observed in those tumors over-expressing VEGFC.

Since the involvement of VEGFC/VEGFR3 in ovarian cancer progression and dissemination offered a promising target for therapy, the therapeutic potential of the blockade of this pathway was investigated in chapter 5.

As there were not VEGFR3 selective inhibitors available, cediranib, a VEGF receptors tyrosine kinase inhibitor, effective in blocking VEGFR3 and VEGFR2 and preventing the formation of lymphatic metastasis was used (Padera, Kuo *et al.* 2008).

This molecule had a dual effect on tumor growth and invasion, by directly targeting the tumor cells and by inhibiting lymphatic vessel activation and blood vessel formation (Heckman, Holopainen *et al.* 2008; Medinger, Esser *et al.* 2009).

Cediranib was effective on tumor growth and survival of both VEGFC over-expressing or wild-type tumors, but the efficacy in counteracting tumor dissemination was observed only in IGROV1-luc over-expressing VEGFC tumors, suggesting relevant role of VEGFC in metastasis. The significant effect of cediranib on the *in vitro* migration of IGROV1-luc cells stimulated with conditioned medium from VEGFC over-expressing cells supported this conclusion.

The activity of cediranib was also investigated on the panel of patient-derived ovarian carcinoma xenografts. These xenografts produced ascites, an important feature of ovarian cancer and were heterogeneous in the amounts of VEGFC released in ascites and serum; in addition VEGFR3 and VEGFR2 expression varied among the HOC tumors.

It was shown that cediranib was effective on all the xenografts but it was more effective on tumor releasing high VEGFC and expressing VEGFR3, thus supporting the importance of the VEGFC/VEGFR3 autocrine loop.

However it cannot be excluded that the effect of cediranib on ovarian carcinoma xenografts might be due to the binding of VEGFC to VEGFR2 that can exert both angiogenic activity and autocrine effect.

Different schedules and regimens of cediranib were tested and cediranib was combined with chemotherapy in order to reproduce the on-going ICON6 clinical trial and to answer some uncertain issues.

It was first demonstrated that maintenance therapy was more effective than the 3 weeks-treatment in prolonging mice survival. Surprisingly, significant prolongation of survival was observed starting the treatment with cediranib (single therapy) on advanced tumors (day 22) and maintaining until day 90. This is particularly important, since ovarian cancer is frequently diagnosed at advanced stage. Reduction of abdominal distention was observed after cediranib administration, suggesting that the efficacy of this TKI on advanced tumors was also due to a decrease in ascites and thus also indicating the importance of maintenance treatment to keep this process under control.

It was shown that treatment benefits were improved combining cediranib with chemotherapy, although no significant difference was observed with cediranib stopped (day 27) or maintained after chemotherapy (day 90). On the contrary, starting cediranib after chemotherapy was not advantageous.

In conclusion, in this thesis it was extensively demonstrated that VEGFC in serum or ascites of ovarian carcinoma bearing mice correlated with tumor progression. To be noted that high levels of VEGFC have been reported in ovarian cancer patients.
Moreover, high VEGFC was detected in mice bearing tumors responsive to cediranib and levels correlated with the response. This points to VEGFC as a possible indicator of tumor burden.

### 6.2 Future directions

As a result of the research performed in this project, further studies can be proposed which would strengthen the promising findings seen here.

First, as it was demonstrated that cediranib was more effective on human ovarian tumor xenografts that released a high amount of VEGFC and had the highest expression of VEGFR3, a larger panel of patient-derived human ovarian xenografts will be characterized for the production of VEGFC and the expression of VEGF receptors. The response to cediranib will be further investigated, in order to find a possible correlation between VEGFC/VEGFR3 expression and the response to therapy. The availability of a "signature" predictive of response to cediranib could be useful to stratify patients for therapy.

Second, ovarian cancers secrete large amounts of VEGFA. VEGFA over-expression is frequently described in ovarian cancer patients and is associated with disease progression and a worse outcome (Bamberger and Perrett 2002). Our previous data with bevacizumab, the humanized antibody directed against VEGFA, showed efficacy in patient-derived ovarian cancer xenografts (Oliva, Decio *et al.* 2012); it would be interesting to "vertically inhibit" the antiangiogenic pathway, combining bevacizumab and cediranib. This was indeed demonstrated in mice bearing human head and neck tumors (Bozec, Gros *et al.* 2008) and in the A431 human vulval tumour xenograft (Kendrew, Odedra *et al.* 2013).
This hypothesis that the double inhibition of VEGFA (bevacizumab) and VEGFC/VEGFRs (cediranib) could improve the efficacy of antiangiogenic therapies also in ovarian cancer is worth exploring.

Then, the search of biomarkers is important for the future of antiangiogenic therapy. To date, reliable biomarkers able to predict the efficacy of these treatments are still far from be identified. The need for validated biomarkers to select those patients that most likely would benefit from antiangiogenic drugs has become even more critical (Jayson, Hicklin *et al.* 2012).

On the basis of the results presented in this thesis, VEGFC, soluble VEGFR1 and soluble VEGFR2 seem to be promising molecules to be investigated for this scope. They will be analyzed and validated in a bigger panel of patient-derived ovarian cancer xenografts.

Another important point related to the search of biomarkers is the involvement of stroma in the response to antiangiogenic therapy. Indeed, among the mechanisms involved in evasive resistance to angiogenic inhibitors, tumor microenvironment (e.g. hypoxia, revascularization, recruitment of pericytes) could be relevant (Bergers and Hanahan 2008; Shojaei and Ferrara 2008). Thus, the effect of the interaction between tumor and mouse stroma on cediranib therapy will be investigated, conscious that the drift of stromal components of these tumor xenografts from human to mouse could present a relevant drawback of these models.

As already discussed in chapter 5, the mature form of VEGFC can bind to and activate also VEGFR2. Furthermore, cediranib, not only blocks VEGFR3, but also VEGFR2 and VEGFR1. For this reason, the influence of VEGFR2 on the results obtained thus far will be investigated.

Cediranib is an antiangiogenic drug and was described to block VEGFC-induced VEGFR3 activity and lymphangiogenesis (Heckman, Hyngstrom *et al.* 2008). In our models it was shown that cediranib is effective in inhibiting tumor growth, metastasis, and ascites formation, but we have no data regarding the lymphangiogenic/antiangiogenic effect of cediranib. Treated tumors will be stained for markers of lymphatic (LYVE-1) and blood vessels (CD31), in order to investigate the possible reduction of vessels after therapy.

Tumor cells were detected in lymphatics in VEGFC-over-expressing tumors only, indicating that lymphatic vessels were somehow activated by VEGFC, favoring tumor cell entry. It was already demonstrated that VEGFC promotes tumor invasion toward lymphatics by increasing lymphatic secretion of CCL21 which, in turn, drives CCR7-dependent chemotactic tumor invasion (Issa, Le *et al.* 2009). Therefore, stain for CCL21 will be performed, in relation to tumor invasion.

Finally, as shown in chapter 5, VEGFR3 expression was analysed by immunohistochemistry in HOC8 xenograft and in a set of 12 patients (Decio, Taraboletti *et al.* in press, 2014). VEGFR3 was expressed by the majority of neoplastic cells and it was mostly localized in the cytoplasmic compartment. To further understand the mechanisms and the role of VEGFC/VEGFR3 pathway in ovarian cancer metastasis, the possible translocation of VEGFC-activated VEGFR3 into the nucleus, where it may activate genes with central role in cancer progression, will be investigated. This had already been hypothesized for lung adenocarcinoma cells and primary lymphatic endothelial cells (Su, Yen *et al.* 2007).

# Bibliography

Achen, M. G., M. Clauss, et al. (1995). "The non-receptor tyrosine kinase Lyn is localised in the developing murine blood-brain barrier." Differentiation **59**(1): 15-24.

Achen, M. G., J. M. Gad, et al. (1997). "Placenta growth factor and vascular endothelial growth factor are co-expressed during early embryonic development." Growth Factors **15**(1): 69-80.

Achen, M. G., B. K. McColl, et al. (2005). "Focus on lymphangiogenesis in tumor metastasis." Cancer Cell **7**(2): 121-7.

Achen, M. G. and S. A. Stacker (1998). "The vascular endothelial growth factor family; proteins which guide the development of the vasculature." Int J Exp Pathol **79**(5): 255-65.

Achen, M. G. and S. A. Stacker (2008). "Molecular control of lymphatic metastasis." Ann N Y Acad Sci **1131**: 225-34.

Aghajanian, C., N. J. Finkler, et al. (2011). OCEANS: a randomized, double-blinded, placebo-controlled phase III trial of chemotherapy with or without bevacizumab (BEV) in patients with platinum-sensitive recurrent epithelial ovarian (EOC), primary peritoneal (PPC), or fallopian tube cancer (FTC). ASCO Annual Meeting, Journal of Clinical Oncology.

Ahmed, A. A., D. Etemadmoghadam, et al. (2010). "Driver mutations in TP53 are ubiquitous in high grade serous carcinoma of the ovary." J Pathol **221**(1): 49-56.

Alam, A., I. Blanc, et al. (2012). "SAR131675, a potent and selective VEGFR-3-TK inhibitor with antilymphangiogenic, antitumoral, and antimetastatic activities." Mol Cancer Ther **11**(8): 1637-49.

Alitalo, A. and M. Detmar (2012). "Interaction of tumor cells and lymphatic vessels in cancer progression." Oncogene **31**(42): 4499-508.

Arinaga, M., T. Noguchi, et al. (2003). "Clinical significance of vascular endothelial growth factor C and vascular endothelial growth factor receptor 3 in patients with nonsmall cell lung carcinoma." Cancer **97**(2): 457-64.

Avraham, H., S. Y. Park, et al. (2000). "RAFTK/Pyk2-mediated cellular signalling." Cell Signal **12**(3): 123-33.

Baeuerle, P. A. and D. Baltimore (1996). "NF-kappa B: ten years after." Cell **87**(1): 13-20.

Baldwin, M. E., S. A. Stacker, et al. (2002). "Molecular control of lymphangiogenesis." Bioessays **24**(11): 1030-40.

Bamberger, E. S. and C. W. Perrett (2002). "Angiogenesis in epithelian ovarian cancer." Mol Pathol **55**(6): 348-59.

Bast, R. C., Jr., B. Hennessy, et al. (2009). "The biology of ovarian cancer: new opportunities for translation." Nat Rev Cancer **9**(6): 415-28.

Batchelor, T., P. Mulholland, et al. (2010). A Phase III randomized study comparing the efficacy of cediranib as monotherapy, and in combination with lomustine alone in recurrent glioblastoma patients. 35th ESMO Congress, Annals of Oncology.

Beasley, N. J., R. Prevo, et al. (2002). "Intratumoral lymphangiogenesis and lymph node metastasis in head and neck cancer." Cancer Res **62**(5): 1315-20.

Beierle, E. A., W. Dai, et al. (2004). "Expression of VEGF receptors in cocultured neuroblastoma cells." J Surg Res **119**(1): 56-65.

Benard, J., J. Da Silva, et al. (1985). "Characterization of a human ovarian adenocarcinoma line, IGROV1, in tissue culture and in nude mice." Cancer Res **45**(10): 4970-9.

Benedet, J. L., H. Bender, et al. (2000). "FIGO staging classifications and clinical practice guidelines in the management of gynecologic cancers. FIGO Committee on Gynecologic Oncology." Int J Gynaecol Obstet **70**(2): 209-62.

Bergers, G. and L. E. Benjamin (2003). "Tumorigenesis and the angiogenic switch." Nat Rev Cancer **3**(6): 401-10.

Bergers, G. and D. Hanahan (2008). "Modes of resistance to anti-angiogenic therapy." Nat Rev Cancer **8**(8): 592-603.

Bhowmick, N. A., E. G. Neilson, et al. (2004). "Stromal fibroblasts in cancer initiation and progression." Nature **432**(7015): 332-7.

Bolis, G., G. Scarfone, et al. (2010). "Paclitaxel/carboplatin versus topotecan/paclitaxel/carboplatin in patients with FIGO suboptimally resected stage III-IV epithelial ovarian cancer a multicenter, randomized study." Eur J Cancer **46**(16): 2905-12.

Bookman, M. A., M. F. Brady, et al. (2009). "Evaluation of new platinum-based treatment regimens in advanced-stage ovarian cancer: a Phase III Trial of the Gynecologic Cancer Intergroup." J Clin Oncol **27**(9): 1419-25.

Bozec, A., F. X. Gros, et al. (2008). "Vertical VEGF targeting: A combination of ligand blockade with receptor tyrosine kinase inhibition." Eur J Cancer **44**(13): 1922-30.

Burger, R. A., M. F. Brady, et al. (2011). "Incorporation of bevacizumab in the primary treatment of ovarian cancer." N Engl J Med **365**(26): 2473-83.

Burghardt, E., H. Pickel, et al. (1986). "Pelvic lymphadenectomy in operative treatment of ovarian cancer." Am J Obstet Gynecol **155**(2): 315-9.

Burns, J. C., T. Friedmann, et al. (1993). "Vesicular stomatitis virus G glycoprotein pseudotyped retroviral vectors: concentration to very high titer and efficient gene transfer into mammalian and nonmammalian cells." Proc Natl Acad Sci U S A **90**(17): 8033-7.

Cannistra, S. A., R. C. Bast, Jr., et al. (2003). "Progress in the management of gynecologic cancer: consensus summary statement." J Clin Oncol **21**(10 Suppl): 129s-132s.

Cao, Y., P. Linden, et al. (1998). "Vascular endothelial growth factor C induces angiogenesis in vivo." Proc Natl Acad Sci U S A **95**(24): 14389-94.

Carmeliet, P. and R. K. Jain (2000). "Angiogenesis in cancer and other diseases." Nature **407**(6801): 249-57.

Carmignani, C. P., T. A. Sugarbaker, et al. (2003). "Intraperitoneal cancer dissemination: mechanisms of the patterns of spread." Cancer Metastasis Rev **22**(4): 465-72.

Cass, I., A. J. Li, et al. (2001). "Pattern of lymph node metastases in clinically unilateral stage I invasive epithelial ovarian carcinomas." Gynecol Oncol **80**(1): 56-61.

Chen, S. S. and L. Lee (1983). "Incidence of para-aortic and pelvic lymph node metastases in epithelial carcinoma of the ovary." Gynecol Oncol **16**(1): 95-100.

Chen, V. W., B. Ruiz, et al. (2003). "Pathology and classification of ovarian tumors." Cancer **97**(10 Suppl): 2631-42.

Chen, Y., L. Jiang, et al. (2010). "Vascular endothelial growth factor-C promotes the growth and invasion of gallbladder cancer via an autocrine mechanism." Mol Cell Biochem **345**(1-2): 77-89.

Chen, Z., M. L. Varney, et al. (2005). "Down-regulation of vascular endothelial cell growth factor-C expression using small interfering RNA vectors in mammary tumors inhibits tumor lymphangiogenesis and spontaneous metastasis and enhances survival." Cancer Res **65**(19): 9004-11.

Cheng, D., B. Liang, et al. (2013). "Serum vascular endothelial growth factor (VEGF-C) as a diagnostic and prognostic marker in patients with ovarian cancer." PLoS One **8**(2): e55309.

Chilov, D., E. Kukk, et al. (1997). "Genomic organization of human and mouse genes for vascular endothelial growth factor C." J Biol Chem **272**(40): 25176-83.

Collinson, F. J., J. Seligmann, et al. (2012). "Ovarian cancer: advances in first-line treatment strategies with a particular focus on anti-angiogenic agents." Curr Oncol Rep **14**(6): 509-18.

Colombo, N. (2011). "Efficacy of trabectedin in platinum-sensitive-relapsed ovarian cancer: new data from the randomized OVA-301 study." Int J Gynecol Cancer **21 Suppl 1**: S12-6.

Connolly, D. C. (2009). "Animal models of ovarian cancer." Cancer Treat Res **149**: 353-91.

Cramer, D. W., G. B. Hutchison, et al. (1983). "Determinants of ovarian cancer risk. I. Reproductive experiences and family history." J Natl Cancer Inst **71**(4): 711-6.

Cramer, D. W. and W. R. Welch (1983). "Determinants of ovarian cancer risk. II. Inferences regarding pathogenesis." J Natl Cancer Inst **71**(4): 717-21.

Cree, I. A., S. Glaysher, et al. (2010). "Efficacy of anti-cancer agents in cell lines versus human primary tumour tissue." Curr Opin Pharmacol **10**(4): 375-9.

Cueni, L. N. and M. Detmar (2006). "New insights into the molecular control of the lymphatic vascular system and its role in disease." J Invest Dermatol **126**(10): 2167-77.

Dadras, S. S., T. Paul, et al. (2003). "Tumor lymphangiogenesis: a novel prognostic indicator for cutaneous melanoma metastasis and survival." Am J Pathol **162**(6): 1951-60.

Daniel, V. C., L. Marchionni, et al. (2009). "A primary xenograft model of small-cell lung cancer reveals irreversible changes in gene expression imposed by culture in vitro." Cancer Res **69**(8): 3364-73.

Decaudin, D. (2011). "Primary human tumor xenografted models ('tumorgrafts') for good management of patients with cancer." Anticancer Drugs **22**(9): 827-41.

Decio, A., G. Taraboletti, et al. (in press, 2014). "Vascular Endothelial Growth Factor C promotes ovarian carcinoma progression through paracrine and autocrine mechanisms." Am J Pathol.

Denduluri, N., S. X. Yang, et al. (2008). "Circulating biomarkers of bevacizumab activity in patients with breast cancer." Cancer Biol Ther 7(1): 15-20.

Deprimo, S. E., C. L. Bello, et al. (2007). "Circulating protein biomarkers of pharmacodynamic activity of sunitinib in patients with metastatic renal cell carcinoma: modulation of VEGF and VEGF-related proteins." J Transl Med **5**: 32.

Dixelius, J., T. Makinen, et al. (2003). "Ligand-induced vascular endothelial growth factor receptor-3 (VEGFR-3) heterodimerization with VEGFR-2 in primary lymphatic endothelial cells regulates tyrosine phosphorylation sites." J Biol Chem **278**(42): 40973-9.

Dowlati, A., R. Gray, et al. (2008). "Cell adhesion molecules, vascular endothelial growth factor, and basic fibroblast growth factor in patients with non-small cell lung cancer treated with chemotherapy with or without bevacizumab--an Eastern Cooperative Oncology Group Study." Clin Cancer Res **14**(5): 1407-12.

du Bois, A., J. Herrstedt, et al. (2010). "Phase III trial of carboplatin plus paclitaxel with or without gemcitabine in first-line treatment of epithelial ovarian cancer." J Clin Oncol **28**(27): 4162-9.

Dumont, D. J., L. Jussila, et al. (1998). "Cardiovascular failure in mouse embryos deficient in VEGF receptor-3." Science **282**(5390): 946-9.

Edmondson, R. J. and J. M. Monaghan (2001). "The epidemiology of ovarian cancer." Int J Gynecol Cancer **11**(6): 423-9.

Ellis, L. M. and D. J. Hicklin (2008). "VEGF-targeted therapy: mechanisms of anti-tumour activity." Nat Rev Cancer **8**(8): 579-91.

Emi, N., T. Friedmann, et al. (1991). "Pseudotype formation of murine leukemia virus with the G protein of vesicular stomatitis virus." J Virol **65**(3): 1202-7.

Eriksson, U. and K. Alitalo (1999). "Structure, expression and receptor-binding properties of novel vascular endothelial growth factors." Curr Top Microbiol Immunol **237**: 41-57.

Evers, B., R. Drost, et al. (2008). "Selective inhibition of BRCA2-deficient mammary tumor cell growth by AZD2281 and cisplatin." Clin Cancer Res **14**(12): 3916-25.

Fadare, O., M. P. Orejudos, et al. (2008). "A comparative analysis of lymphatic vessel density in ovarian serous tumors of low malignant potential (borderline tumors) with and without lymph node involvement." Int J Gynecol Pathol **27**(4): 483-90.

Fathalla, M. F. (1971). "Incessant ovulation--a factor in ovarian neoplasia?" Lancet **2**(7716): 163.

Feki, A., P. Berardi, et al. (2009). "Dissemination of intraperitoneal ovarian cancer: Discussion of mechanisms and demonstration of lymphatic spreading in ovarian cancer model." Crit Rev Oncol Hematol **72**(1): 1-9.

Fernando, A., S. Glaysher, et al. (2006). "Effect of culture conditions on the chemosensitivity of ovarian cancer cell lines." Anticancer Drugs **17**(8): 913-9.

Ferrara, N. (1999). "Vascular endothelial growth factor: molecular and biological aspects." Curr Top Microbiol Immunol **237**: 1-30.

Ferrara, N. and K. Alitalo (1999). "Clinical applications of angiogenic growth factors and their inhibitors." Nat Med **5**(12): 1359-64.

Ferrell, R. E., K. L. Levinson, et al. (1998). "Hereditary lymphedema: evidence for linkage and genetic heterogeneity." Hum Mol Genet **7**(13): 2073-8.

Fiebig, H. H., A. Maier, et al. (2004). "Clonogenic assay with established human tumour xenografts: correlation of in vitro to in vivo activity as a basis for anticancer drug discovery." Eur J Cancer **40**(6): 802-20.

Fiedler, W., R. Mesters, et al. (2010). "An open-label, Phase I study of cediranib (RECENTIN) in patients with acute myeloid leukemia." Leuk Res **34**(2): 196-202.

Folkman, J. (1995). "Angiogenesis in cancer, vascular, rheumatoid and other disease." Nat Med **1**(1): 27-31.

Fu, X. and R. M. Hoffman (1993). "Human ovarian carcinoma metastatic models constructed in nude mice by orthotopic transplantation of histologically-intact patient specimens." Anticancer Res **13**(2): 283-6.

Garofalo, A., E. Naumova, et al. (2003). "The combination of the tyrosine kinase receptor inhibitor SU6668 with paclitaxel affects ascites formation and tumor spread in ovarian carcinoma xenografts growing orthotopically." Clin Cancer Res **9**(9): 3476-85.

Ghosh, S., C. A. Sullivan, et al. (2008). "High levels of vascular endothelial growth factor and its receptors (VEGFR-1, VEGFR-2, neuropilin-1) are associated with worse outcome in breast cancer." Hum Pathol **39**(12): 1835-43.

Giavazzi, R., B. Sennino, et al. (2003). "Distinct role of fibroblast growth factor-2 and vascular endothelial growth factor on tumor growth and angiogenesis." Am J Pathol **162**(6): 1913-26.

Gille, J., R. A. Swerlick, et al. (1997). "Transforming growth factor-alpha-induced transcriptional activation of the vascular permeability factor (VPF/VEGF) gene requires AP-2-dependent DNA binding and transactivation." EMBO J **16**(4): 750-9.

Gorelik, B., I. Ziv, et al. (2008). "Efficacy of weekly docetaxel and bevacizumab in mesenchymal chondrosarcoma: a new theranostic method combining xenografted biopsies with a mathematical model." Cancer Res **68**(21): 9033-40.

Goss, G. D., A. Arnold, et al. (2010). "Randomized, double-blind trial of carboplatin and paclitaxel with either daily oral cediranib or placebo in advanced non-small-cell lung cancer: NCIC clinical trials group BR24 study." J Clin Oncol **28**(1): 49-55.

Hanahan, D. and J. Folkman (1996). "Patterns and emerging mechanisms of the angiogenic switch during tumorigenesis." Cell **86**(3): 353-64.

Hanahan, D. and R. A. Weinberg (2011). "Hallmarks of cancer: the next generation." Cell **144**(5): 646-74.

Hanrahan, E. O., H. Y. Lin, et al. (2010). "Distinct patterns of cytokine and angiogenic factor modulation and markers of benefit for vandetanib and/or chemotherapy in patients with non-small-cell lung cancer." J Clin Oncol **28**(2): 193-201.

Harrell, M. I., B. M. Iritani, et al. (2007). "Tumor-induced sentinel lymph node lymphangiogenesis and increased lymph flow precede melanoma metastasis." Am J Pathol **170**(2): 774-86.

He, Y., K. Kozaki, et al. (2002). "Suppression of tumor lymphangiogenesis and lymph node metastasis by blocking vascular endothelial growth factor receptor 3 signaling." J Natl Cancer Inst **94**(11): 819-25.

Heckman, C. A., T. Holopainen, et al. (2008). "The tyrosine kinase inhibitor cediranib blocks ligand-induced vascular endothelial growth factor receptor-3 activity and lymphangiogenesis." Cancer Res **68**(12): 4754-62.

Heckman, C. J., A. S. Hyngstrom, et al. (2008). "Active properties of motoneurone dendrites: diffuse descending neuromodulation, focused local inhibition." J Physiol **586**(5): 1225-31.

Hirakawa, S., L. F. Brown, et al. (2007). "VEGF-C-induced lymphangiogenesis in sentinel lymph nodes promotes tumor metastasis to distant sites." Blood **109**(3): 1010-7.

Hirte, H. W., L. Vidal, et al. (2008). A phase II study of cediranib (AZD2171) in recurrent or persistent ovarian, peritoneal or fallopian tube cancer: final results of a PMH, Chicago and California consortia trial. ASCO Annual Meeting, Journal of Clinical Oncology.

Hoshida, T., N. Isaka, et al. (2006). "Imaging steps of lymphatic metastasis reveals that vascular endothelial growth factor-C increases metastasis by increasing delivery of cancer cells to lymph nodes: therapeutic implications." Cancer Res **66**(16): 8065-75.

Hoskins, P., I. Vergote, et al. (2010). "Advanced ovarian cancer: phase III randomized study of sequential cisplatin-topotecan and carboplatin-paclitaxel vs carboplatin-paclitaxel." J Natl Cancer Inst **102**(20): 1547-56.

Huang, K. J. and L. H. Sui (2012). "The relevance and role of vascular endothelial growth factor C, matrix metalloproteinase-2 and E-cadherin in epithelial ovarian cancer." Med Oncol **29**(1): 318-23.

Imagawa, M., R. Chiu, et al. (1987). "Transcription factor AP-2 mediates induction by two different signal-transduction pathways: protein kinase C and cAMP." Cell **51**(2): 251-60.

Irrthum, A., M. J. Karkkainen, et al. (2000). "Congenital hereditary lymphedema caused by a mutation that inactivates VEGFR3 tyrosine kinase." Am J Hum Genet **67**(2): 295-301.

Issa, A., T. X. Le, et al. (2009). "Vascular endothelial growth factor-C and C-C chemokine receptor 7 in tumor cell-lymphatic cross-talk promote invasive phenotype." Cancer Res **69**(1): 349-57.

Jackson, D. G., R. Prevo, et al. (2001). "LYVE-1, the lymphatic system and tumor lymphangiogenesis." Trends Immunol **22**(6): 317-21.

Jayson, G. C., D. J. Hicklin, et al. (2012). "Antiangiogenic therapy-evolving view based on clinical trial results." Nat Rev Clin Oncol **9**(5): 297-303.

Jeltsch, M., A. Kaipainen, et al. (1997). "Hyperplasia of lymphatic vessels in VEGF-C transgenic mice." Science **276**(5317): 1423-5.

Jeltsch, M., T. Karpanen, et al. (2006). "Vascular endothelial growth factor (VEGF)/VEGF-C mosaic molecules reveal specificity determinants and feature novel receptor binding patterns." J Biol Chem **281**(17): 12187-95.

Jemal, A., F. Bray, et al. (2011). "Global cancer statistics." CA Cancer J Clin **61**(2): 69-90.

Jeon, B. H., C. Jang, et al. (2008). "Profound but dysfunctional lymphangiogenesis via vascular endothelial growth factor ligands from CD11b+ macrophages in advanced ovarian cancer." Cancer Res **68**(4): 1100-9.

Ji, R. C. (2007). "Lymphatic endothelial cells, inflammatory lymphangiogenesis, and prospective players." Curr Med Chem **14**(22): 2359-68.

Jones, S., T. L. Wang, et al. (2010). "Frequent mutations of chromatin remodeling gene ARID1A in ovarian clear cell carcinoma." Science **330**(6001): 228-31.

Jones, S., X. Zhang, et al. (2008). "Core signaling pathways in human pancreatic cancers revealed by global genomic analyses." Science **321**(5897): 1801-6.

Joukov, V., K. Pajusola, et al. (1996). "A novel vascular endothelial growth factor, VEGF-C, is a ligand for the Flt4 (VEGFR-3) and KDR (VEGFR-2) receptor tyrosine kinases." Embo J **15**(7): 1751.

Joukov, V., T. Sorsa, et al. (1997). "Proteolytic processing regulates receptor specificity and activity of VEGF-C." Embo J **16**(13): 3898-911.

Kaipainen, A., J. Korhonen, et al. (1995). "Expression of the fms-like tyrosine kinase 4 gene becomes restricted to lymphatic endothelium during development." Proc Natl Acad Sci U S A **92**(8): 3566-70.

Karkkainen, M. J., R. E. Ferrell, et al. (2000). "Missense mutations interfere with VEGFR-3 signalling in primary lymphoedema." Nat Genet **25**(2): 153-9.

Karkkainen, M. J., P. Haiko, et al. (2004). "Vascular endothelial growth factor C is required for sprouting of the first lymphatic vessels from embryonic veins." Nat Immunol **5**(1): 74-80.

Karpanen, T. and K. Alitalo (2008). "Molecular biology and pathology of lymphangiogenesis." Annu Rev Pathol **3**: 367-97.

Karpanen, T., M. Egeblad, et al. (2001). "Vascular endothelial growth factor C promotes tumor lymphangiogenesis and intralymphatic tumor growth." Cancer Res **61**(5): 1786-90.

Karpanen, T., M. Wirzenius, et al. (2006). "Lymphangiogenic growth factor responsiveness is modulated by postnatal lymphatic vessel maturation." Am J Pathol **169**(2): 708-18.

Karst, A. M. and R. Drapkin (2010). "Ovarian cancer pathogenesis: a model in evolution." J Oncol **2010**: 932371.

Kaushal, V., P. Mukunyadzi, et al. (2005). "Stage-specific characterization of the vascular endothelial growth factor axis in prostate cancer: expression of lymphangiogenic markers is associated with advanced-stage disease." Clin Cancer Res **11**(2 Pt 1): 584-93.

Kendrew, J., R. Odedra, et al. (2013). "Anti-tumour and anti-vascular effects of cediranib (AZD2171) alone and in combination with other anti-tumour therapies." Cancer Chemother Pharmacol **71**(4): 1021-32.

Kim, K. E., C. H. Cho, et al. (2007). "In vivo actions of angiopoietins on quiescent and remodeling blood and lymphatic vessels in mouse airways and skin." Arterioscler Thromb Vasc Biol **27**(3): 564-70.

Klasa-Mazurkiewicz, D., M. Jarzab, et al. (2011). "Clinical significance of VEGFR-2 and VEGFR-3 expression in ovarian cancer patients." Pol J Pathol **62**(1): 31-40.

Koch, S., S. Tugues, et al. (2011). "Signal transduction by vascular endothelial growth factor receptors." Biochem J **437**(2): 169-83.

Kodama, M., Y. Kitadai, et al. (2008). "Vascular endothelial growth factor C stimulates progression of human gastric cancer via both autocrine and paracrine mechanisms." Clin Cancer Res **14**(22): 7205-14.

Kriehuber, E., S. Breiteneder-Geleff, et al. (2001). "Isolation and characterization of dermal lymphatic and blood endothelial cells reveal stable and functionally specialized cell lineages." J Exp Med **194**(6): 797-808.

Krishnan, J., V. Kirkin, et al. (2003). "Differential in vivo and in vitro expression of vascular endothelial growth factor (VEGF)-C and VEGF-D in tumors and its relationship to lymphatic metastasis in immunocompetent rats." Cancer Res **63**(3): 713-22.

Kukk, E., A. Lymboussaki, et al. (1996). "VEGF-C receptor binding and pattern of expression with VEGFR-3 suggests a role in lymphatic vascular development." Development **122**(12): 3829-37.

Kummar, S., D. Allen, et al. (2013). "Cediranib for Metastatic Alveolar Soft Part Sarcoma." J Clin Oncol.

Kurman, R. J. and M. Shih Ie (2010). "The origin and pathogenesis of epithelial ovarian cancer: a proposed unifying theory." Am J Surg Pathol **34**(3): 433-43.

Laakkonen, P., M. Waltari, et al. (2007). "Vascular endothelial growth factor receptor 3 is involved in tumor angiogenesis and growth." Cancer Res **67**(2): 593-9.

Lahat, G., A. Lazar, et al. (2009). "Increased vascular endothelial growth factor-C expression is insufficient to induce lymphatic metastasis in human soft-tissue sarcomas." Clin Cancer Res **15**(8): 2637-46.

Landy, A. (1989). "Dynamic, structural, and regulatory aspects of lambda site-specific recombination." Annu Rev Biochem **58**: 913-49.

Langdon, S. P. (2012). "Animal modeling of cancer pathology and studying tumor response to therapy." Curr Drug Targets **13**(12): 1535-47.

Lenardo, M. J. and D. Baltimore (1989). "NF-kappa B: a pleiotropic mediator of inducible and tissue-specific gene control." Cell **58**(2): 227-9.

Lengyel, E. (2010). "Ovarian cancer development and metastasis." Am J Pathol **177**(3): 1053-64.

Leppanen, V. M., A. E. Prota, et al. (2010). "Structural determinants of growth factor binding and specificity by VEGF receptor 2." Proc Natl Acad Sci U S A **107**(6): 2425-30.

Li, X. and U. Eriksson (2001). "Novel VEGF family members: VEGF-B, VEGF-C and VEGF-D." Int J Biochem Cell Biol **33**(4): 421-6.

Liersch, R., S. Hirakawa, et al. (2012). "Induced lymphatic sinus hyperplasia in sentinel lymph nodes by VEGF-C as the earliest premetastatic indicator." Int J Oncol **41**(6): 2073-8.

Lin, J., A. S. Lalani, et al. (2005). "Inhibition of lymphogenous metastasis using adeno-associated virus-mediated gene transfer of a soluble VEGFR-3 decoy receptor." Cancer Res **65**(15): 6901-9.

Lohela, M., M. Bry, et al. (2009). "VEGFs and receptors involved in angiogenesis versus lymphangiogenesis." Curr Opin Cell Biol **21**(2): 154-65.

Lowe, K. A., V. M. Chia, et al. (2013). "An international assessment of ovarian cancer incidence and mortality." Gynecol Oncol **130**(1): 107-14.

Luciw, P. A. (1996). Fields Virology. Philadelphia, PA, Lippincott-Raven Publishers.

Maggioni, A., P. Benedetti Panici, et al. (2006). "Randomised study of systematic lymphadenectomy in patients with epithelial ovarian cancer macroscopically confined to the pelvis." Br J Cancer **95**(6): 699-704.

Makinen, T., L. Jussila, et al. (2001). "Inhibition of lymphangiogenesis with resulting lymphedema in transgenic mice expressing soluble VEGF receptor-3." Nat Med **7**(2): 199-205.

Makinen, T., T. Veikkola, et al. (2001). "Isolated lymphatic endothelial cells transduce growth, survival and migratory signals via the VEGF-C/D receptor VEGFR-3." Embo J **20**(17): 4762-73.

Mandriota, S. J., L. Jussila, et al. (2001). "Vascular endothelial growth factor-C-mediated lymphangiogenesis promotes tumour metastasis." EMBO J **20**(4): 672-82.

Manenti, L., E. Riccardi, et al. (2005). "Circulating plasma vascular endothelial growth factor in mice bearing human ovarian carcinoma xenograft correlates with tumor progression and response to therapy." Mol Cancer Ther **4**(5): 715-25.

Marconcini, L., S. Marchio, et al. (1999). "c-fos-induced growth factor/vascular endothelial growth factor D induces angiogenesis in vivo and in vitro." Proc Natl Acad Sci U S A **96**(17): 9671-6.

Massazza, G., A. Tomasoni, et al. (1989). "Intraperitoneal and subcutaneous xenografts of human ovarian carcinoma in nude mice and their potential in experimental therapy." Int J Cancer **44**(3): 494-500.

Matsuura, M., M. Onimaru, et al. (2009). "Autocrine loop between vascular endothelial growth factor (VEGF)-C and VEGF receptor-3 positively regulates tumor-associated lymphangiogenesis in oral squamoid cancer cells." Am J Pathol **175**(4): 1709-21.

Matulonis, U. A., S. Berlin, et al. (2009). "Cediranib, an oral inhibitor of vascular endothelial growth factor receptor kinases, is an active drug in recurrent epithelial ovarian, fallopian tube, and peritoneal cancer." J Clin Oncol **27**(33): 5601-6.

McColl, B. K., M. E. Baldwin, et al. (2003). "Plasmin activates the lymphangiogenic growth factors VEGF-C and VEGF-D." J Exp Med **198**(6): 863-8.

Medinger, M., N. Esser, et al. (2009). "Antitumor and antiangiogenic activity of cediranib in a preclinical model of renal cell carcinoma." Anticancer Res **29**(12): 5065-76.

Mitchell, P. J., C. Wang, et al. (1987). "Positive and negative regulation of transcription in vitro: enhancer-binding protein AP-2 is inhibited by SV40 T antigen." Cell **50**(6): 847-61.

Morisada, T., Y. Oike, et al. (2005). "Angiopoietin-1 promotes LYVE-1-positive lymphatic vessel formation." Blood **105**(12): 4649-56.

Moro, M., G. Bertolini, et al. (2012). "Patient-derived xenografts of non small cell lung cancer: resurgence of an old model for investigation of modern concepts of tailored therapy and cancer stem cells." J Biomed Biotechnol **2012**: 568567.

Mouawad, R., J. P. Spano, et al. (2009). "Tumoural expression and circulating level of VEGFR-3 (Flt-4) in metastatic melanoma patients: correlation with clinical parameters and outcome." Eur J Cancer **45**(8): 1407-14.

Mounzer, R. H., O. S. Svendsen, et al. (2010). "Lymphotoxin-alpha contributes to lymphangiogenesis." Blood **116**(12): 2173-82.

Mulders, P., R. Hawkins, et al. (2012). "Cediranib monotherapy in patients with advanced renal cell carcinoma: results of a randomised phase II study." Eur J Cancer **48**(4): 527-37.

Nagy, J. A., E. Vasile, et al. (2002). "Vascular permeability factor/vascular endothelial growth factor induces lymphangiogenesis as well as angiogenesis." J Exp Med **196**(11): 1497-506.

Naldini, L., U. Blomer, et al. (1996). "Efficient transfer, integration, and sustained long-term expression of the transgene in adult rat brains injected with a lentiviral vector." Proc Natl Acad Sci U S A **93**(21): 11382-8.

Nicoletti, M. I., V. Lucchini, et al. (1993). "Antitumor activity of taxol (NSC-125973) in human ovarian carcinomas growing in the peritoneal cavity of nude mice." Ann Oncol **4**(2): 151-5.

Nilsson, I., F. Bahram, et al. (2010). "VEGF receptor 2/-3 heterodimers detected in situ by proximity ligation on angiogenic sprouts." EMBO J **29**(8): 1377-88.

Nishida, N., H. Yano, et al. (2004). "Vascular endothelial growth factor C and vascular endothelial growth factor receptor 2 are related closely to the prognosis of patients with ovarian carcinoma." Cancer **101**(6): 1364-74.

Oliva, P., A. Decio, et al. (2012). "Cisplatin plus paclitaxel and maintenance of bevacizumab on tumour progression, dissemination, and survival of ovarian carcinoma xenograft models." Br J Cancer **107**(2): 360-9.

Ozols, R. (2003). "Progress in ovarian cancer: an overview and perspective." Eur J Cancer **Supplement Vol 1**(2): 43-55.

Ozols, R., S. Rubin, et al. (2000). Epithelial Ovarian Cancer. Principles and Practice of Gynecologic Oncology. . Hoskins WJ, Perez CA and Y. RC. Philadelphia, Lippincott Williams & Wilkins: 981–1057.

Paavonen, K., P. Puolakkainen, et al. (2000). "Vascular endothelial growth factor receptor-3 in lymphangiogenesis in wound healing." Am J Pathol **156**(5): 1499-504.

Padera, T. P., A. H. Kuo, et al. (2008). "Differential response of primary tumor versus lymphatic metastasis to VEGFR-2 and VEGFR-3 kinase inhibitors cediranib and vandetanib." Mol Cancer Ther **7**(8): 2272-9.

Pena, C., C. Lathia, et al. (2010). "Biomarkers predicting outcome in patients with advanced renal cell carcinoma: Results from sorafenib phase III Treatment Approaches in Renal Cancer Global Evaluation Trial." Clin Cancer Res **16**(19): 4853-63.

Pepper, M. S. (2001). "Lymphangiogenesis and tumor metastasis: myth or reality?" Clin Cancer Res **7**(3): 462-8.

Pepper, M. S., S. J. Mandriota, et al. (1998). "Vascular endothelial growth factor (VEGF)-C synergizes with basic fibroblast growth factor and VEGF in the induction of

angiogenesis in vitro and alters endothelial cell extracellular proteolytic activity." J Cell Physiol **177**(3): 439-52.

Perren, T. J., A. M. Swart, et al. (2011). "A phase 3 trial of bevacizumab in ovarian cancer." N Engl J Med **365**(26): 2484-96.

Peterson, J. K. and P. J. Houghton (2004). "Integrating pharmacology and in vivo cancer models in preclinical and clinical drug development." Eur J Cancer **40**(6): 837-44.

Petrova, T. V., P. Bono, et al. (2008). "VEGFR-3 expression is restricted to blood and lymphatic vessels in solid tumors." Cancer Cell **13**(6): 554-6.

Petrova, T. V., T. Makinen, et al. (2002). "Lymphatic endothelial reprogramming of vascular endothelial cells by the Prox-1 homeobox transcription factor." EMBO J **21**(17): 4593-9.

Plentl, A. A. and E. A. Friedman (1971). "Lymphatic system of the female genitalia. The morphologic basis of oncologic diagnosis and therapy." Major Probl Obstet Gynecol **2**: 1-223.

Podgrabinska, S., P. Braun, et al. (2002). "Molecular characterization of lymphatic endothelial cells." Proc Natl Acad Sci U S A **99**(25): 16069-74.

Pugh, B. F. and R. Tjian (1990). "Mechanism of transcriptional activation by Sp1: evidence for coactivators." Cell **61**(7): 1187-97.

Pujade-Lauraine, E., F. Hilpert, et al. (2012). AURELIA: A randomized phase III trial evaluating bevacizumab (BEV) plus chemotherapy (CT) for platinum (PT)-resistant recurrent ovarian cancer (OC). 2012 ASCO Annual Meeting, Chicago, IL, USA, Journal of Clinical Oncology.

Qian, C. N., B. Berghuis, et al. (2006). "Preparing the "soil": the primary tumor induces vasculature reorganization in the sentinel lymph node before the arrival of metastatic cancer cells." Cancer Res **66**(21): 10365-76.

Raja, F. A., C. L. Griffin, et al. (2011). "Initial toxicity assessment of ICON6: a randomised trial of cediranib plus chemotherapy in platinum-sensitive relapsed ovarian cancer." Br J Cancer **105**(7): 884-9.

Rinderknecht, M. and M. Detmar (2008). "Tumor lymphangiogenesis and melanoma metastasis." J Cell Physiol **216**(2): 347-54.

Rini, B. I., M. D. Michaelson, et al. (2008). "Antitumor activity and biomarker analysis of sunitinib in patients with bevacizumab-refractory metastatic renal cell carcinoma." J Clin Oncol **26**(22): 3743-8.

Roberts, N., B. Kloos, et al. (2006). "Inhibition of VEGFR-3 activation with the antagonistic antibody more potently suppresses lymph node and distant metastases than inactivation of VEGFR-2." Cancer Res **66**(5): 2650-7.

Rottenberg, S., J. E. Jaspers, et al. (2008). "High sensitivity of BRCA1-deficient mammary tumors to the PARP inhibitor AZD2281 alone and in combination with platinum drugs." Proc Natl Acad Sci U S A **105**(44): 17079-84.

Saaristo, A., T. Tammela, et al. (2006). "Vascular endothelial growth factor-C accelerates diabetic wound healing." Am J Pathol **169**(3): 1080-7.

Saaristo, A., T. Veikkola, et al. (2002). "Adenoviral VEGF-C overexpression induces blood vessel enlargement, tortuosity, and leakiness but no sprouting angiogenesis in the skin or mucous membranes." FASEB J **16**(9): 1041-9.

Sallinen, H., M. Anttila, et al. (2011). "Cotargeting of VEGFR-1 and -3 and angiopoietin receptor Tie2 reduces the growth of solid human ovarian cancer in mice." Cancer Gene Ther **18**(2): 100-9.

Sallinen, H., M. Anttila, et al. (2009). "Antiangiogenic gene therapy with soluble VEGFR-1, -2, and -3 reduces the growth of solid human ovarian carcinoma in mice." Mol Ther **17**(2): 278-84.

Schmittgen, T. D. and K. J. Livak (2008). "Analyzing real-time PCR data by the comparative C(T) method." Nat Protoc **3**(6): 1101-8.

Schmoll, H. J., D. Cunningham, et al. (2012). "Cediranib with mFOLFOX6 versus bevacizumab with mFOLFOX6 as first-line treatment for patients with advanced colorectal cancer: a double-blind, randomized phase III study (HORIZON III)." J Clin Oncol **30**(29): 3588-95.

Schoppmann, S. F., R. Horvat, et al. (2002). "Lymphatic vessels and lymphangiogenesis in female cancer: mechanisms, clinical impact and possible implications for anti-lymphangiogenic therapies (Review)." Oncol Rep **9**(3): 455-60.

Sehouli, J., F. Senyuva, et al. (2009). "Intra-abdominal tumor dissemination pattern and surgical outcome in 214 patients with primary ovarian cancer." J Surg Oncol **99**(7): 424-7.

Senturk, E., S. Cohen, et al. (2010). "A critical re-appraisal of BRCA1 methylation studies in ovarian cancer." Gynecol Oncol **119**(2): 376-83.

Shaner, N. C., P. A. Steinbach, et al. (2005). "A guide to choosing fluorescent proteins." Nat Methods **2**(12): 905-9.

Shcherbo, D., E. M. Merzlyak, et al. (2007). "Bright far-red fluorescent protein for whole-body imaging." Nat Methods **4**(9): 741-6.

Shemiakina, II, G. V. Ermakova, et al. (2012). "A monomeric red fluorescent protein with low cytotoxicity." Nat Commun **3**: 1204.

Shih Ie, M. and R. J. Kurman (2004). "Ovarian tumorigenesis: a proposed model based on morphological and molecular genetic analysis." Am J Pathol **164**(5): 1511-8.

Shimizu, K., H. Kubo, et al. (2004). "Suppression of VEGFR-3 signaling inhibits lymph node metastasis in gastric cancer." Cancer Sci **95**(4): 328-33.

Shojaei, F. and N. Ferrara (2008). "Role of the microenvironment in tumor growth and in refractoriness/resistance to anti-angiogenic therapies." Drug Resist Updat **11**(6): 219-30.

Siegel, R., D. Naishadham, et al. (2013). "Cancer statistics, 2013." CA Cancer J Clin **63**(1): 11-30.

Siegfried, G., A. Basak, et al. (2003). "The secretory proprotein convertases furin, PC5, and PC7 activate VEGF-C to induce tumorigenesis." J Clin Invest **111**(11): 1723-32.

Sironi, M., A. Conti, et al. (2006). "Generation and characterization of a mouse lymphatic endothelial cell line." Cell Tissue Res **325**(1): 91-100.

Skobe, M., L. M. Hamberg, et al. (2001). "Concurrent induction of lymphangiogenesis, angiogenesis, and macrophage recruitment by vascular endothelial growth factor-C in melanoma." Am J Pathol **159**(3): 893-903.

Skobe, M., T. Hawighorst, et al. (2001). "Induction of tumor lymphangiogenesis by VEGF-C promotes breast cancer metastasis." Nat Med **7**(2): 192-8.

Smith, N. R., D. Baker, et al. (2010). "Vascular endothelial growth factor receptors VEGFR-2 and VEGFR-3 are localized primarily to the vasculature in human primary solid cancers." Clin Cancer Res **16**(14): 3548-61.

Sopo, M., M. Anttila, et al. (2012). "Antiangiogenic gene therapy with soluble VEGF-receptors -1, -2 and -3 together with paclitaxel prolongs survival of mice with human ovarian carcinoma." Int J Cancer **131**(10): 2394-401.

Stacker, S. A., M. G. Achen, et al. (2002). "Lymphangiogenesis and cancer metastasis." Nat Rev Cancer **2**(8): 573-83.

Stacker, S. A., M. E. Baldwin, et al. (2002). "The role of tumor lymphangiogenesis in metastatic spread." FASEB J **16**(9): 922-34.

Stacker, S. A., C. Caesar, et al. (2001). "VEGF-D promotes the metastatic spread of tumor cells via the lymphatics." Nat Med 7(2): 186-91.

Stuart, G. C., H. Kitchener, et al. (2011). "2010 Gynecologic Cancer InterGroup (GCIG) consensus statement on clinical trials in ovarian cancer: report from the Fourth Ovarian Cancer Consensus Conference." Int J Gynecol Cancer **21**(4): 750-5.

Su, J. L., P. C. Yang, et al. (2006). "The VEGF-C/Flt-4 axis promotes invasion and metastasis of cancer cells." Cancer Cell 9(3): 209-23.

Su, J. L., C. J. Yen, et al. (2007). "The role of the VEGF-C/VEGFR-3 axis in cancer progression." Br J Cancer **96**(4): 541-5.

Sundar, S. S., H. Zhang, et al. (2006). "Role of lymphangiogenesis in epithelial ovarian cancer." Br J Cancer **94**(11): 1650-7.

Tammela, T., A. Saaristo, et al. (2005). "Angiopoietin-1 promotes lymphatic sprouting and hyperplasia." Blood **105**(12): 4642-8.

Taraboletti, G., D. Belotti, et al. (1993). "Endothelial cell migration and invasiveness are induced by a soluble factor produced by murine endothelioma cells transformed by polyoma virus middle T oncogene." Cancer Res **53**(16): 3812-6.

Tavassoli, F. and P. Devilee (2003). Pathology and Genetics of Tumours of the Breast and Female Genital Organs. a. W. H. O. International Agency for Research on Cancer. Lyon, France, IAPS Press.

Tentler, J. J., A. C. Tan, et al. (2012). "Patient-derived tumour xenografts as models for oncology drug development." Nat Rev Clin Oncol 9(6): 338-50.

Tischer, E., R. Mitchell, et al. (1991). "The human gene for vascular endothelial growth factor. Multiple protein forms are encoded through alternative exon splicing." J Biol Chem **266**(18): 11947-54.

Tobler, N. E. and M. Detmar (2006). "Tumor and lymph node lymphangiogenesis--impact on cancer metastasis." J Leukoc Biol **80**(4): 691-6.

Ueda, M., Y. C. Hung, et al. (2005). "Vascular endothelial growth factor-C expression and invasive phenotype in ovarian carcinomas." Clin Cancer Res **11**(9): 3225-32.

Valoti, G., M. I. Nicoletti, et al. (1998). "Ecteinascidin-743, a new marine natural product with potent antitumor activity on human ovarian carcinoma xenografts." Clin Cancer Res **4**(8): 1977-83.

Van den Eynden, G. G., M. K. Vandenberghe, et al. (2007). "Increased sentinel lymph node lymphangiogenesis is associated with nonsentinel axillary lymph node involvement in breast cancer patients with a positive sentinel node." Clin Cancer Res **13**(18 Pt 1): 5391-7.

van der Burg, M. E., M. van Lent, et al. (1995). "The effect of debulking surgery after induction chemotherapy on the prognosis in advanced epithelial ovarian cancer. Gynecological Cancer Cooperative Group of the European Organization for Research and Treatment of Cancer." N Engl J Med **332**(10): 629-34.

Veikkola, T., L. Jussila, et al. (2001). "Signalling via vascular endothelial growth factor receptor-3 is sufficient for lymphangiogenesis in transgenic mice." EMBO J **20**(6): 1223-31.

Wirzenius, M., T. Tammela, et al. (2007). "Distinct vascular endothelial growth factor signals for lymphatic vessel enlargement and sprouting." J Exp Med **204**(6): 1431-40.

Witte, D., A. Thomas, et al. (2002). "Expression of the vascular endothelial growth factor receptor-3 (VEGFR-3) and its ligand VEGF-C in human colorectal adenocarcinoma." Anticancer Res **22**(3): 1463-6.

Witzenbichler, B., T. Asahara, et al. (1998). "Vascular endothelial growth factor-C (VEGF-C/VEGF-2) promotes angiogenesis in the setting of tissue ischemia." Am J Pathol **153**(2): 381-94.

Wong, N. S., R. A. Buckman, et al. (2010). "Phase I/II trial of metronomic chemotherapy with daily dalteparin and cyclophosphamide, twice-weekly methotrexate, and daily prednisone as therapy for metastatic breast cancer using vascular endothelial growth factor and soluble vascular endothelial growth factor receptor levels as markers of response." J Clin Oncol **28**(5): 723-30.

Workman, P., E. O. Aboagye, et al. (2010). "Guidelines for the welfare and use of animals in cancer research." Br J Cancer **102**(11): 1555-77.

Yavuzcan, A., A. Baloglu, et al. (2009). "The investigation of the factors affecting retroperitoneal lymph node metastasis in stage IIIC and IV epithelial ovarian cancer." Arch Gynecol Obstet **280**(6): 939-44.

Yee, J. K., A. Miyanohara, et al. (1994). "A general method for the generation of high-titer, pantropic retroviral vectors: highly efficient infection of primary hepatocytes." Proc Natl Acad Sci U S A **91**(20): 9564-8.

# Appendices

## A.1 Work by the candidate emanating from the work described in this thesis

PUBLICATIONS

Manuscript in press in American Journal of Pathology (January 2014):

Decio A, Taraboletti G, Patton V, Alzani R, Perego P, Fruscio R, Jürgensmeier JM, Giavazzi R and Belotti D. *Vascular Endothelial Growth Factor C promotes ovarian carcinoma progression through paracrine and autocrine mechanisms.*

Manuscript in preparation:

Decio A, Cesca M, Oliva P, Scarlato V, Bassi A, Jürgensmeier JM, Giavazzi R and Belotti D. *Maintenance treatment with cediranib prolongs survival in a patient-derived ovarian carcinoma xenografts in mice.*

CONGRESS PRESENTATIONS

Belotti D, Decio A, Taraboletti G and Giavazzi R. *Ovarian carcinoma xenografts as a model to study lymphangiogenesis.* Gordon Research Conferences: Molecular Mechanisms in Lymphatic function and disease, Ventura, CA, March 2008.

Decio A, Ceruti R, Taraboletti G, Giavazzi R and Belotti D. *Lymphangiogenesis in ovarian carcinoma xenografts.* Workshop SIICA, "Angiogenesis: basi molecolari ed implicazioni terapeutiche II", Certosa di Pontignano (Si), Italy, May 21-23, 2008. Abstract selected for Oral Presentation and awarded a travel grant.

Decio A, Taraboletti G, Giavazzi R and Belotti D. *Ovarian tumor models to study lymphatic spread.* ESH Conference ANGIOGENESIS, Helsinki, Finland, June 6-7, 2009.

Decio A, Patton V, Scabini M, Losa M, Alzani R, Taraboletti G, Giavazzi R and Belotti D. *Lymphatic spread: models of ovarian carcinoma xenografts.* 51st National Congress of Italian Society of Cancerology (SIC), Sesto San Giovanni (Milan), Italy, November 23-26, 2009.

Decio A, Patton V, Scabini M, Losa M, Alzani R, Taraboletti G, Giavazzi R and Belotti D. *VEGF-C and VEGFR-3 in ovarian tumor progression.* 2010 Gordon Research Conferences: Molecular Mechanisms of Lymphatic Function & Disease Conference, Il Ciocco in Lucca (Barga), Italy, June 13-18, 2010.

Decio A, Cesca M, Scarlato V, Jürgensmeier JM, Taraboletti G, Giavazzi R and Belotti D. *Cediranib affects tumor progression and survival of mice bearing human ovarian carcinoma xenografts expressing VEGFC.* 22nd Biennal EACR Congress, Barcelona, Spain, July 7-10, 2012.

Decio A, Taraboletti G, Patton V, Alzani R, Jürgensmeier JM, Giavazzi R and Belotti D. *Vascular Endothelial Growth Factor C promotes ovarian carcinoma progression through paracrine and autocrine mechanisms.* 16th Beatson International Cancer Conference: Targeting the Tumour Stroma, Glasgow, Scotland, July 7-10, 2013.

## A.2 Work not pertaining, or previous, to the work described in this thesis

PUBLICATIONS

Rovida A, Castiglioni V, Decio A, Scarlato V, Scanziani E, Giavazzi G and Cesca M. *Chemotherapy counteracts metastatic dissemination induced by antiangiogenic treatment in mice.* Mol Cancer Ther, 2013 Aug; Epub ahead of print.

Oliva, P*, Decio A*, Castiglioni V, Bassi A, Pesenti E, Cesca M, Scanziani E, Belotti D, Giavazzi R. *Cisplatin plus paclitaxel and maintenance of bevacizumab on tumour progression, dissemination, and survival of ovarian carcinoma xenograft models.* Br J Cancer, 2012 Jul; 107 (2):360-9. **Equal contribution*

Zecchini S, Bombardelli L, Decio A, Bianchi M, Mazzarol G, Sanguineti F, Aletti G, Maddaluno L, Berezin V, Bock E, Casadio C, Viale G, Colombo N,Giavazzi R and Cavallaro U. *The adhesion molecule NCAM promotes ovarian cancer progression via FGFR signalling.* EMBO Mol Med. 2011 Aug; 3(8):480-94.

Giavazzi R, Decio A. *Syngeneic murine metastasis models: B16 melanoma.* In Methods in Molecular Biology: Metastasis Research Protocols, Brooks SA (ed.), Humana Press Inc, Totowa, NJ, In press.

Sagredo O, García-Arencibia M, de Lago E, Finetti S, Decio A and Fernández-Ruiz J. *Cannabinoids and neuroprotection in basal ganglia disorders.* Molecular Neurobiology 2007 Aug; 36 (1):82-91.

Sagredo O, Ramos JA, Decio A, Mechoulam R, Fernández-Ruiz J. *Cannabidiol reduced the striatal atrophy caused 3-nitropropionic acid in vivo by mechanisms independent of the activation of cannabinoid, vanilloid TRPV(1) and adenosine A(2A) receptors.* Eur. J. Neurosci. 2007 Aug; 26 (4):843-51.

CONGRESS PRESENTATIONS

Sagredo O, Decio A, Ramos JA, Cabranes A, Mechoulam R and Fernandez-Ruiz J. *Cannabidiol reduced the striatal atrophy caused 3-nitropropionic acid in vivo by mechanisms independent of the activation of cannabinoid receptors.* 16th Annual Symposium on the Cannabinoids of the International Cannabinoid Research Society (ICRS), Tihany, Hungary, June 25-28, 2006.

Belotti D, Decio A, Borsotti P, Yiotakis A, Dive V, and Taraboletti G. *Antineoplastic activity of the selective MMP-12 inhibitor 470.1 in ovarian carcinoma.* Cancerdegradome Annual Meeting, Kranjska Gora, Slovenia, March 30th to April 1st 2008.

Oliva P, Decio A, Castiglioni V, Bassi A, Belotti D, Bani MR and Giavazzi R. *Combinations of chemotherapy and bevacizumab in a xenograft model of human ovarian carcinoma.* 52nd

National Congress of Italian Society of Cancerology (SIC), Roma, Italy, October 4-7, 2010. Abstract selected for "Oral Poster Discussion" and awarded a travel grant.

Oliva P, Decio A, Castiglioni V, Bassi A, Bani MR, Belotti D and Giavazzi R. *Combination of chemotherapy with bevacizumab in xenograft models of human ovarian carcinoma.* 102nd AACR Annual Meeting, Orlando, Florida, April 2-6, 2011.

Cesca M, Rovida A, Castiglioni V, Decio A and Giavazzi R. *Proper scheduling of chemotherapy regimens to counteract tumor metastasis after inhibition of angiogenesis.* 54th National Congress of Italian Society of Cancerology (SIC), Bologna, Italy, October 1-4 2012. Awarded a "Premio Trivella" for best posters.

Decio A, Cesca M, Bizzaro F, Scarlato V, Ghilardi C, Bani MR and Giavazzi R. *Heterogeneous response to antiangiogenic therapy in ovarian cancer xenografts: a tool to investigate biomarkers of response.* AACR Meeting 2013, Washington DC, USA, April 6-10, 2013. Recipient of the 2013 AACR-SIC Scholar-in-training Award.

Bizzaro F, Cesca M, Decio A, Scarlato V, Figini S, Ghilardi C, Bani MR and Giavazzi R. *A panel of patient-derived tumor xenografts representing the heterogeneity of epithelial ovarian cancer (EOC).* 5th Freiburg Symposium on Anticancer Drug Discovery, Freiburg, Germany, April 24-27, 2013.